



CHALMERS
UNIVERSITY OF TECHNOLOGY



Gas exchange modeling of a single-cylinder engine

GT-Power modeling of a compression ignition engine running on DME

Master thesis programme Sustainable Energy Systems

SARA SOMMARSJÖ
MAGNUS LENGQUIST

Department of Applied Mechanics
CHALMERS UNIVERSITY OF TECHNOLOGY
Gothenburg, Sweden 2015

MASTER'S THESIS 2015:90

Gas exchange modeling of a single-cylinder engine

GT-Power modeling of a compression ignition engine running on DME

Master's Thesis within the Sustainable Energy Systems programme

SARA SOMMARSJÖ
MAGNUS LENGUIST

Department of Applied Mechanics
Division of Combustion
CHALMERS UNIVERSITY OF TECHNOLOGY
Gothenburg, Sweden 2015

Gas exchange modeling of a single-cylinder engine
GT-Power modeling of a compression ignition engine running on DME
Master's Thesis within the Sustainable Energy Systems programme
SARA SOMMARSJÖ
MAGNUS LENGQUIST

© SARA SOMMARSJÖ & MAGNUS LENGQUIST, 2015-12-19

Supervisors: Henrik Salsing & Martin Sundqvist, Volvo Group Trucks Technology
Examiner: Ingemar Denbratt, Department of Applied Mechanics

Master's Thesis 2015:90
ISSN 1652-8557
Department of Applied Mechanics
Division of Combustion
Chalmers University of Technology
SE-412 96 Gothenburg
Sweden
Telephone: + 46 (0)31-772 1000

Cover:
Volvo FH DME D13 Truck, Volvo Truck Corporation, images.volvotrucks.com

Department of Applied Mechanics
Gothenburg, Sweden 2015-12-19

Gas exchange modeling of a single-cylinder engine
GT-Power modeling of a compression ignition engine running on DME
Master's thesis in the Sustainable Energy Systems programme

SARA SOMMARSJÖ
MAGNUS LENGQUIST
Department of Applied Mechanics
Division of Combustion
Chalmers University of Technology

Abstract

Fossil fuels are dominating the transport sector but due to concerns regarding the climate change, oil resources availability and conflicts in the world, the interest of alternative fuels has increased.

Therefore, the purpose of this work is to model a single-cylinder GT-Power gas exchange model that is running on the alternative fuel, dimethyl ether (DME). The model aims to simulate in-data necessary for further development of the combustion process that will be carried out through CFD analyses. The model will be verified through measured test data of previously performed DME engine tests.

This thesis work resulted in a predictive combustion model, DIPulse, with exhaust gas recirculation (EGR) that is calibrated for two engine load points, B50 and C100. It is able to handle a wide range of EGR amounts and injected fuel masses.

CO₂ predictions for inlet- and exhaust gases have 9.5% and 4.8% accuracy respectively compared with measured lab data and the maximum cylinder pressure has an accuracy of 1.2%.

However, the model can neither handle transient behaviors nor load points other than B50 and C100. It was difficult to achieve accurate CO₂ concentration levels that agrees with the measured data. However, consistent results from the simulations are expected to be difficult to achieve due to significant variations in measured CO₂ concentrations during engine tests.

Keywords: Combustion, DME, EGR, Gas exchange, GT-Power, Single-Cylinder Engine, Simulation

Acknowledgements

This work has been performed as a corporation with Volvo Group Trucks Technology in Gothenburg, Sweden as a part of the master's programme Sustainable Energy Systems at Chalmers University of Technology.

When we started with the thesis, we had limited knowledge in the gas exchange and combustion processes, which are the main areas in this thesis. However, it has been a gratifying challenge and we have learned a lot during this work. We are very thankful for all help that we have acquired and we would like to thank Volvo for giving us the opportunity to perform this thesis work.

We are especially thankful to our supervisors at Volvo, Henrik Salsing and Martin Sundqvist, for giving your time, knowledge, experience, support and welcoming during this work and for believing in us despite our initial knowledge in the field. We would also like to thank Karl Wågman, who is a simulation engineer working with various simulations in GT-Power as a consultant at Volvo. Thank you for sharing your knowledge and experience and for your support throughout this work. All of you have been crucial for the accomplishing the thesis and we will carry your positive attitude with us as an experience to our future undertakings and tasks.

Finally, we would like to thank all of you that have helped us collecting information and data needed for the work. We have been greeted with a welcoming and helpful attitude and a willingness to share knowledge and experience from everyone that we have met during this time.

Sara Sommarsjö and Magnus Lengquist

Abbreviations

#	Load step number
AHRR	Apparent Heat Release Rate
ATDC	After Top Dead Center
ATDCF	After Top Dead Center Firing
BDC (BC)	Bottom Dead Center (Bottom Center)
BNR	Build number
BTDC	Before Top Dead Center
CAD	Crank Angle Degree
CCS	Carbon Capture and Storage
CFD	Computational Fluid Dynamics
CI	Compression Ignition
CN	Cetane Number
DI	Direct Injection
DME	Dimethyl Ether
DPF	Diesel Particulate Filter
EGR	Exhaust Gas Recirculation
EOI	End Of Injection
ESC	European Stationary Cycle
EVC	Exhaust Valve Closing
EVO	Exhaust Valve Opening
GWP	Global Warming Potential
ICE	Internal combustion engines
IVC	Intake Valve Closing
IVO	Intake Valve Opening
LHV	Lower Heating Value
PM	Particulate Matter
RoHR	Rate of Heat Release
SCR	Selective Catalytic Reduction
SOC	Start Of Combustion
SOI	Start Of Injection
TDC (TC)	Top Dead Center (Top Center)
TTW	Tank To Wheel
WTT	Well To Tank
WTW	Well To Wheel

Table of Contents

1	Introduction	1
1.1	Background	1
1.2	Purpose	1
1.3	Scope	1
1.4	Method	2
1.5	Thesis outline	2
2	Engine and modeling theory	3
2.1	Compression-ignition engines and the four-stroke cycle	3
2.2	Components in diesel engines	5
2.3	Engine operating parameters and definitions	6
2.4	The gas exchange process	9
2.4.1	Effects on volumetric efficiency	9
2.4.2	Valves and valve lash	10
2.4.3	Exhaust Gas Recirculation (EGR)	11
2.5	Combustion in compression ignition engines	12
2.5.1	Rate of Heat Release and Apparent Heat Release Rate	12
2.5.2	Combustion phases and events	14
2.6	Modeling theory	16
2.6.1	GT-Power specific expressions and definitions	16
2.6.2	Heat transfer	17
2.6.3	Discretization Length	18
2.6.4	Cylinder ports	19
2.6.5	Non-predictive and predictive combustion models	19
2.6.6	Combustion model DIPulse	20
2.7	Dimethyl Ether (DME)	21
2.7.1	Fuel properties	21
2.7.2	Production and transport aspects	23
2.7.3	Environmental aspects	23
2.8	Load points and European Stationary Cycle (ESC)	25
2.9	Design of Experiments (DOE)	26
3	Engine at Chalmers	27
3.1	Measurement equipment	28
4	Engine modeling and calibration	30
4.1	Measured data	30
4.2	Engine calibration process	30
4.3	Fuel specification	31
4.4	Case 1: Non-predictive combustion model without EGR	32
4.4.1	Boundary conditions	32
4.4.2	Modeling of cylinder head ports and valves	32
4.4.3	Combustion profile	34
4.4.4	Injection system	34
4.4.5	In-cylinder heat transfer	34
4.4.6	Cylinder calibration	34
4.4.7	Inlet tank modeling	35
4.4.8	Pressure calibration	36

4.5	Case 2: Predictive combustion model without EGR	37
4.5.1	Definition of injection events	37
4.5.2	Adjustment of fuel injection rate curves	38
4.5.3	Calibration of DIPulse	39
4.5.4	Enthalpy in liquid fuel	41
4.6	Case 3: Imposed combustion profile with EGR	41
4.6.1	Heat transfer from cylinder ports	41
4.6.2	EGR cooler	41
4.6.3	EGR valve	42
4.6.4	Back pressure	42
4.6.5	Extra inlet tank	42
4.6.6	Calibration	43
4.7	Case 4: Predictive combustion model with EGR	44
4.7.1	Model validation	44
4.7.2	Final model check	45
5	Results	46
5.1	Case 1: Without EGR and imposed combustion rate	46
5.1.1	Cylinder pressure calibration	46
5.1.2	System pressure calibration	46
5.2	Case 2: Predictive combustion without EGR	48
5.2.1	DIPulse multipliers	48
5.2.2	Pressure adjustments during the compression stroke	50
5.2.3	Nozzle hole diameter and discharge coefficient	53
5.2.4	Convection multiplier	53
5.2.5	LHV multiplier	55
5.2.6	Sensitivity analysis of injection rate curves	55
5.2.7	Enthalpy in liquid fuel	57
5.3	Case 3: Imposed combustion profile with EGR	58
5.4	Case 4: Predictive combustion with EGR	59
5.4.1	Cylinder pressure	60
5.4.2	Rate of heat release	61
5.4.3	Final model validation	62
6	Discussion	67
6.1	EGR circuit	67
6.2	Calibration of EGR circuit	67
6.3	Predictive combustion model (DIPulse)	68
6.3.1	The convection and LHV multiplier	68
6.3.2	Matching the RoHR curves in the calibration model	69
6.3.3	Enthalpy in the liquid fuel	69
6.3.4	Sensitivity analysis of injection rate curves	70
6.4	Final model results and behavior	72
6.5	Sources of errors	72
7	Conclusion	73
8	References	74
9	Appendices	77

1 Introduction

This report summarizes the work behind the development of a single-cylinder GT-Power gas exchange model that is running on the alternative fuel dimethyl ether (DME). It includes the model's accuracy in comparison with measured data achieved during engine lab tests and its weaknesses and strengths. The model aims to simulate in-data necessary for further development of the combustion process.

1.1 Background

Fossil fuels have dominated the transport sector during the past century but due to concerns regarding the climate change, oil resources availability and conflicts in the world, the interest of alternative fuels has increased.

Dimethyl ether (DME) is an alternative fuel that provides the possibility to be CO₂ neutral if produced from by-products like black liquor or renewable feedstock. Its properties makes it suitable to use in diesel engines, due to the similar combustion characteristics as diesel fuel, which makes it a promising biofuel from an energy security, economic and environmental perspective. Research and development of DME has led to test trucks running on the fuel and in order to improve the combustion process and thus make the use of the fuel more efficient, further development on the combustion system using a simulation software is needed.

Modeling the combustion processes using simulation software has become an important tool in research and development of engines. It increases the understanding of the complex processes taking place in the cylinder and in combination with lab tests, engine simulations contribute to development of engines and engine components to improve the combustion efficiency among other things.

1.2 Purpose

In order to increase the predictability of computational fluid dynamics (CFD) analyses, accurate in-data and boundary conditions are necessary and can be produced with simulations. In order to obtain data that cannot be measured and increase the understanding of the DME combustion process, simulations is one important tool. This work will focus on using the simulation tool GT-Power to model and verify the gas exchange process in a single-cylinder engine running on DME that will be able to produce necessary data for CFD analyses.

1.3 Scope

This work contains simulations of a single-cylinder engine by using the simulation tool GT-Power. The engine model is run on DME and is verified through measured test data of previously performed DME engine tests. The result consists of a model with a predictive combustion process and EGR with the possibility to adjust the EGR rate and injected fuel amount at specific load points. The model is able to produce relevant output data for further CFD analyses of the combustion process of DME.

The simulation model is calibrated at two engine loads and two engine speeds. Hence, it cannot handle any engine accelerations or any intermediate engine speeds or loads.

1.4 Method

The software used to make a simulation model of the engine is GT-Power v7.4 Build 4. It performs 1-D simulations of the flows and has a wide range of possibilities when it comes to calculation and simulation of internal combustion engines, such as composition, pressure and temperature during combustion. The model was built from scratch with some geometries collected through external measurements and engine data, like valve openings, specific pressure drops and cylinder head geometries, were collected from drawings and other documentations.

The development of the model was divided in four different cases where the model was built up gradually and calibrated in smaller steps to make error searching and calibration easier.

Calibration of the model was made by adjusting geometries and other parameters so as they became consistent with measured data from engine lab tests. The simulation results were compared and validated with measured data.

1.5 Thesis outline

The thesis begins with providing relevant engine theory necessary to understand the modeling process and results achieved and discussed. The theory is addressed to readers with fundamental technical knowledge. Relevant modeling theory related to the software GT-Power is also included as well as explanation of the fuel DME used in this work. The thesis will also explain the process and steps taken to obtain the final model and finally present the results achieved and what accuracy that can be expected from the model. Conclusions and recommendations for future work is also included.

2 Engine and modeling theory

Reciprocating engines, also known as piston engines, are engines that transmit power from a piston that moves back and forth in a cylinder to a drive shaft through a connected rod and crank mechanism, where a cyclical piston motion is produced by the rotating crank (Heywood, 1988). These types of engines are very common and are used in all kinds of transport modes like private cars and freight transport by truck and maritime.

This chapter will provide fundamental knowledge about compression-ignition four-stroke combustion engines including the gas exchange and combustion process. The fuel DME used in this work will also be introduced as well as necessary terms and information about the source of measured lab data.

2.1 Compression-ignition engines and the four-stroke cycle

There are different methods for fuel ignition in an engine, like spark-ignition and compression-ignition (Heywood, 1988; Mollenhauer & Tschöcke, 2010). In spark-ignition engines, it is common that the air and fuel are mixed in the intake system before entering the cylinder. The mixture is then ignited by a spark from an electrical discharge, across a spark plug, which starts the combustion process.

Compression-ignition engines do not need an external spark to start the combustion process, since the fuel is auto-ignited by the hot and compressed air in the cylinder. The fuel is directly injected into the cylinder shortly before the wanted start of combustion. Thereafter, the combustion starts and the cylinder pressure increases. The flame is thereafter spread to the amount of fuel that has been sufficiently mixed with air to burn. The fuel and air mixing, and thus the combustion, continues during the expansion process. It is important that the amount of fuel is appropriate to the fraction of the air inducted to enhance a complete combustion. This is normally done by having excess air in relation to the stoichiometric air to fuel ratio.

The compression ratio in compression-ignition engines is higher than spark-ignition engines and the range depends on if the engine is naturally aspirated or turbo-/super-charged. By varying the amount of fuel injected to the engine, load control is achieved but as long as the engine's speed is held constant, the inlet airflow remains unchanged.

To clarify, the diesel engine/process refers to the diesel process not the combustion of diesel fuel itself. Hence, a diesel engine is a compression ignition engine using direct injected fuel. An alternative fuel like DME with similar properties can be used in diesel engines and thus be related to the diesel process.

There are several types of working cycles; the most commonly used are the four-stroke cycle and the two-stroke cycle. In the four-stroke cycle presented in figure 2.1, one power stroke requires two crankshaft revolutions and four piston strokes. Whereas the two-stroke engine requires one crankshaft revolution and two piston strokes. After the strokes are completed, the cycle repeats.

The four strokes in diesel engines seen in figure 2.1 are further described below:

A) Intake stroke:

Air is inducted during the intake stroke through the intake valve at a pressure below atmospheric pressure or above if the engine is turbo/super charged.

B) Compression stroke:

The air is compressed during the compression stroke, which results in increased temperature and pressure to above the fuel's auto-ignition point.

C) Power stroke:

The fuel injection starts at around TDC, depending on the load and speed. Once the fuel is injected into the cylinder it evaporates and mixes with the air. Spontaneous ignition starts just after the fuel has been injected and the combustion continues during the expansion process. The combustion process is further described in section 2.5.

D) Exhaust stroke:

The exhaust stroke starts after the power stroke from BDC and force the exhaust gases out of the cylinder through the exhaust valve.

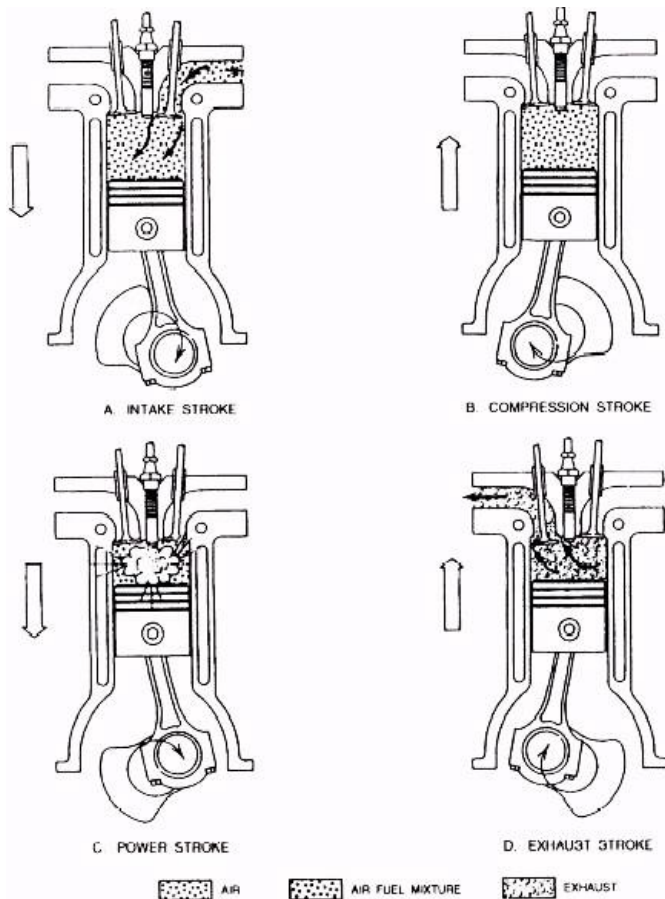


Figure 2.1 The four-stroke diesel engine (www.tpub.com, 2015)

2.2 Components in diesel engines

A typical diesel engine (compression ignited, direct injected, four-stroke engine), can be divided into subsystems according to the following:

- Charging system
- Combustion system
- Fuel delivery and fuel injection system
- Cooling system
- Mechanical system
- Lubrication system
- Exhaust system

In the charging system, a turbo or supercharger can be included. In order to increase the engine's efficiency and power, the air mass flow into the engine is increased through forcing compressed air into the engine (Heywood, 1988; Mollenhauer & Tschoeke, 2010). This can be done by using a compressor that is powered by a turbine, driven by the engine's exhaust gas or by using a supercharger, which is mechanically driven by the engine. It is common that diesel engines are equipped with a turbo, to achieve higher power density.

The combustion system for diesel engines are commonly direct injected. In direct injection systems, the momentum energy from the injected fuel jets is used to distribute the fuel and obtain a combustible mixture. The formation of the air swirl is connected to the inlet valve port design, lift and injection nozzle design. Piston geometry is crucial to archive a good mixing between fuel spray and fresh air and thereby getting a good combustion efficiency.

Compression ignition engines use a different fuel injection system than spark ignition engines, since they do not use a carburetor or port injector, which mixes the air and fuel before the mixture enters the engine. The fuel injection system is an important part of the diesel engine since it is crucial for the internal mixture formation and thus the combustion.

Fuel systems can be divided into two major component groups, low-pressure side components and high-pressure side components (Khair & Jääskeläinen, 2013; Mollenhauer & Tschoeke, 2010). The low pressure side components deliver the fuel from the tank through a low pressure circuit typically consisting of fuel tank, filters, feed pump and control valves. The low pressure circuit is connected to a high pressure circuit with a high pressure pump, valves and accumulator or high pressure pump plungers driven by a cam. The high-pressure side components creates high pressure, meters the fuel and deliver the fuel to the combustion chamber containing a high pressure pump, fuel injector and fuel-injection nozzles.

There are three common fuel injection systems for diesel engines:

1. Pump-Line-Nozzle systems that are driven by a central injection pump from the engine's geartrain and contains fuel lines that links the pump to each nozzle located above the cylinder head.
2. Unit injector systems that have a single device containing a high-pressure pumping element, fuel metering and injector. In a single device, wave superposition decreases when eliminating the injection lines, which reduce injection delays and induces high injection pressure. It is common to have unit pump systems in this design, where each cylinder has its own camshaft driven injection pumping element.

3. Common rail systems have a so called rail with a common pressure accumulator mounted along the engine block. The fuel is delivered through the rail with a high pressure pump driven at e.g. crankshaft speed from engine or twice the camshaft speed. The fuel is then further delivered through high pressure injection lines to the fuel injectors.

It is also important to cool the engine in order to lower the emissions, lower the fuel consumption, prevent components from excessive temperatures, lower temperatures of the incoming air (improved charging) and improve the efficiency of turbocharger compressors. Engine cooling is divided according to the cooling medium; air cooling and liquid cooling. Liquid cooling is most common and typical cooling mediums are water or water/ethylene glycol blends to lower the freezing point.

When it comes to the mechanical system, it contains among other things piston, crankshaft, connection rod and camshaft. The main purpose of the system is to convert chemically released energy into kinetic rotational energy. The mechanical system also controls intake and exhaust valve opening and closing through transferring motion from the camshaft to the valve stems through a so called valve rocker arm.

The mechanical components also need lubrication to work properly. Therefore, the lubrication system is meant to keep the moving parts in the mechanical system lubricated so it will not wear and break premature. It can sometimes act as a cooling system as well when cooled lubricant is purposely ejected towards the bottom side of the piston, which generates a cooling effect.

Exhaust systems take care of emissions and sound. Here one will find the selective catalytic reduction (SCR) catalyst and diesel particulate filter (DPF) whose purpose are to handle NO_x emissions and soot particulates. In the exhaust system there is often a turbine making use of the lower pressure in the exhaust gas to be able to run the compressor at the intake air side.

2.3 Engine operating parameters and definitions

There are many different parameters that can be derived from basic geometrical shapes of the cylinder and crankshaft. This section will address some that are of importance for this work and common abbreviations can be seen figure 2.2. Equation (2.1) to (2.9) is collected from Internal Combustion Engine Fundamentals (Heywood, 1988).

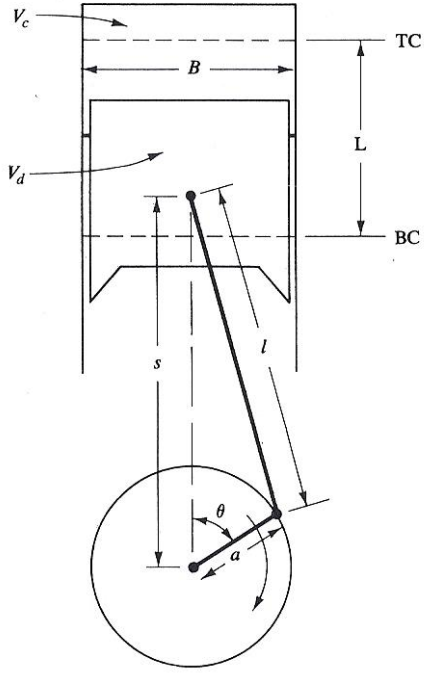


Figure 2.2 Cylinder geometry (Heywood, 1988)

Compression ratio, r_c is the volume of the cylinder when the piston is at the bottom of the stroke (maximum volume) divided by the volume of the cylinder when the piston is at the top of its stroke (minimum volume). The compression ratio is calculated according to equation (2.1).

$$r_c = \frac{\text{maximum cylinder volume}}{\text{minimum cylinder volume}} = \frac{V_d + V_c}{V_c} \quad (2.1)$$

Where V_d is the displacement volume and V_c the clearance volume.

One important parameter is the present volume in the cylinder at any given moment and can be expressed as equation (2.2), where s can be calculated according to equation (2.3)

$$V = V_c + \frac{\pi B^2}{4} (l + a - s) \quad (2.2)$$

$$s = a \cos(\theta) + (l^2 - a^2 \sin^2(\theta))^{1/2} \quad (2.3)$$

Where B is the cylinder bore [m], l is the crank rod length [m], a is the crank radius, θ is the crank angle.

The mechanical efficiency, η_m is the relation between the useful power and the indicated power according to equation (2.4).

$$\eta_m = \frac{P_b}{P_i} \quad (2.4)$$

Where the indicated power, P_i is the net power produced in the cylinder (the area in the pressure-volume diagram) and the brake power, P_b is the useful power at the output shaft.

Mean effective pressure, mep is the average pressure exerted on the piston during a power stroke divided by the displacement volume and thus independent on the engine's size. Where n_g is number of crank revolutions per power stroke and thus two for four-stroke engines.

$$mep = \frac{P n_g}{V_d N} \quad (2.5)$$

Air/fuel ratio, A/F is a measure of the air to fuel mass flow rate according to equation (2.6).

$$A/F = \frac{\dot{m}_{air}}{\dot{m}_{fuel}} \quad (2.6)$$

Volumetric efficiency is a measure of the overall effectiveness of the engine as an air pumping device and is defined in equation (2.7).

$$\eta_v = \frac{m_a}{\rho_{a,i} V_d} \quad (2.7)$$

Where $\rho_{a,i}$ is the density of inlet air at a reference pressure (usually atmospheric or charge pressure), m_a is the mass of air inducted per cycle and V_d is the displaced volume.

Air trapping ratio is the ratio of air trapped in the cylinder to the air delivered to the cylinder. This value is less than one if there is any incoming air flowing through the cylinder out through the exhaust port at the intake stroke. This results in loss of fresh air out from the cylinder that could have been trapped instead and used during the combustion.

Residual Fraction at inlet valve closing (IVC) is the total mass fraction of exhaust gases trapped in the cylinder, from previous combustion, at IVC. This value includes both the amount of EGR and the amount of trapped residual gases.

Some definitions and parameters when it comes to the injection system are also of interest. First of all, the injection pressure, which controls the rate of fuel injected into the combustion chamber and kinetic energy into the cylinder through the fuel spray. Higher pressure leads to a higher driving force and thus higher mass flow. Other parameters, such as the number of nozzle holes and the nozzle hole diameter. If fuel mass flow remains constant when changing flow area, this can be used to control the fuel jet velocity that can affect the mixing of fuel and air in the cylinder and thus affect the combustion. However, in reality fuel mass flow will not remain constant and fuel jet velocity will be independent of the hole diameter as can be seen in equation (2.8).

$$U = \frac{\dot{m}_{actual}}{A_n} = C_d \sqrt{2 \rho \Delta p} \quad (2.8)$$

Where U is the velocity of the fluid, \dot{m}_{actual} is the actual mass flow, A_n is the minimum flow area, ρ is the density of the fluid, Δp is the pressure drop across the flow object i.e. nozzle or valve.

The discharge coefficient, C_d , which is used both in the fuel injection system and the inlet/exhaust valves, is often defined as the ratio of the actual discharge to the theoretical discharge. In this case the actual mass flow rate at the discharge end of the nozzle to that of an ideal nozzle. The discharge coefficient can be calculated according to equation (2.9).

$$C_d = \frac{\dot{m}_{actual}}{A_n \sqrt{2 \rho \Delta p}} \quad (2.9)$$

2.4 The gas exchange process

The gas exchange process contains the intake and exhaust strokes in a four-stroke engine. The purpose is to remove burned gases at the end of the power stroke and introduce fresh air to the next cycle (Heywood, 1988). To get an understanding of which state the inlet and outlet gases are in, one needs to understand the rest of the air intake and exhaust system. In a diesel engine, the intake system usually consists of air filter and turbo charger. The exhaust system often contains exhaust manifold, exhaust pipe and catalytic converter and silencer.

The major problem with modeling the gas exchange system is that it is not stationary. Due to the movements of the cylinder and piston, the flow in the intake and exhaust system is pulsating, which makes it a complex system.

2.4.1 Effects on volumetric efficiency

One measure of how well the gas exchange process is performed is the volumetric efficiency mentioned in section 2.3 (Heywood, 1988). For naturally aspirated engines, the volumetric efficiency can be around 0.9 since the inlet air is driven by the motion of the piston alone, creating a vacuum to force the air into the cylinder. In engines with a charging system, the volumetric efficiency can be much higher. However, this depends on what reference state of air that is chosen when calculating the volumetric efficiency. If the reference state is air at atmospheric pressure and a charging system is used, then the volumetric efficiency is most likely above one. If the reference state of air is chosen as the pressure after the compressor, then the direct effect of the compressor on the volumetric efficiency is not taken into account and thereby, the volumetric efficiency can end up below 1.0 for the same engine. Hence, when stating volumetric efficiency, it is important to know what reference state of air has been used in the calculations.

Other parameters that can affect the volumetric efficiency are:

- **Residence time in inlet manifold**
Heat from the inlet manifold increases temperature, which lowers density of air and reduces the air mass entered into the cylinder and thus decreasing the volumetric efficiency.
- **EGR**
Described in section 2.4.3.
- **Flow friction**
Increased friction in example pipes reduces the overall flow in the system and thus decreases the volumetric efficiency.

- **Backflow**
Late IVC can cause flow to go back into the inlet manifold, which decreases the volumetric efficiency.
- **Ram effect**
Described in section 2.4.2, Valves and valve lash.
- **Chocking**
Chocking occur when the velocity of incoming or outgoing gas from the cylinder reaches supersonic speeds, which results in decreased volumetric efficiency.
- **Tuning**
Can be done through changing the manifold lengths causing the pressure fluctuations in system to be in phase with valve timings. This can increase the volumetric efficiency if done correctly.

2.4.2 Valves and valve lash

Valves are the components that controls more precise at what crank angle the gas will be allowed to enter the cylinder during the intake stroke and when it will be released from the cylinder during the exhaust stroke (Heywood, 1988). Often in modern engines there are two intake valves and two exhaust valves. Usually, the intake valves have a larger diameter than the exhaust valves to be able to trap a larger amount of fresh air into the cylinder. Exhaust valves can be smaller due to much higher differential pressure during the exhaust stroke, that act as the driving force at the same time as the piston forces the exhaust gases out.

Valve timing refers to the crank angle at which the valves open or close and can be set differently to achieve various effects. As an example, an advanced exhaust valve opening before the power stroke is completed can result in less torque from the engine due to loss of energy to the exhaust. However, at the same time with the extra energy delivered to the exhaust, increased pressure and temperature gives more power to the turbo if applied and thereby compresses more air resulting in a larger amount of air mass delivered to the cylinder.

To improve the volumetric efficiency, one can try with closing the intake valves later than BDC and more into the compression stroke. At high engine speeds, this lets the inertia of the incoming air to be forced into the cylinder even when the cylinder is entering the compression stroke. This is called the *ram effect*. On the other hand, if the engine speed is low, the air has not enough inertia and therefore, due to the late closing of the intake valve, air can flow backwards out of the cylinder at the compression stroke and thus reducing the volumetric efficiency during lower engine speeds.

Another important parameter when it comes to valves is the valve lash or valve clearance. This is a small gap between the valve stem and the rocker arm (an arm that transfers the motion from the camshaft) and is measured in mm. The purpose of this clearance is to make sure that the valves are completely closed in all cases. If the valves are not completely closed, severe performance issues can occur. Too much valve lash is not good either, since the force of which the rocker arm hits the valve stem increases with increased valve lash, which increases wear.

Increased valve lash will also affect the overall valve timings, as can be seen in figure 2.3, where the total valve opening time becomes smaller with increased valve lash. With increased valve lash, a lower valve lift is achieved with an amplitude change related to the amount of valve lash. Valve lash is also often larger at exhaust valves than intake valves due to the increased temperatures at exhaust that will cause the valves to expand more. The valve lash

also affects valve overlap, between intake- and exhaust-valve, which can affect trapping ratio and volumetric efficiency.

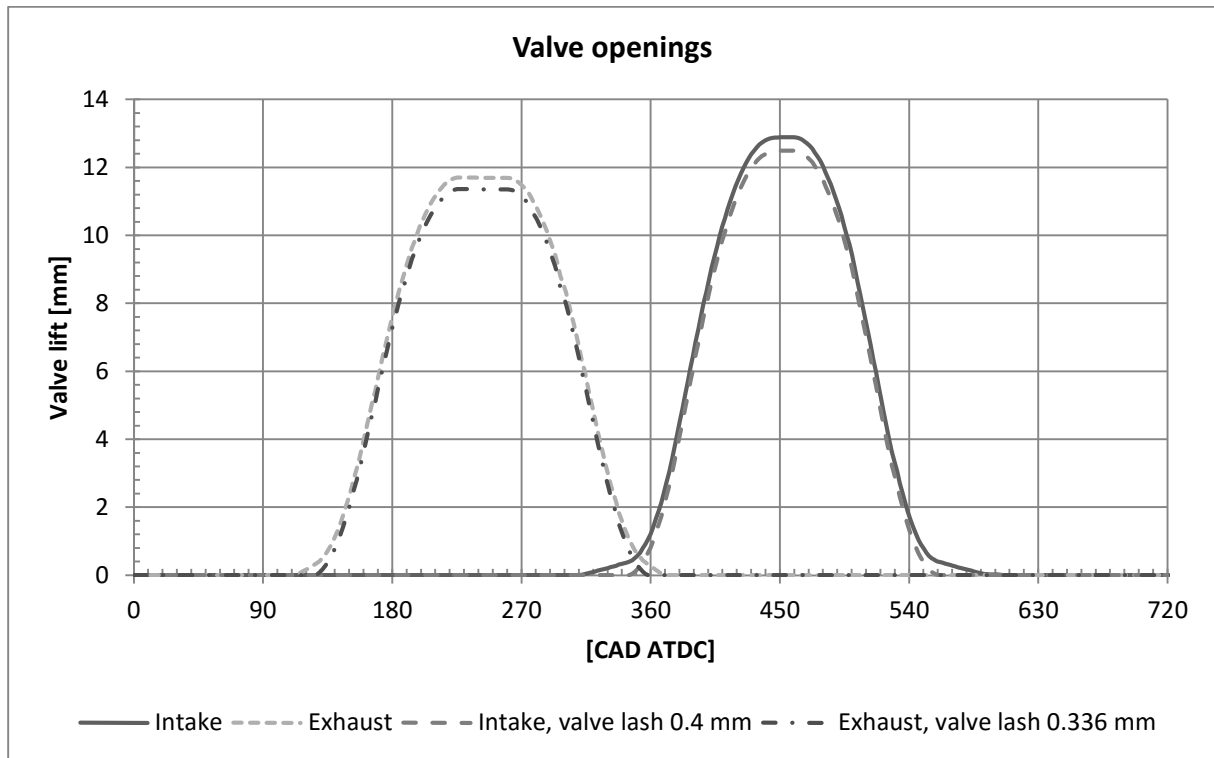


Figure 2.3 Valve timings and the effect of valve lash for exhaust and intake valve separately. The amount of valve lash chosen here is a result of later calibration of the GT-Power model.

2.4.3 Exhaust Gas Recirculation (EGR)

Nitrogen oxides, NO_x , levels are regulated by different environmental legislations in, amongst others, United States and Europe and are regulated mainly because of their harmful effects on humans (Heywood, 1988). NO_x emissions can be reduced through using selective catalytic reduction (SCR) catalyst, which uses urea (AdBlue) that transforms to ammonia in the reactor. Ammonia, NH_3 , then reacts with NO_x , whose products are converted into nitrogen, N_2 , and water, H_2O .

Another way to decrease NO_x emissions is through using exhaust gas recirculation (EGR), which is recirculation of a portion of burned gases back to the inlet where it is first mixed with the fresh air before entering the cylinder. EGR reduces NO_x through lowering the combustion temperature and reducing oxygen content in the cylinder. High temperature and high oxygen concentration in the cylinder has a direct positive effect on the formation of NO_x .

Since volumetric efficiency often is based on fresh air as reference state, and the purpose of the EGR is to send burned gases back to the cylinder, this will affect volumetric efficiency significantly both directly and indirectly. The direct effect is that the fraction of fresh air into the cylinder becomes less, and thereby reducing the volumetric efficiency. The indirect effect is that the burned gases from the EGR circuit often has a high temperature, and when mixing with the fresh air it increases the overall temperature, which reduces the density of the incoming gases to the cylinder. This will reduce the total mass of the gases entering the cylinder and thus lowering the volumetric efficiency.

The amount of EGR can be defined either through a fraction of EGR mass flow in relation to total engine mass flow according to equation (2.10). Although, sometimes the mass of the fuel injected is neglected. The amount of EGR can also be estimated through measuring the CO₂ concentration in inlet flow compared to CO₂ concentration in the outlet flow according to equation (2.11).

$$EGR_{Mass}[\%] = \frac{\dot{m}_{EGR}}{\dot{m}_{fresh\ air} + \dot{m}_{EGR} + \dot{m}_{fuel\ injected}} \cdot 100 \quad (2.10)$$

$$EGR_{CO_2}[\%] = \frac{CO_2\ into\ cylinder\ [\%]}{CO_2\ out\ from\ cylinder\ [\%]} \cdot 100 \quad (2.11)$$

2.5 Combustion in compression ignition engines

Combustion in compression ignition engines is started shortly after the fuel is injected. As the liquid fuel is turned in to fuel vapor which mixes with the air and then auto-ignites due to the high pressure and temperature in the cylinder. The combustion process is very fast and is completed after a couple of milliseconds. However, the combustion can be divided into different sub-phases in which, the combustion can be analyzed in each phase using e.g. rate of heat release analysis.

2.5.1 Rate of Heat Release and Apparent Heat Release Rate

Rate of Heat Release (RoHR) or Heat Release Rate is the instantaneous rate of chemical energy released from the fuel molecules in the cylinder during the combustion i.e. chemical energy release rate (Gamma Technologies, 2014a; Heywood, 1988). The heat release lags the burn rate, which is caused by a delay in the formation of the final products during the combustion since the whole share of the fuel-air mixture does not react immediately. The delay is also caused by the inhomogeneous mixture of the fuel and gases, which makes the fuel equivalence ratio (i.e. the ratio of actual fuel-to-air ratio divided by the stoichiometric fuel-to-air ratio) of the burning mix discontinuous. A change of equivalence ratio and temperature affects the energy released per mass of fuel and thus changes the difference between the burn rate and heat release rate.

The chemical RoHR can be calculated during simulations but is not possible to measure during engine lab tests. Hence, one needs an alternative method to estimate the RoHR when doing experiments, which is done through analyzing the cylinder pressure during the combustion. Apparent Heat Release Rate (AHRR) is a result of analyzing the cylinder pressure profile. However, cylinder pressure is not just an effect of the chemical energy release, but also an effect of compression ratio, heat transfer and in-cylinder gas composition among other factors. Different assumptions are need to filter the heat release from other physical phenomena and thus an exact match will not be achieved, which is why this method and the result obtained from it is often called Apparent Heat Release Rate (AHRR). Due to different assumptions, one can obtain several different AHRR curves from the same pressure profile depending on how it is calculated. This is illustrated in figure 2.5, where two different curves use the same pressure profile according to figure 2.4.

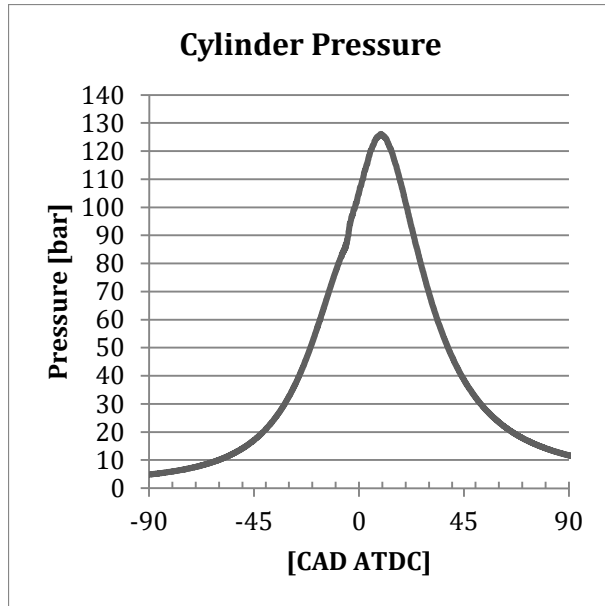


Figure 2.4 Cylinder pressure

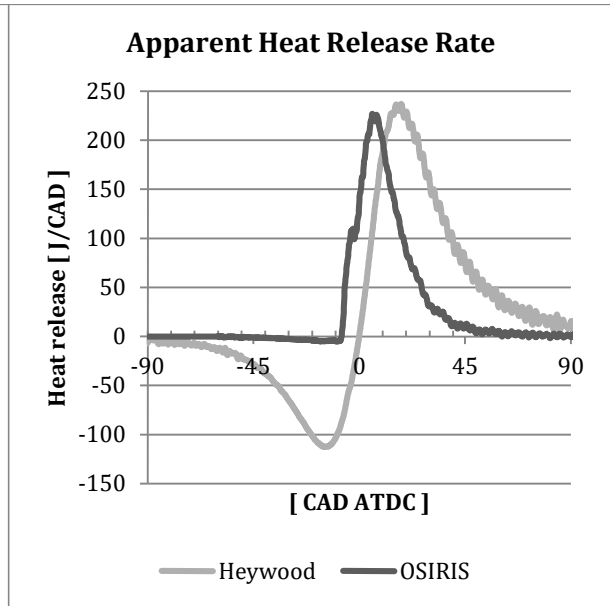


Figure 2.5 Comparison of AHRR. Output data from rig-software OSIRIS compared to calculated AHRR suggested by Heywood.

It should be mentioned that to get the Heywood AHRR curve, like in figure 2.5, it is necessary to apply a filter to the cylinder pressure data. The filter used in this case is the Savitzky-Golay filter, which is applied about 500 times (Maurya, et al., 2013). Without using a filter or filtering procedure, it would be difficult to see any meaningful trend in the AHRR curve.

Heywood suggests calculating the apparent rate of heat release according to equation (2.12) (Heywood, 1988, p. 510). This equation includes rough assumptions as ideal gases, no crevice flow past the piston and does not take into consideration any heat transfer from cylinder (adiabatic).

$$\frac{dQ_n}{dt} = \frac{\gamma}{\gamma - 1} p \frac{dV}{dt} + \frac{1}{\gamma - 1} V \frac{dp}{dt} \quad (2.12)$$

Where Q_n is released heat, γ is the ratio of specific heats c_p/c_v , p is the cylinder pressure and t is the time.

γ varies during a cycle and is not the same during the compression stroke as during the power stroke due to differences in temperature, pressure and composition. In addition, it is also affected by the amount of EGR used since the compositions are affected by changes in EGR.

GT-Power on the other hand, uses another methodology where the heat transfer Q_{tot} from the cylinder is included, which can be seen in equation (2.13), and heat transfer from cylinder is further mentioned in section 2.6.2. In this equation, AHRR is also normalized with the total available energy in the fuel by division with the fuel mass multiplied with its lower heating value, LHV_i . LHV_i is the LHV value of the fuel evaluated at the overall equivalence ratio and the instantaneous cylinder pressure and temperature. More information about the LHV value and how it is used in the AHRR analysis is obtained in section 2.6.1.

$$AHRR = \frac{-p \frac{dV_{tot}}{dt} - Q_{tot} - \frac{d(m_{tot}e_{tot,s})}{dt}}{m_{f,tot} \cdot LHV_i} \quad (2.13)$$

Where p is the cylinder pressure, V_{tot} is the instantaneous volume of the cylinder, Q_{tot} is the total heat transfer from the cylinder, m_{tot} is the total mass of the content in the cylinder, $e_{tot,s}$ is the specific sensible energy of the content in the cylinder, t is the time, $m_{f,tot}$ is the total fuel mass injected during one cycle.

Since the AHRR, independent of calculation method used, is greatly dependent on the cylinder pressure, it is important that it is measured correctly. Errors may occur in the measured cylinder pressure curve that will affect the AHRR extensively. These errors can originate from:

- Insufficient cooling of pressure sensor
- Placement of pressure sensor
- Calibration of pressure sensor, which can affect translation in x- and y-direction
- Calibration of TDC in relation to crank angle degrees
- Gas composition related to specific heats

An example of calibration error is if the cylinder pressure sensor is not calibrated accurately enough in the beginning of the cycle. This pressure will then deviate from the theoretical pressure during e.g. the compression stroke. Since the pressure deviates, this will look like heat release, either negative or positive depending on the pressure deviation. This is a false heat release that will not occur in reality. The same kind of phenomenon can occur if the cylinder pressure deviates in crank angle direction.

All these different methods that estimates the rate of heat release are only estimations. They can be more or less advanced, like the method proposed by Heywood, which lacks an interpretation of heat transfer from the cylinder and thereby results in a negative heat release. Therefore, it is important to use the same calculation methods, including the same phenomena, when comparing rate of heat release curves.

In GT-Power there are two types of predicted heat release curves available when running the so called calibration model (case 2), more about this model can be read in section 4.5. The first one is the predicted heat release curve, which can be compared with a simulated heat release curve based on the cylinder pressure and these can be achieved only when running the calibration model. The other method used to predict the heat release can be achieved both in the final model (case 4) and in the calibration model. The difference is that the heat release is predicted using different assumptions, which results in non-homogenous predicted heat release curves.

2.5.2 Combustion phases and events

The combustion process of a compression ignition engine can be divided into different phases in which, the combustion rate is controlled by different phenomena. Figure 2.6 shows the combustion process expressed as crank angle resolved heat release divided into four phases from start of injection to end of combustion. It also shows how the heat release relates to measured cylinder pressure.

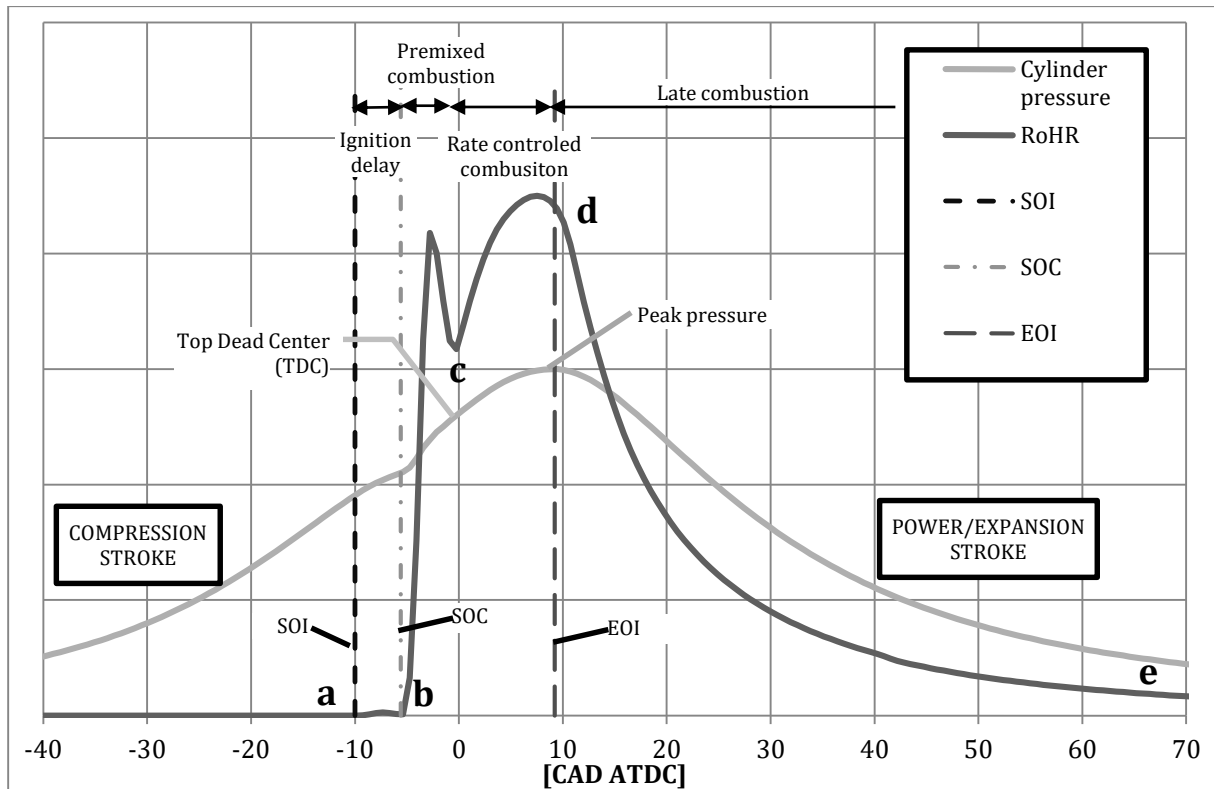


Figure 2.6 Combustion phases in CI engines

The first phase, a to b, is called ignition delay and it is defined as the time between start of injection (SOI) and start of combustion (SOC) (Heywood, 1988; Khair & Jääskeläinen, 2013). SOC is typically defined at the point where the net heat release returns to zero from being negative engendered by the energy consumed from the fuel's vaporization and other energy losses that are not included in the model. The physical processes that occur before start of combustion are atomization of the liquid fuel, vaporization of fuel's droplets and mixing of the fuel vapor with the surrounding gas.

The chemical processes occurring during the ignition delay period generates radicals through breaking down hydrocarbons in the fuel, and local ignition that occur at several places in the cylinder simultaneously. The chemical reactions start just after the fuel vapor makes contact with the air.

The fuel's properties and fuel injection parameters will impact the ignition delay significantly. Cetane number (CN) is a measure of a fuel's auto-ignition quality and thus indicates how easy the fuel ignites and thus, the higher CN, the shorter ignition delay. Other fuel related parameters that shortens the ignition delay are higher injection pressure and temperature, later SOI, less fuel quantity due to less energy required to evaporate the fuel and the injection nozzle type, hole diameter and geometry.

Inducted air properties also have significant effect on the ignition delay. Increased air temperature and pressure, compression ratio and turbulence decrease the ignition delay due to changed charge state. Engine speed at constant load slightly decreases the ignition delay due to changed pressure/time and temperature/time changes, increased injection pressure and higher peak temperature caused by less heat loss during compression. The oxygen concentration in the incoming gas mixture shortens the ignition delay with increasing amount of oxygen.

The second phase, b to c, is called premixed combustion and it represents the combustion occurring at the fuel jet in the cylinder during the ignition when the fuel and surrounding gas have mixed sufficiently to form a combustible mix. The combustion rate during this phase is very high, which causes high temperature and pressure rates increase inside the cylinder. The amount of fuel burned during this phase is governed by how much fuel is injected during the ignition delay period, which itself is affected by engine speed/load and injection timing.

The third phase, c to d, is the diffusion or mixing-controlled combustion phase and the majority of the fuel is burned during this phase in a heavy duty engine. The remaining fuel from the premixed combustion that has not yet been injected, evaporated or sufficiently mixed to be combustible is burned during this phase. The combustion rate of the fuel, in this phase, is controlled by the fuel injection rate and the subsequent mixing with air.

A fourth phase can also be defined as at which the combustion continues after end of injection and prior opening of the exhaust valve. During this phase, the fuel that has not yet been burned, will combust but at lower rate. Some of the heat release from the previous phase can occur in this phase since the heat release lags the burn rate and carbon, that has already been formed, can release energy if oxidized. As long as there is motion inside the cylinder and sufficient temperature, mixing will continue and thus provide opportunities for continuous combustion, as long as the temperature is not too low. As the piston moves downwards the volume increases, resulting in reduced pressure and temperature. A sign of efficient combustion is when the late combustion, the “tail” in the RoHR curve, is decreasing quickly after the rate controlled combustion. Hence, the fuel has been combusted more advanced and thereby more efficient.

2.6 Modeling theory

The modeling theory section describes definitions and relevant theory needed to understand the results and thus the discussion in this report. GT-Power specific terms and how different phenomena are handled, such as heat transfer and combustion models, will be described.

2.6.1 GT-Power specific expressions and definitions

Some definitions that GT-Power uses that are of importance for understanding the content in this report will be stated in this section.

Forward Run

When calculating heat release, this is the normal mode used in GT-Power simulations and uses the burn rate as an input and calculates the cylinder pressure as a result of the energy released during the combustion (Gamma Technologies, 2014a).

Reverse Run

Uses the same calculation methods as in the forward run but uses cylinder pressure as an input and calculates the apparent burn rate required to reproduce the same cylinder pressure in the forward run. This is done through an iterative process that calculates the amount of fuel transferred from the unburned to the burned zone within each timestep until it matches the measured cylinder pressure.

Combustion

GT-Power defines combustion as the amount of total fuel mass and gases transferred from the unburned to the burned zone through enthalpy change inside the cylinder. The results consist of release of chemical energy in the fuel-gas mixture and calculation of species and concentrations.

Burn Rate

The instantaneous rate at which the fuel is consumed inside the cylinder during the combustion i.e. the rate at which a fuel and air mixture is converted to combustion products. GT-Power calculates the burn rate as the rate of which the fuel and gas molecules are transferred from the unburned to the burned zone and start to participate in chemical reactions.

LHV Multiplier

The lower heating value (LHV) multiplier is a multiplier that is used to adjust the energy content in the fuel that is required to achieve the target cumulative burn fraction and is used during the reverse run in the calibration model (case 2), more about this model can be read in section 4.5. The multiplier is adjusted in the reverse run when the burn rate is calculated through using the imposed cylinder pressure to target either the combustion efficiency or the burned fuel fraction in the calibration model. The purpose with the LHV multiplier is to compensate for any disparity between the measured and the predicted cylinder pressure caused by a cumulative error between the available fuel mass in the cylinder and the predicted fuel burned. The error is therefore adjusted through adjusting the fuel energy content with the LHV multiplier.

If the LHV multiplier deviates too much from one, the deviation is flagged as an error and in many cases, error in the LHV multiplier can be due to errors in the cylinder pressure measurements, errors in other measurements that are used as inputs to the calculations, inaccuracies and simplified assumptions in the model. Gamma Technologies recommendation is a maximum deviation of 5% for the LHV multiplier.

2.6.2 Heat transfer

The total heat transfer in pipes is calculated from (Gamma Technologies, 2014b):

- The internal heat transfer coefficient
- The predicted fluid temperature
- The internal wall temperature

The wall temperatures are calculated by the internal and external heat transfer, the thermal capacitance of the walls and the user defined initial wall temperature. The external heat transfer is the heat transfer from outside of the pipe walls to the environment.

In-cylinder heat transfer

The in-cylinder heat transfer is performed by conduction, convection and radiation according to equations (2.14), (2.15) and (2.16) (Heywood, 1988).

Conduction:

$$\dot{q} = -k\nabla T \quad (2.14)$$

Convection:

$$\dot{q} = h_c(T - T_w) \quad (2.15)$$

Radiation:

$$\dot{q} = \sigma(T_1^4 - T_2^4) \quad (2.16)$$

Where \dot{q} is the heat transfer per unit area and time for conduction, convection and radiation respectively. k is the thermal conductivity, h_c is the convective heat transfer coefficient, T_w is the wall temperature, T is the surrounding fluid temperature, σ^1 is the Stefan-Boltzmann constant for a black body, T_1 and T_2 are the temperatures of two different black bodies.

In an engine operating cycle, parameters like fluid velocity, pressure, composition and surface area varies, which makes the heat transfer in a cylinder complex and many simplifications are made along with the heat transfer process that is often assumed to be quasi steady.

Several different empirical correlations have been proposed to predict the convective heat transfer coefficient h_c . Woschni's correlation is one of the most common and it is summarized in equation (2.17):

$$h_c = 3.26B^{-0.2}p^{0.8}T^{-0.55}w^{0.8} \quad (2.17)$$

Where B [m] is the cylinder bore, p [kPa] is the pressure, T [K] is the cylinder gas temperature and w [m/s] is the average cylinder gas velocity.

Hohenberg examined and made changes to Woschni's formula to give better prediction of heat transfer in direct injection diesel engines with and without swirl (Hohenberg, 1980). The modifications use characteristic length based on instantaneous cylinder volume instead of cylinder bore, changes in the effective gas velocity and in the temperature term exponent have been made. Hohenberg's correlation can be seen in equation (2.18).

$$h_c = 130 \cdot V^{-0.06}p^{0.8}T^{-0.4} \cdot (\bar{v}_p + 1.4)^{0.8} \quad (2.18)$$

Where V [m³] is the instantaneous cylinder volume, p [bar] is the pressure, T [K] is the cylinder gas temperature and \bar{v}_p [m/sec] is the average cylinder gas velocity.

2.6.3 Discretization Length

In order to approve a model's accuracy, the discretization length needs to be adjusted (Gamma Technologies, 2014b). Discretization is the division of larger parts or volumes into smaller with the aim to improve the accuracy. This can be done through dividing a system into several components or divide a pipe into multiple sub-volumes, where each of the volumes performs their own calculation. Flow models are solved by Navier-Stokes equations for continuity, momentum and energy and the time integration method can be explicit or implicit. The explicit method uses only the values of the sub-volume in question and its

¹ Usually real surfaces are not considered as "black" and only emits radiation to a certain extend and are therefore often multiplied with an emissivity factor ϵ to compensate for this.

neighboring sub-volumes with values from the previous time step, while the implicit method solves the values of all sub-volumes at the new time step simultaneously by an iterative non-linear system of algebraic equations solving. The explicit method's primary variables are mass flow, density and internal energy and for the implicit method mass flow, pressure and total enthalpy. The explicit method is beneficial where smaller time steps are required and will result in more accurate predictions of pressure pulsations that occur in the engine gas flows and when pressure wave dynamics is important. The explicit method is recommended for most GT-Power engine simulations.

For engine cycle simulations using the explicit method, the recommended discretization lengths are:

- 0.4 times cylinder bore for the intake system
- 0.55 times cylinder bore for the exhaust system

The reason for using different discretization lengths for the intake and exhaust systems is due to the difference in speed of sound due to the temperature differences.

2.6.4 Cylinder ports

The intake and exhaust ports to the cylinder can be modeled using pipe and flowsplit parts in GT-Power (Gamma Technologies, 2014b). Flow coefficients of the valves are calculated from measurements of mass flow rates for a given pressure difference. The flow coefficients include flow losses caused by the port and the pressure losses caused by geometrical changes. Such as angles, changes in diameter and surface roughness where each of them cannot be easily distinguished from the measured pressure loss. Therefore, the friction multiplier and pressure loss coefficients for pipes and flowsplits have to be set to zero in order to avoid pressure losses in the port to be calculated twice.

The inlet and outlet diameters of the ports should be the diameter at the opening of the cylinder head to the intake and exhaust manifold in order to provide correct losses from contraction or expansion. Flowsplits between valves and ports should be added for engines with three or more valves per cylinder. One can make a simplification of the intake and exhaust ports and avoid flowsplits by changing a parameter in the intake valve, controlling the number of equal valves connected to the cylinder. The expansion diameter of the opening of a flowsplit connected to the intake or exhaust manifold should be the same as the opening of the cylinder head in order to achieve the correct losses from contraction or expansion of the flow as it enters or leaves the cylinder head.

2.6.5 Non-predictive and predictive combustion models

When simulating an engine in GT-Power, one can use both non-predictive and predictive combustion models. The choice depends on what the goal with the simulation is and the available input data. Predictive models are generally a good choice for various simulations but are more advanced, require more detailed data and run slower than non-predictive models (Gamma Technologies, 2014a).

The characteristics of a non-predictive combustion model is that the crank angle resolved burn rate is imposed, and imposing the burn rate assumes that there is enough fuel-air mixture available in the cylinder to support the burn rate independent of the conditions in the cylinder. Non-predictive combustion models do not take injection timing, injection profile, residual gas

fractions or other variables that affect the burn rate into account and should therefore not be used when the purpose is to study variables that have direct or indirect effect on the burn rate. Non-predictive combustion models can however be an appropriate choice when studying variables that has little or no effect on the burn rate due to the shorter simulation time required.

Predictive combustion models predict the burn rate and the related variables that affects or are affected by the burn rate, such as rate of heat release and composition. Using predictive combustion models is always recommended according to Gamma Technologies (2014a) but they do run slower than non-predictive models depending on the model's complexity and design. Predictive models also require good measured lab data to calibrate the model in order to achieve meaningful results and enough measured data to validate the model.

Therefore, non-predictive models should be used when it is appropriate and predictive models when it is required. There are several predictive combustion models available in GT-Power, which are suitable for different engine types. Therefore, the choice of combustion model should be made carefully according to the engine type studied.

However, despite that the predictive combustion models in GT-Power can imply that they are very advanced, they are still simplified combustion models that cannot predict 3D effects. They are unable to estimate the effects of changes in piston geometries, angle of fuel injection etc. For those analyses, more detailed modeling is needed e.g. combustion CFD simulations. Advanced way of working is to use a predictive model first to get initial conditions for the whole system, which is used in combustion CFD simulations. Afterwards a non-predictive model can then use the results from the combustion CFD simulation as inputs. For analyzing the system impact of the more resolved combustion.

2.6.6 Combustion model DIPulse

The predictive combustion model used is the “EngCylCombDIPulse” model, which will hereafter be called “DIPulse”, and it predicts the combustion rate and the emissions for direct injected liquid fuels (Gamma Technologies, 2014a). An alternative, earlier developed and similar combustion model (DIJet) is available but not chosen due to much slower runtime. DIPulse works through tracking the fuel when it is injected and evaporated and then mixed with the surrounding gas and finally burned. The model is designed to predict the pressure, temperature and the mixture composition of fresh air, fuel and EGR/residual gases (Gamma Technologies, 2015).

Various data is required to build a DIPulse combustion model and the most important is accurate injection rate profiles and injected mass per cycle. The different input data needed is specified in table 9.3, appendix A - 2.

Since the combustion is greatly controlled by the injection rate, amongst other parameters. However, the combustion process calculated by DIPulse is also adjusted using four multipliers, which are described in table 2.1, to better match lab data.

Table 2.1 DIPulse multipliers description (Gamma Technologies, 2014a)

Multiplier	Description
Entrainment Rate Multiplier	The spray slows down when it enters the cylinder as the surrounding unburned and burned gases entrain into the spray. The rate of the entrainment is calculated by using the law of momentum applied in a “spray penetration law”, which can be modified using this multiplier.
Ignition Delay Multiplier	The ignition delay of the mixture can be modified using this multiplier. However, its effect of the ignition delay does not dominate the effect of the injection rate profiles used.
Premixed Combustion Rate Multiplier:	The mixture present at the time that a spray ignites is called premixed combustion. The premixed combustion is assumed to be kinetically controlled and the rate of this combustion can be modified with this multiplier.
Diffusion Combustion Rate Multiplier	The fuel and the entrained gas in the spray that is insufficiently mixed after a spray is ignited continue to burn primarily in a diffusion/mixing-controlled phase, this combustion rate can be modified using this multiplier.

To validate the model, the measured data needed is intake, exhaust and cylinder pressures and temperatures. The cylinder pressure needs to be crank angle resolved. Depending on the amount of load points and EGR rates the model is intended to be valid for, several injection rate profiles and cylinder pressure curves are needed to achieve an accurate model.

2.7 Dimethyl Ether (DME)

The need for transportation is increasing around the world and for the past decades, diesel and gasoline have been the leading fuels for road transportation vehicles (Semelsberger, et al., 2005). In order to reduce the oil dependency, research has been conducted with the aim to find alternative fuels that is not oil based. Volvo Group has been working on a long-term strategy for alternative fuels through developing trucks running on DME since the beginning of 1990 (Strandhede, 2013). Field tests have been performed in US and Sweden since 2011, ten trucks running on DME were put into traffic through a project sponsored by the Swedish Energy Agency and the European Union.

2.7.1 Fuel properties

The chemical formula for DME is CH_3OCH_3 and molecule can be seen in figure 2.7. DME has a gaseous state at atmospheric pressure and 20°C but is heavier than air and therefore sinks when released in air (Semelsberger, et al., 2005). DME liquefies at around 5 bar absolute pressure and therefore needs pressurized fuel tanks. A summary of properties for

DME compared to diesel fuel are listed in table 2.2 (Semelsberger, et al., 2005; Gable & Gable , 2015; AMF, 2015).

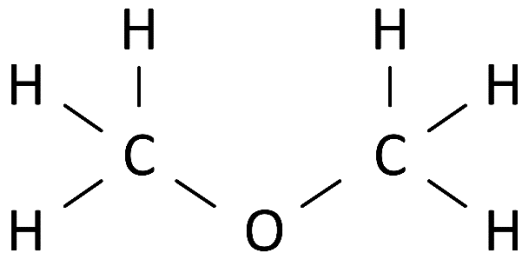


Figure 2.7 DME molecule

DME is considered as a good diesel fuel with a short ignition delay, due to its high cetane number (CN), which provides a good start of the combustion. It also emits no soot from the combustion in comparison to diesel and contains oxygen which improves the combustion (Salomonsson, 2015).

Table 2.2 Thermodynamic properties of DME and diesel
(Semelsberger, et al., 2005; Gable & Gable , 2015; AMF, 2015)

	DME	Diesel
Formula	CH ₃ OCH ₃	C ₁₄ H ₃₀
Molecular weight [g/mol]	46.07	198.4
Density [kg/m³]	661	856
Normal boiling point [°C]	-24.9	125-400
LHV [kJ/cm³]	18.92	35.66
LHV [MJ/kg]	28.62	41.66
Exergy [MJ/L]	20.63	33.32
Exergy [MJ/kg]	30.75	46.94
Carbon Content [wt.%]	52.2	87
Sulfur Content [ppm]	0	~250
Viscosity @40°C, [mm²/s]	~0.21 ²	~1.3 – 4.0
CN³	55-60	45-60

DME is not without drawbacks, like it is considered as a solvent and therefore, one needs to carefully choose sealing materials that are compatible with the fuel. The low viscosity, listed in table 2.2, makes it harder for the fuel pumps to work and therefore reduces efficiency. The LHV value for DME is also low compared to diesel and it depends on e.g. the oxygen content in the fuel and the molecule structure. Approximately twice as much volume of DME is needed to release the same amount of energy as for diesel fuel due its lower energy content. As DME is gaseous at ambient conditions and therefore the fuel system pressure needs to be held at least 12 – 30 bar to avoid vaporization (Semelsberger, et al., 2005; AMF, 2015). This

² Kinematic viscosity for DME varies greatly with pressure and temperature due to its compressibility (Teng, et al., 2002)

³ Cetane number is a measure of the combustion performance of fuels in compression ignition engines with 100 as base index. The higher cetane number, the shorter ignition-delay time.

is usually not a problem in the injection system, due to the high pressure pump delivers several hundreds of bars, but can be a problem in the truck's fuel delivery system.

2.7.2 Production and transport aspects

DME can be produced from various energy resources including natural gas, coal or biomass like farmed wood and wood waste. As an example, in Sweden, a pilot plant for bio DME has been developed (Salomonsson, 2015). The pilot plant uses synthesis gas (or syngas), which is a gaseous mixture of carbon monoxide, carbon dioxide and hydrogen, and it is produced through gasification of carbon containing feedstocks in a pressurized black liquor gasifier. The different pathways from feedstock to fuel can be seen in figure 2.8.

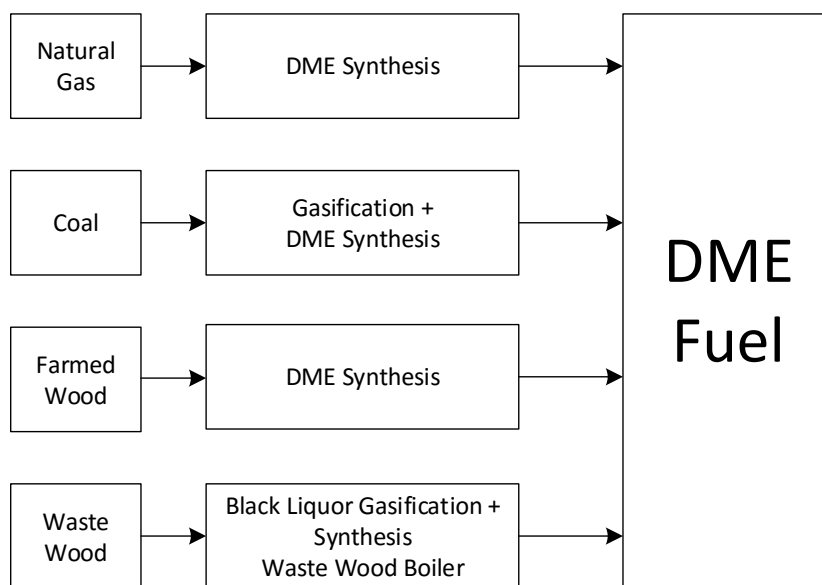


Figure 2.8 DME fuel production pathways

DME is similar to LPG through being gaseous at ambient conditions but liquid at moderate pressure, which makes the logistics similar to that of LPG, which is beneficial since LPG already is used as transport fuel in many countries. Shipping of the fuel to other regions is also similar to how LPG is shipped. Although, today there is no large-scale supply and distribution system for DME as transport fuel and modifications on existing LPG infrastructure, like on pumps, seals and gaskets, are necessary to enable using the existing LPG infrastructure.

In the field tests included in the BioDME project there were four filling stations in Sweden (Stockholm, Jönköping, Gothenburg and Piteå) that delivered fuel to ten DME test trucks within Sweden. The trucks had a common rail fuel-injection system with a rail pressure at around 300 bar and a EGR system for NO_x reduction to reach Euro V emission levels.

2.7.3 Environmental aspects

Global warming potential (GWP) is an index with CO₂ as base that can be used to compare different greenhouse gases' residence time and how effective they absorb outgoing infrared radiation that contributes to global warming (United Nations Framework Convention On Climate Change, 2014). Regarding DME and GWP, research has shown that DME has a GWP of 1.2 for a 20-year time period and 0.3 for 100 years. Indications of tropospheric

lifetime are shown to be around 5 days, which is beneficial from environmental point of view (Semelsberger, et al., 2005).

DME can provide an efficient diesel process, low emissions and reduced noise. The chemical structure of DME leads to low particulate matter (PM) emissions and by using selective catalytic reduction (SCR) or exhaust gas recirculation (EGR), NO_x emissions can be controlled and thus reduced (AMF, 2015; Greszler, 2013). In addition, since DME combustion is soot free, no diesel particulate filter (DPF) is needed.

The related energy consumption and greenhouse gas emissions from a specific fuel can be estimated using a well-to-wheel (WTW) analysis. WTW analyses can be divided into well-to-tank (WTT), which includes the fuels' production process, and tank-to-wheel (TTW), which includes the energy use or emissions emitted by the vehicle.

When it comes to energy use for DME fuel production, the wood pathway is less energy efficient compared to the black liquor pathway and when looking at the well-to-tank greenhouse gas emissions, black liquor has shown to result in lowest emissions, closely followed by farmed wood. Producing DME from coal has so far not been seriously considered but is a possibility. However, the process would emit the largest amount of greenhouse gas emissions (European Commission, Joint Research Centre, 2014).

Comparison between DME, other alternative fuels and conventional fuels for heavy vehicles can be seen in figure 2.9. The figure shows a typical value and a best and worst case depending on the feedstock that the fuel is derived from (Volvo Truck Cooperation, 2015). The values in the graph shows the carbon dioxide equivalents with conventional diesel fuel as a base. It can be seen in the figure that DME can have a low climate impact if it is produced from renewable feedstocks, but DME can also have a significant climate impact if produced from natural gas.

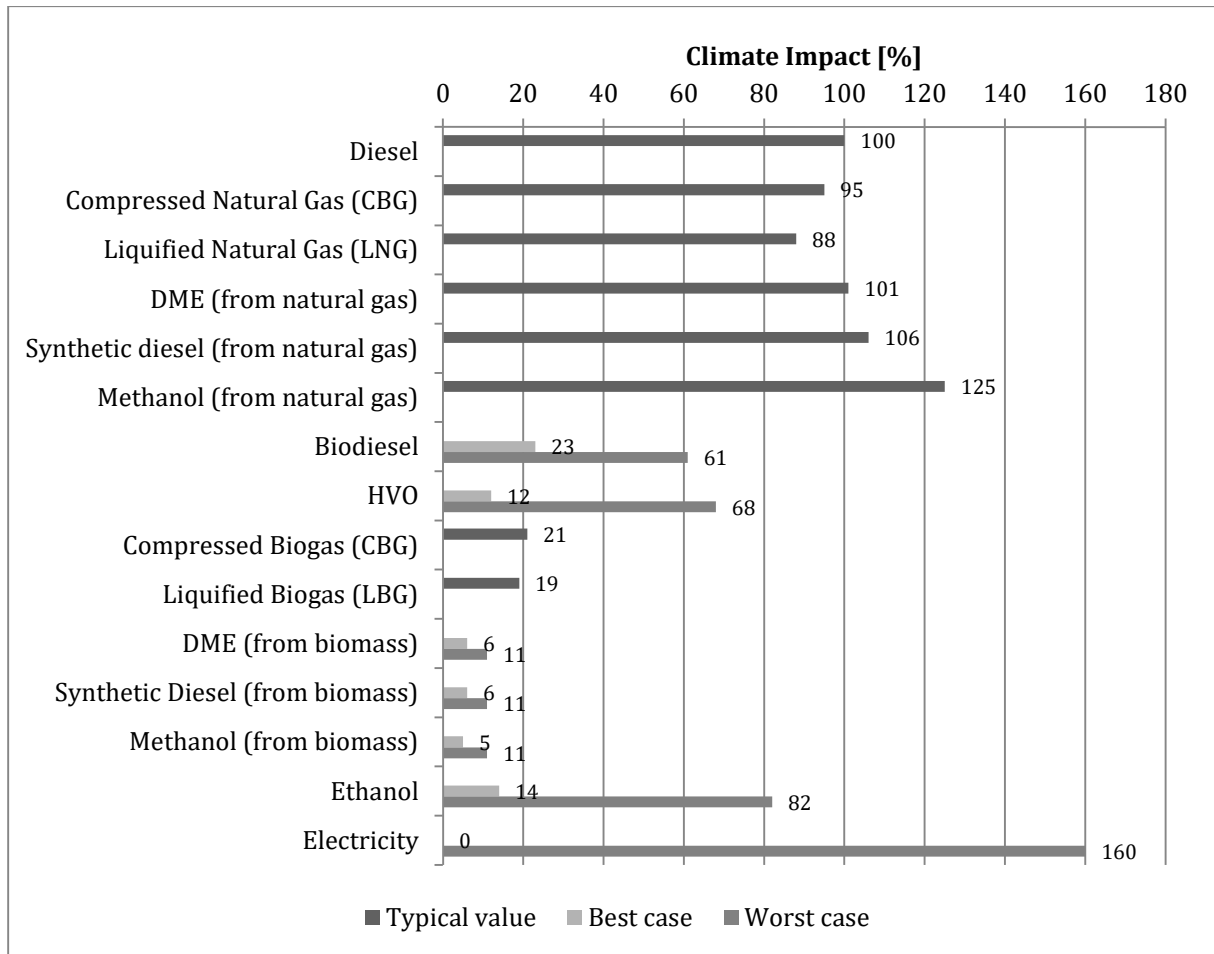


Figure 2.9 Climate impact for a complete well-to-wheel chain in terms of CO₂ equivalents (Volvo Truck Cooperation, 2015)

2.8 Load points and European Stationary Cycle (ESC)

A load point is specified by its engine speed and engine torque and a cycle consists of several load points. The European Stationary Cycle (ESC) is used in this report to define load points for the engine.

ESC was introduced by the Euro III emission regulation for emission measurement for heavy-duty diesel engines (DieselNet, 2015). It is a way of defining steady state load modes at different locations in the engine's power band. A mode consists of a letter, A to C, representing a certain engine speed and a percentage number that defines the amount of power at that engine speed. These engine speeds are calculated through a defined high speed, n_{hi} , and a low engine speed, n_{lo} . The high engine speed, n_{hi} , is defined as the engine speed where 70% of declared maximum power is achieved. The lower engine speed n_{lo} is where 50% of maximum power is achieved. The engine speed for A, B and C is calculated according to equation (2.19) to (2.21).

$$A = n_{lo} + 0.25(n_{hi} - n_{lo}) \quad (2.19)$$

$$B = n_{lo} + 0.50(n_{hi} - n_{lo}) \quad (2.20)$$

$$C = n_{lo} + 0.75(n_{hi} - n_{lo}) \quad (2.21)$$

2.9 Design of Experiments (DOE)

Design of experiments (DOE) is a way of statistically determine the effect that different factors have on certain responses. It can be used to see which factors that are dominant for certain responses and it can also be used to optimize towards desired results.

The experiments are set up by choosing the factors that should be included and varied and also how many different variations of each factor that should be included. One also choose what kinds of responses that should be looked at. As an example, it is possible to see how the valve lash for the intake and exhaust valve separately affects the trapped mass in the cylinder. Then two factors are present, intake and exhaust valve lash, and one response, the trapped mass. If five different valve lashes for each valve is chosen, maybe to look for nonlinear responses, this will result in 25 unique combinations.

In this way, the number of experiments can increase easily since the number of experiments are the product each factors' number of levels ($Number\ of\ runs = \prod_i^{factors} levels_i$). As an example if one have four factors with 8 different values each it will become 4096 experiments ($8 \cdot 8 \cdot 8 \cdot 8 = 4096$).

GT-Power has a specific software aimed for analyzing the data collected called DOE-Post. The software creates a model based on the DOE analysis and how the results respond to a change in a factor's value. This model can be used to provide an optimized solution. For example, if the valve lash was chosen to 2, 4 and 6 mm in the DOE analysis, the model can predict an optimal solution in between these at for example 3.5 mm. However, since these are fitted curves they might not match exactly with simulated data and therefore a separate simulation with the optimized factors should always be done to validate the result.

3 Engine at Chalmers

The engine that has been modeled and used during previous research studies is a single-cylinder research engine based on the Volvo D12C Diesel engine and was built based on the AVL 501 research engine (Salsing, 2011). This engine was originally delivered to Volvo in 1988 but it was later disassembled, maintained and thereafter reassembled in 1996 at Chalmers (Mittermaier, 1996).

A simplified schematics of Chalmers single-cylinder research engine can be seen in figure 3.1 and is focused on the gas side of the engine, hence fuel, oil and coolant flows are simplified. The engine has an EGR system and two gas tanks to reduce flow pulsations that otherwise occur in single-cylinder engines.

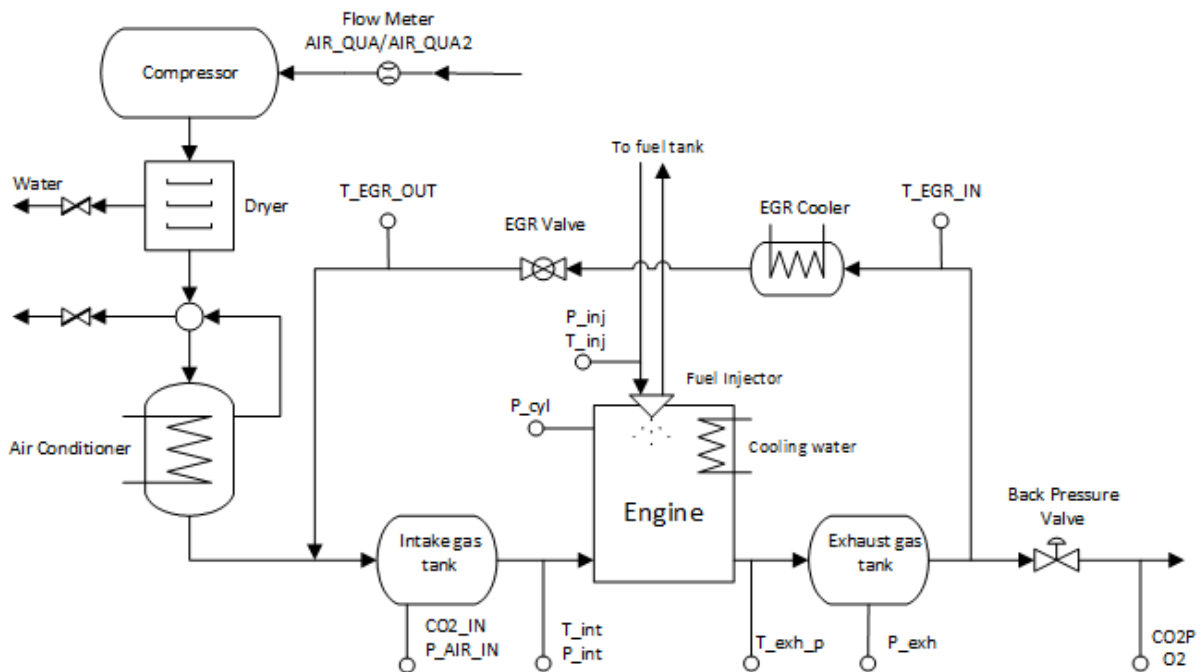


Figure 3.1 Gas side schematic of Chalmers single-cylinder research-rig

The air is compressed by a screw compressor and dried in a dryer working with a coil temperature of 4°C and then the temperature is regulated with the air conditioner. A summary of the main properties of the engine can be seen in table 3.1.

The cylinder has a displaced volume of 2.02 liters with a cylinder bore of Ø131 mm and a stroke of 150 mm. The cylinder head has two inlet and two exhaust valves.

The injection system used for DME is a so called common rail system working at a pressure of 300 to 550 bar and has a centrally placed injector. The injection system has been under continuous development and details around the different setups used are found in (Salsing, 2011).

The EGR circuit basically consists of an EGR cooler designed for a 13 liter engine, a valve and pipes. The valve is a ball valve and can be set in any position between completely closed to fully open. This valve has some play and if an intermediate position is chosen, it might be difficult to set the same position twice. This increases the complexity when simulating the EGR circuit. The amount of EGR is controlled by the back pressure control valve that is placed downstream the split to the EGR/exhaust circuit, as can be seen in figure 3.1.

Table 3.1 Specification of the Volvo D12C single-cylinder engine in DME configuration.
Adapted from (Salsing, 2011).

Bore x Stroke, [mm]	131 x 150
Displaced volume, [l]	2.02
Compression ratio, [-]	17:1 and 15:1
Fuel injection system	Common rail
Common rail pressure, [bar]	<300 – 550
Fuel feed pressure, [bar]	12 – 18
Nozzle flow @ 100 bar, [l/min]	4.5
Number of orifices, [-]	8
Included angle, [°]	155
Piston	Diesel variant: Ø92 DME variant: Ø88-REC
Inlet valve opening/closing, [CAD ATDCF]	310/-115
Exhaust valve opening/closing, [CAD ATDCF]	111/-347
Fluid inlet temperatures, air/oil/water, [°C]	30 ⁴ /90/85

3.1 Measurement equipment

Below in table 3.2 is a summary of the sensors in the research rig that are most important for this work. There are several other sensors and equipment used but that are of little importance to this work and therefore not mentioned.

There are two different kinds of resolution of the sensors. Fast sensors that are crank angle resolved and thereby enabling studying how it varies in the cycle. Slow sensors are cycle averaged values and do not have fast enough sampling rate to see changes within a cycle.

⁴ Applicable only when no EGR is present, since the temperature at inlet increase with increased EGR rate.

Table 3.2 Summary of measurement equipment at Chalmers single-cylinder engine

Sensor	Abbreviation	Measures	Type	Resolution
Flow Meter	AIR_QUA / AIR_QUA2 ⁵	Air mass flow	Endress/Hauser	Slow
Flow Meter	ENG_FLW2	Fuel mass flow	Micro Motion, CMF010	Slow
CO ₂ inlet	CO2_IN	CO ₂ dry volume fraction	Non-dispersive infrared detector	Slow
Pressure at intake	P_int_K	Absolute pressure	Kistler 4045A5 piezo-resistive	Fast
Temperature at intake	T_int	Temperature	Pentronic, Pt100	Fast
Cylinder pressure	P_cyl	Relative pressure	Kistler 7061B piezo- electric	Fast
Temperature at exhaust	T_exh_p	Temperature	Pentronic, TC	Slow
Pressure at exhaust	P_exh	Pressure		Slow
Temperature at EGR cooler inlet	T_EGR_IN	Temperature	Pentronic, TC	Slow
Temperature at EGR outlet	T_EGR_OUT	Temperature	Pentronic, Pt100	Slow
CO ₂ exhaust	CO2P	CO ₂ dry volume fraction	Non-dispersive infrared detector	Slow
O ₂ exhaust	O2_%	O ₂ dry volume fraction	Paramagnetic analyzer	Slow

⁵ Two different abbreviations for this sensor because between measurements the sensor broke down and had to be replaced, hence the number two at the end. The second air flow meter is also placed downstream of the dryer and not at the same place as the first air flow meter.

4 Engine modeling and calibration

The content in this chapter will describe the steps taken and how they were done to finalizing the engine model. The software used is GT-Power v7.4 Build 4 from Gamma Technology. The software performs 1-D simulations of the flows and has a wide range of possibilities when it comes to calculation and simulation of internal combustion engines, such as composition, pressure and temperature during combustion. The simulation results were compared and validated with measured data. In order to collect missing data needed in the models, measurements in the engine's lab test cell were made. The measurements include external geometrical measurements.

4.1 Measured data

The term “measured data” is commonly used in this report and refers to data collected during lab tests on a single-cylinder engine at Chalmers University of Technology (Salsing, 2011).

The measurements have been categorized in two different steps. By build number (BNR), which is a time period of continuous measurements at the research engine. Changed BNR means that instruments may have been changed and equipment adjusted compared to the previous BNR. Load step number, sometime uses a hashtag symbol, #, and indicates an engine run at which the engine's parameters are constant. Consecutive load steps, with the same parameter settings, uses the same designation (number) and should therefore give comparable results. When load step number is changed, one or more parameters has changed like the amount of EGR or the charge air pressure. A summary of the input data parameters for an engine run can be seen in appendix A - 1.

4.2 Engine calibration process

The calibration and validation of the GT-Power model was made through dividing the model into different cases according to Table 4.1. A more detailed description of each case can be found under their respective section. The calibration procedure for most cases is done through changing parameters from their theoretical values so that simulated data at different sensors, described in section 3.1, are comparable to measured data. An exception is case 2 where calibration multipliers are used that has no theoretical starting value.

Table 4.1 Summary of cases' objectives

Case 1	Without EGR and imposed combustion profile Tuning of inlet and exhaust conditions including inlet and exhaust tank
Case 2	Without EGR and predictive combustion model (calibration model) Tuning of the combustion profile
Case 3	With EGR and Imposed combustion profile Tuning of EGR
Case 4	With EGR and predictive combustion model (final model) Tuning the complete system together

Measured data was available with and without EGR, so the model validation started with the simplest case using an imposed heat release curve to simulate the combustion, which is called

a non-predictive combustion model. When inlet and outlet conditions in the non-predictive combustion model were calibrated, a predictive combustion model without EGR was developed and thereafter validated. A non-predictive model with EGR was also developed simultaneously as the predictive model without EGR, which corresponds to case 2 and case 3. Case 4 is the final model and a combination of case 2 and 3, a predictive combustion model with EGR. The processes for the four cases are further described in section 4.4 to 4.7.

4.3 Fuel specification

The fuel DME, which was used in the model throughout the whole modeling process, had to be specified since it was not available in GT-Power as standard. It was specified using two templates in GT-Power called “FluidLiqIncompress” and “FluidGas”. The first template is the liquid state of the fuel and is intended to be used when the liquid share of the total mixture is very small, like during the combustion. The other template is used to specify the gaseous part of the fuel.

Amongst other things needed in the templates, thermal and transport properties had to be specified, which was made through using a modified Redlich-Kwong equation of state proposed by Ho, et al. (2004). Since some of the properties in the templates should be given as a polynomial, a curve-fitting tool in MATLAB was used to convert the equation of state into a more simple relationship.

Due to problems of getting the modified Redlich-Kwong equation of state to produce reasonable properties for gaseous DME, the transport properties in “FluidGas” were assumed to be the same as those for air. Similar assumptions have been made by Gamma Technologies in some of their own specified fuels and it was therefore considered as a reasonable simplification.

The enthalpy in the liquid DME fuel object at 1 bar is calculated according to:

$$h = h_{ref,liq} + a_1(T - T_{ref}) + a_2(T - T_{ref})^2 + a_3(T - T_{ref})^3 \text{ [J/kg]} \quad (4.1)$$

Where T is the actual temperature [K], $T_{ref} = 298$ [K], $h_{ref,liq} = h_{ref,vap} - \Delta h_{vaporization}$ J/kg, $h_{ref,vap}$ is the enthalpy of the vapor fluid object at 1 bar and 298 K [J/kg], $\Delta h_{vaporization}$ is the heat of vaporization at 298 K [J/kg]

If enthalpy data at 1 bar and 298 K is unavailable, then data for constant pressure specific heat, c_p , can be used which is the derivative of enthalpy with respect to temperature. The equation is then:

$$\frac{\partial h}{\partial T} = c_p = a_1 + 2a_2(T - T_{ref}) + 3a_3(T - T_{ref})^2 \text{ [J/kg]} \quad (4.2)$$

4.4 Case 1: Non-predictive combustion model without EGR

The main purpose of case 1 was to calibrate the system so that the temperatures and pressures are coherent with the measured data and thus match the pressure losses and heat transfer losses in the system. To achieve this, a simple combustion model was chosen where the combustion profile was imposed.

4.4.1 Boundary conditions

The inlet boundary condition was defined as a combination of the compressor, dryer and air conditioner to make the model simpler and easier to use since there was no interest in simulating the components separately. Measured data was available for the incoming air including temperature and pressure and the name of the inlet boundary condition is “Compressor”. Relative humidity have been calculated based on an absolute water vapor content of $0.63 \text{ g}_{\text{water}}/\text{kg}_{\text{dry air}}$ and the charge air pressure. The absolute water content is based on the air conditioner cooling temperature of 4°C (Salsing, 2011).

The outlet boundary condition was set after the exhaust pipe with the back-pressure and temperature known from the measured data. The outlet boundary condition is called “ExhaustEnv”.

4.4.2 Modeling of cylinder head ports and valves

Valve ports and valves were modeled using flow data measurements for the valve and port together, which means that they have the same properties. The pressure drop across the two objects were modeled in the valve only and not in the pipe part, meaning no pressure drop calculations in the ports. This is how the valves and ports are recommended to be modeled to get accurate pressure drop and thus avoid defining the pressure drop twice (Gamma Technologies, 2014a).

Special considerations were made for the heat transfer from the valves. To simulate that heat transfer, a higher value of the heat transfer coefficient of the ports was set to compensate for that of the valves. The heat transfer coefficient and the imposed wall temperature of the ports were calibrated to achieve more accurate inlet and outlet temperatures.

The volumes of the ports were collected from a CAD model of the cylinder head according to figure 4.1. Even though the model was for a 13 liter engine and not a 12 liter engine like the one at Chalmers, it should be little or no difference between the two cylinder heads. When specifying the diameter, it is recommended to use the hydraulic diameter of the inlet opening of intake port and the outlet end of the exhaust port.

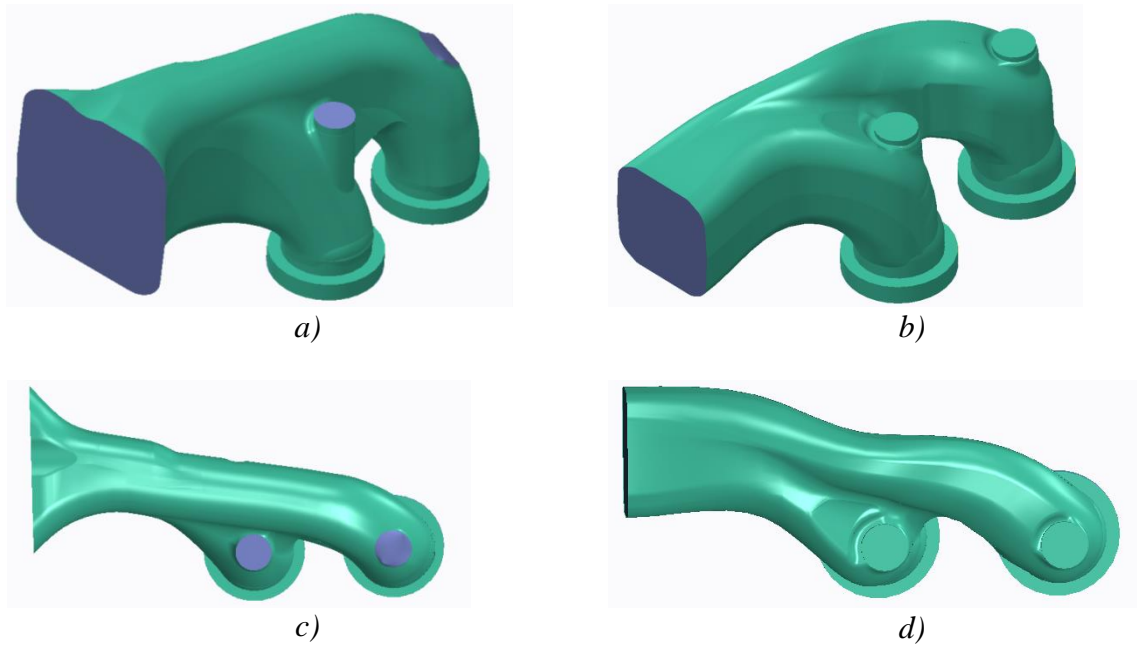


Figure 4.1 Intake and exhaust port volumes. a) Intake, b) Exhaust, c) Intake top view, d) Exhaust top view.

The total volume of the port is important and therefore, the length of the ports was altered to get as accurate volume as possible. Each port is also modeled as a single pipe with one inlet and one outlet, not two outlets as in figure 4.1. This simplifies the modeling procedure and the division of port volumes leading to each valve is avoided, which would otherwise be necessary.

Due to the lack of measured flow data for the 12 liter engine, the valve geometries and discharge coefficients were taken from the 13 liter engine instead. The measured valve lift curves, without valve lash, are presented in figure 4.2.

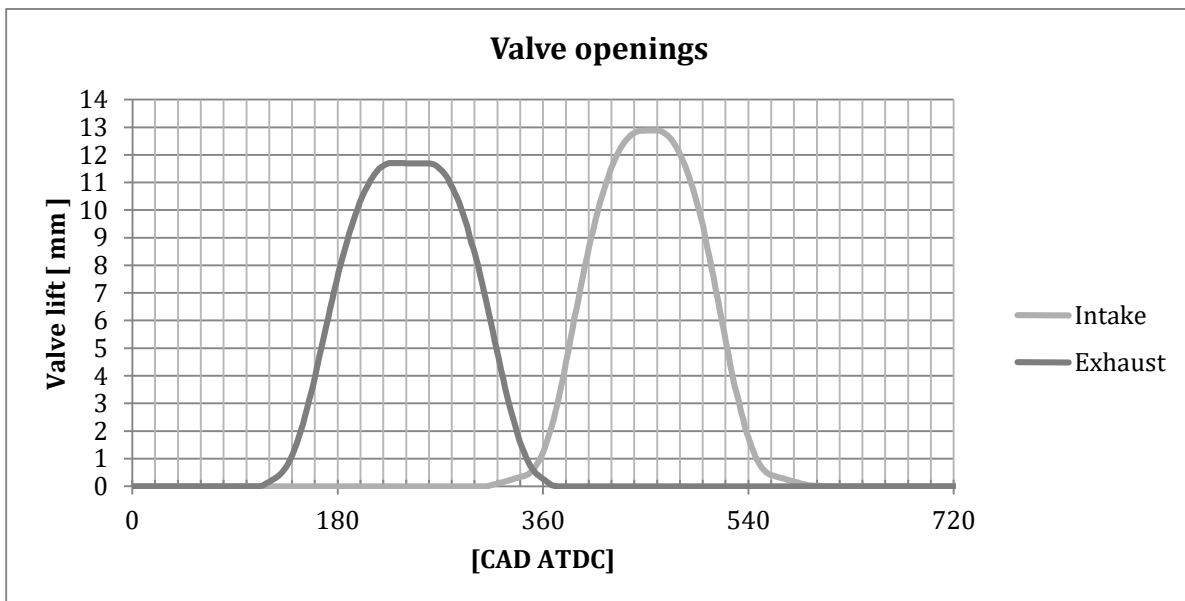


Figure 4.2 Valve openings with no valve lash (Salsing, 2011)

4.4.3 Combustion profile

Calculated apparent heat release rate data based on the measured cylinder pressure was used as input to the non-predictive combustion profile. The model will assume, if nothing else is specified, that 100% of the fuel injected in the cylinder will be burned at the specified imposed combustion rate. When using imposed combustion profiles, one combustion profile for each engine run is necessary and new settings are needed.

The combustion profile used was the imposed combustion profile called "EngCylCombProfile" in GT-Power. This is a general option that allows a directly imposed crank angle resolved burn rate profile, which is the reason why this combustion profile object was chosen. The burn rate can also be calculated directly from the measured cylinder pressure if it is available. However, the apparent rate of heat release was chosen as input throughout this work.

4.4.4 Injection system

The injection system is modeled using a basic injection template called "InjDieselSimpleConn". This simple template requires only the injected mass, fluid temperature, injection timing and injection duration to be specified. This template was chosen since the combustion model used does not need any detailed injection data and is recommended by Gamma Technologies (2014a).

4.4.5 In-cylinder heat transfer

The heat transfer object used in the cylinder, to calculate the in-cylinder convection coefficient, is the Hohenberg model. This correlation has shown to give more accurate heat transfer results for direct injected diesel engines than the similar classical Woschni correlation without swirl, which is why this model has been chosen (Gamma Technologies, 2014a).

The heat transfer model needs cylinder wall, piston and cylinder head temperatures to calculate the heat transfer. Different models to calculate the cylinder wall temperatures were available but most of them needed accurate cooling system data and since this data was not available, a simple model containing three different zones was used. The temperatures for these zones were imposed and the initial values were chosen based on recommendations from Gamma Technologies (2014a).

4.4.6 Cylinder calibration

All the parts that the cylinder consists of need to be calibrated with measured data to make sure that the central part of the model, seen in figure 4.3, is as accurate as possible. This makes it easier to find the source of errors in the model. The model that was calibrated can be seen in figure 4.3. A "bellmouth" was added to make sure that no pressure losses occurred between the environment parts and the ports.

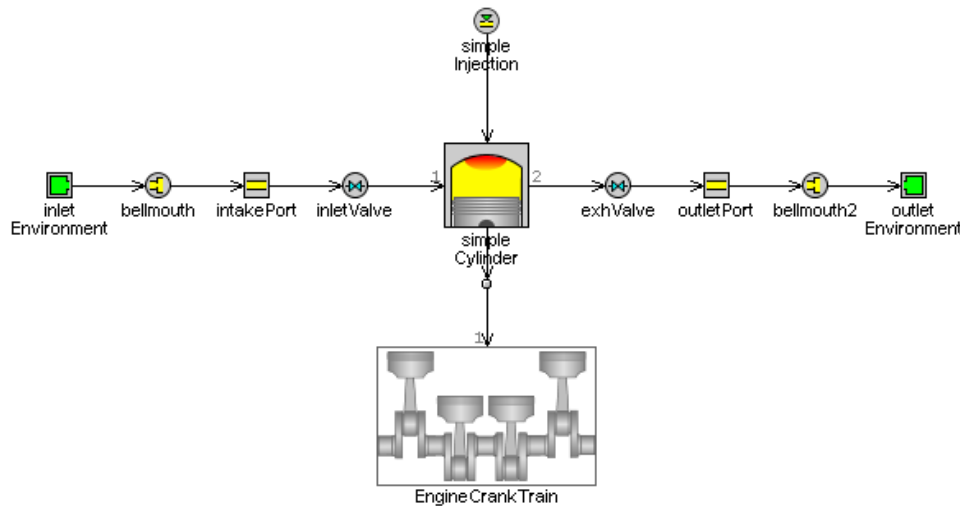


Figure 4.3 Calibration model of single-cylinder engine

4.4.7 Inlet tank modeling

The inlet tank was first modeled as a single pipe volume with length and diameter corresponding to the total volume of the tank. The inlet tank was also modeled with multiple pipes together with a flowsplit on each side to investigate how the number of pipes affects the gas exchange and the pressure of the fast pressure sensor “P_int_K”. This corresponds to a more realistic approach since the real tank consists of a bundle of pipes. The layouts for the two different inlet tanks are shown in figure 4.4 and figure 4.5 and the fast pressure sensor “P_int_K” is further described in section 3.1.

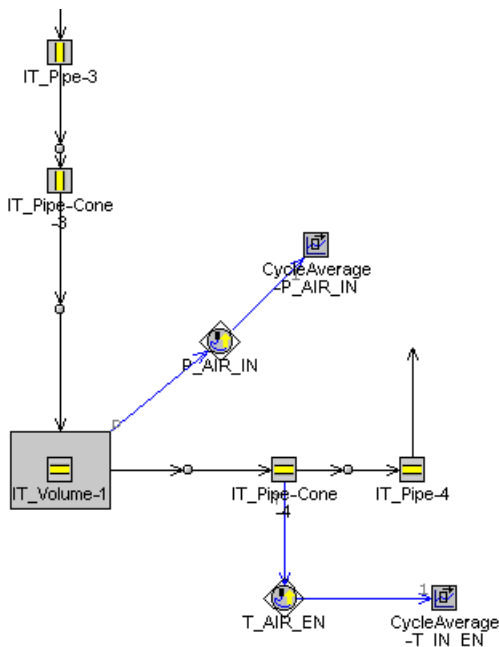


Figure 4.4 Inlet tank as single volume

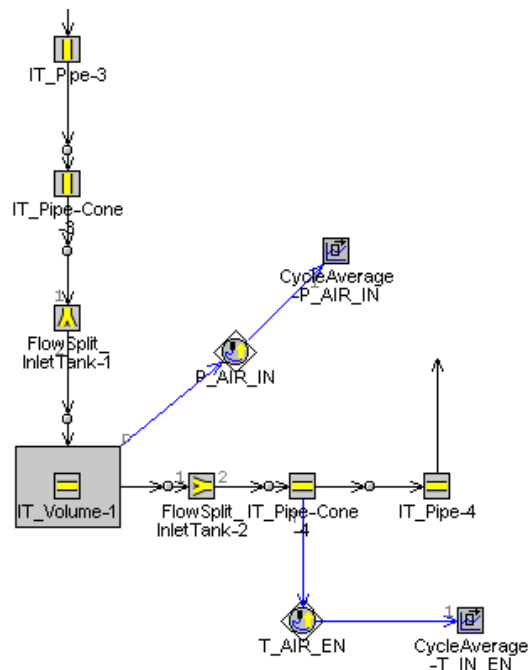


Figure 4.5 Inlet tank as multiple pipes

Four cases were simulated during two different simulations. One simulation with 100, 2500, 5000 and 10000 pipes and the other with 1, 10, 100 and 1000 pipes. The volume of the

flowsplits were adjusted correspondingly to achieve the correct total volume of 70 liters. The pipes had all an inner diameter of 3 mm. The results can be seen in section 5.1.2.

4.4.8 Pressure calibration

Due to the fact that the pressure in the system is pulsating, which means not constant/static, they need to be calibrated so that they are in phase with measured data from the “P_int_K” pressure sensor. This is even more important when the intake valves are opening since it can have a severe effect on the volumetric efficiency.

To calibrate the pressure curve, two things were changed in the model:

1. Volume of the intake system
 - By changing diameter of inlet tank
 - By changing the length of intake runner
2. Adjusting intake valve lash

Changing the volume in these two ways affects the pressure curve differently; through changing the length, the phase of the pulsations can be altered and through changing the diameter of the tank, the overall amplitude of the curve will change. Modifications of the valve lash will affect a section of the P_int_K pressure profile around the inlet valve opening more than other sections of the pressure curve. Measured pressure and valve opening and closing can be seen in figure 4.6.

It is important that the model is more accurate between IVO and IVC since this is the only condition affecting the gas exchange from the intake side of the system.

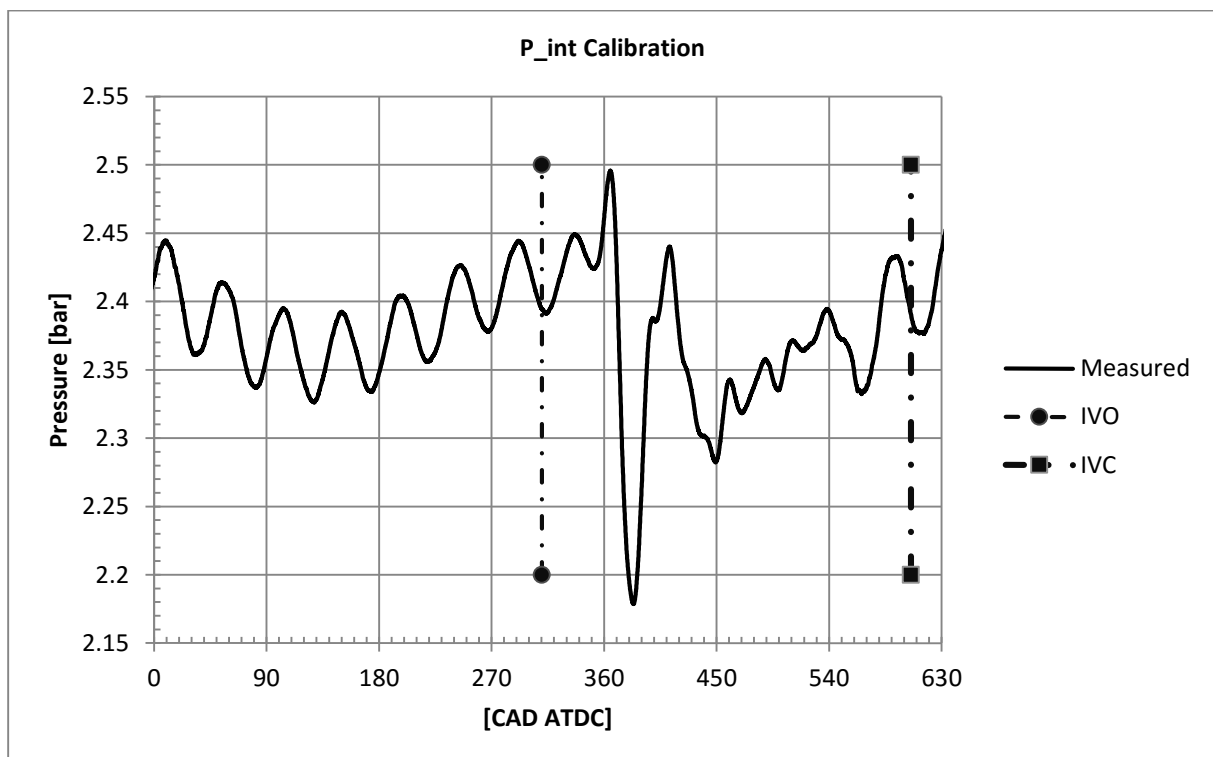


Figure 4.6 Measured pressure from P_int_K sensor

4.5 Case 2: Predictive combustion model without EGR

The changes made from case 1 will be presented in this chapter. Case 2 includes a predictive combustion model without EGR. The only components changed are the fuel injection component and the cylinder, which contains other objects and parameters.

The injection profile template used in case 2 is “InjProfileConn”, which uses single pulse injection with an imposed crank angle resolved mass flow rate profile. This template was chosen because it is commonly used for direct injection engines in GT-Power (Gamma Technologies, 2014a).

The predictive combustion model used is DIPulse because it is the most suitable combustion model for compression ignition engines. Even though it is developed for diesel fuel specifically, it can also run using other fuels. The predictive model was calibrated through setting up a calibration model, which means using the “measured+predicted” cylinder pressure analysis mode, which can be set in the cylinder object. The calibration model consisted of three components based on the following templates:

1. InjProfileConn
2. EngCylinder
3. EngineCrankTrain

The reason for using a simpler calibration model is because it reduces the simulation time significantly and provides the possibility to compare forward and reversed run results, like apparent and predicted heat release. More about forward and reversed run can be read in section 2.6.1. The calibration model uses imposed initial states and exhaust emissions based on measured data instead of simulating the whole gas exchange process, which enabled calibration of the combustion model when run both with and without EGR. A more detailed explanation of the objects and parameters specified in the calibration model can be found in appendix A - 2.

4.5.1 Definition of injection events

DIPulse requires specification of start of injection (SOI), which was achieved from measured data at the first distinctive minimum in the injection line pressure curve. End of injection (EOI) was also specified as the maximum value in the injection line pressure curve to enable calculation of the injection duration. Figure 4.7 shows an example of how SOI and EOI were specified.

Start of combustion was specified through using the apparent heat release rates, that had already been calculated using a software called OSIRIS, at the first positive value of the heat release according to the example in figure 4.8.

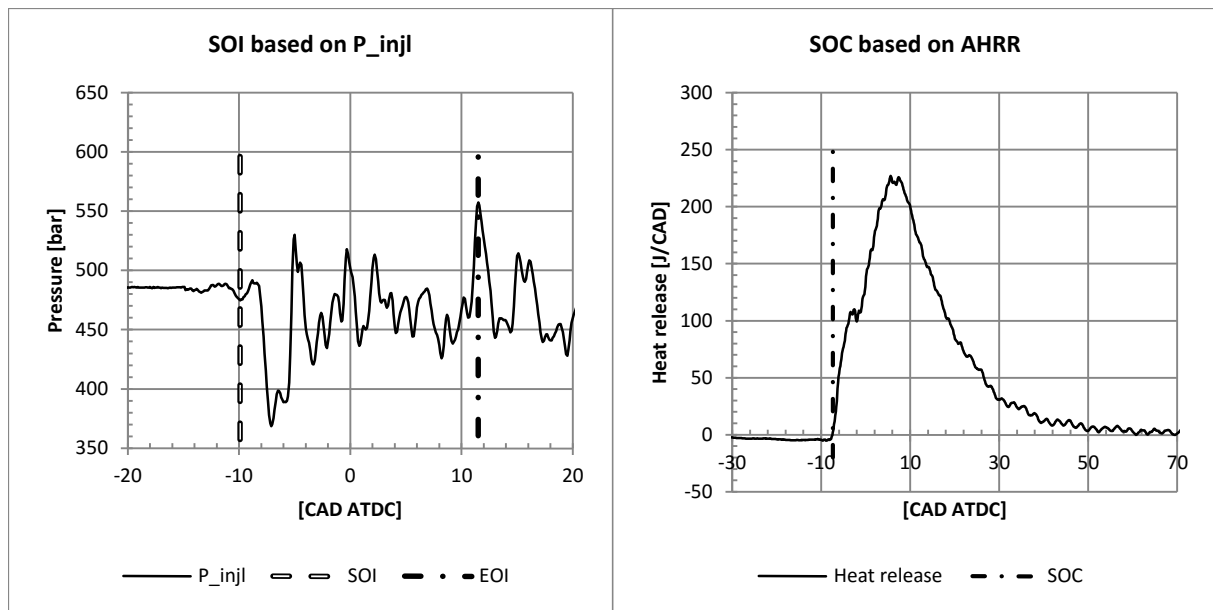


Figure 4.7 Start of injection and end of injection based on pressure from injection line (P_{injl})

Figure 4.8 Start of combustion based on apparent heat release rate

4.5.2 Adjustment of fuel injection rate curves

Injection rate profiles used by the predictive combustion model DIPulse have been, prior to this report, simulated by Volvo using AMESim software. Two simulated injection rates for DME were available with different EGR rates. During this work it was not possible to simulate new injection profiles and therefore, the existing profiles were modified to fit the measured data's load points, EGR rates and rail pressures.

To achieve the right amount of fuel injected from the initial simulated injection rates, the area of the injection curves was either enlarged or reduced. This was done through a MATLAB program by either removing a section or by enlarging an area at a plateau in the profile. The profile in figure 4.9 has been enlarged by increasing the later part of the curve and thus avoiding adjustments at the first 25 CAD of the curve.

In the simulated injection profile data there were a lot of scrap data that needed to be processed such as:

- Doublets (same data point appeared twice)
- Negative injection rates
- Sharp edges (two or more different injection rates at same CAD)

The simulated curve in figure 4.9 has been adjusted according to the procedure described above. Doublets and negative injection rates were removed to obtain a more realistic profile. Sharp edges, where two or more injection rate data points have the same CAD, were removed and replaced by one point consisting of the average value of the removed points.

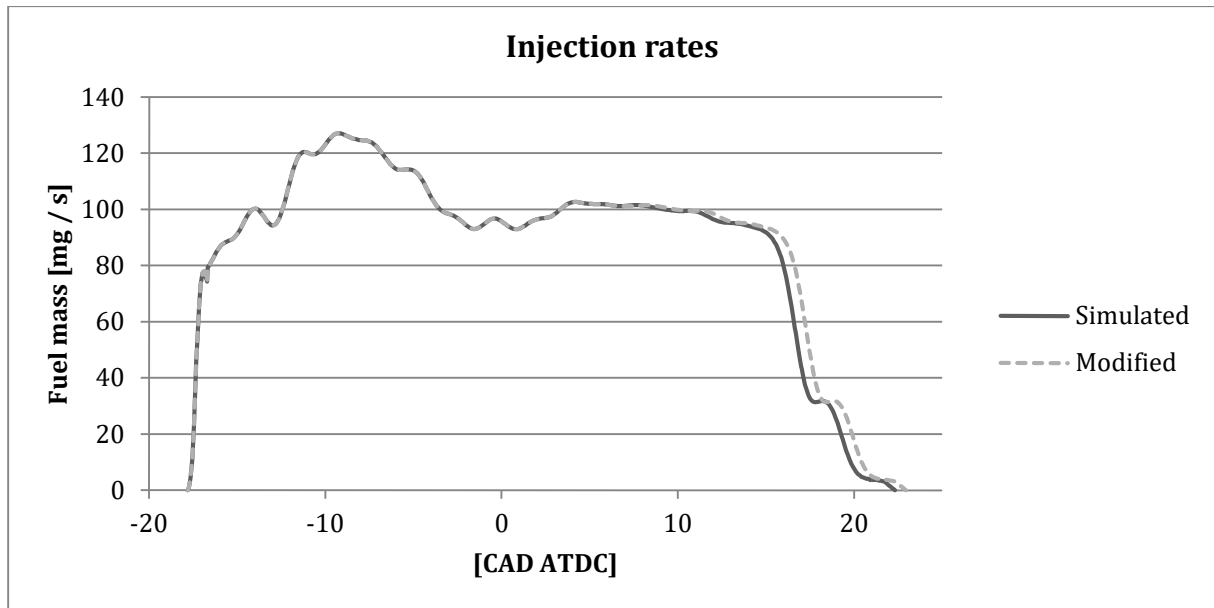


Figure 4.9 Simulated and modified injection rate profile

Due to the fact that DIPulse is sensitive to the injection rates used in the model and that the simulated injection rates used in this work were not verified with measured data, it is of interest to see how the heat release and cylinder pressure curve react to changes of the injection rate. This was done through implying small to major changes in the beginning of the injection rate profile and at the same time keep the total amount of fuel injected constant.

The injection rate profiles' injection duration has not been adjusted to correlate with that of measured data. They have only been adapted to achieve the right amount of injected mass per cycle. The difference between the simulated and measured injection duration varies between 1.5 % to 12.9 % for the diesel piston and -10.9 % and 3.6 % for the DME piston as seen in table 9.6 in appendix A - 6.

4.5.3 Calibration of DIPulse

DIPulse uses multipliers, described in section 2.6.6, to calibrate and optimize the combustion process. But before the optimization could be initiated, a DOE analysis in GT-Power was made to achieve data sets of combinations for the multipliers. The recommended limits for the multipliers were achieved from Gamma Technologies (2015) according to table 4.2.

However, the maximum value for the ignition delay was increased from 1.7 to 2.0 because the maximum limit was reached during the simulations.

Table 4.2 Recommended values for DIPulse multipliers for diesel combustion (Gamma Technologies, 2015)

Multiplier	Min	Max
Entrainment Rate	0.95	2.8
Ignition Delay	0.3	1.7 ⁶
Premixed Combustion Rate	0.05	2.5
Diffusion Combustion Rate	0.4	1.4

⁶ The value of this upper limit was changed to 2.0 to better suit optimizations for DME

The DOE analyses were run with and without EGR for B50 and C100 separately and each of them with the diesel and DME piston respectively. As a first attempt, the values seen in table 4.3 were used as initial values for the DOE analyses based on measured data and recommendations from Gamma Technology.

Table 4.3 Initial values for the calibration model

Parameter	Initial Value	Unit
Air Trapping Ratio	1	[-]
Residual Fraction	3%+EGR%	[mass %]
Convection Multiplier	1.2	[-]
Crank-Slider System Stiffness (Compression)	Ign (stiff)	[kN/mm]
Compression Ratio	15.1	[-]
Nozzle Hole Diameter	0.327	mm
Nozzle Discharge Coefficient	0.85	[-]
SOI, B50	-10	[CAD ATDC]
SOI, C100	-15	[CAD ATDC]

After the DOE analyses had been run, a spreadsheet developed by Gamma Technologies was used to optimize the multipliers automatically. The effect of changing the multipliers was thereafter tested to see if the model could be improved by manually adjusting the multipliers. It was done through changing the multipliers one at a time with appropriate step lengths depending on the range they were tested for and the initial value achieved from the optimization results.

Besides the DIPulse multipliers, there are other parameters that affects the combustion process that are also of interest. The convection multiplier affects the in-cylinder heat transfer, the crank-slider system compression stiffness controls the elasticity in the mechanical components, the compression ratio affects the pressure in the cylinder and the nozzle discharge coefficient affects the injection pressure and thus the mass flow rate of the injected fuel. These parameters can be seen in table 4.4 and have values and ranges based on recommendations from Gamma Technologies.

Table 4.4 Ranges for calibration parameters given by Gamma Technologies

Parameter	Simulated Value Range	Unit
Convection Multiplier	0.85-1.6	[-]
Crank-Slider System Stiffness (Compression)	100-1000 or ign (totally stiff)	[kN/mm]
Compression Ratio	14.1-15.1	[-]
Nozzle Discharge Coefficient	0.6-0.85	[-]

The parameters used for calibrating the model that did not have recommended values or ranges are presented in table 4.5, whose test range was a question of judgment related to the initial test results.

Table 4.5 Other calibration parameters

Parameter	Simulated Value Range	Unit
Compression Ratio	14.1 to 15.1	[-]
SOI, B50	-10 to -12	[CAD ATDC]
SOI, C100	-15 to -17	[CAD ATDC]

4.5.4 Enthalpy in liquid fuel

The results from the calibration model contained an initial heat release that is not a physical phenomenon occurring in reality. Therefore, the enthalpy in the liquid fuel object was modified as a test to investigate how changes of the enthalpy affect the rate of heat release. This was made through changing the constants a_1 , a_2 and a_3 that are used to calculate the enthalpy according to equation (4.1) and (4.2) in section 4.3. The result of this can be seen in section 5.2.7.

4.6 Case 3: Imposed combustion profile with EGR

This model is similar to case 1 through using the same imposed combustion profile but the EGR circuit is added that was not present in case 1. The purpose is to calibrate the EGR circuit before combining it with the predictive combustion model, which was done in case 4. Unspecified changes remain the same as in case 1.

4.6.1 Heat transfer from cylinder ports

As mentioned in section 4.4.2, case 1 used imposed wall temperature and that is also the recommended procedure by Gamma Technologies. However, when calibrating the EGR circuit, better result was obtained when the wall temperature was calculated rather than imposed and therefore calculated wall temperature is hereafter used.

4.6.2 EGR cooler

The EGR cooler is modeled as semi-predictive, meaning that the cooler's effectiveness as a function of exhaust mass flow at a specific cooling media temperature is specified. This gives the cooler a reasonable accuracy when changing the amount of EGR used at different engine speeds. The effectiveness of the cooler is then multiplied with a calibration factor so that the simulated performance becomes equal to the measured. A part of the GT-Power model showing the EGR cooler circuit can be seen in figure 4.10.

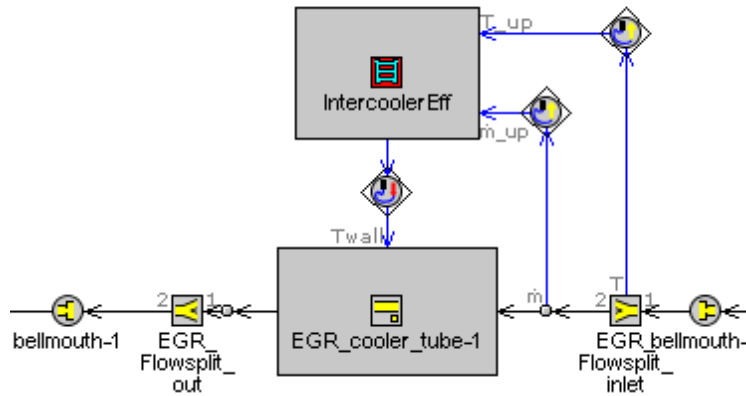


Figure 4.10 EGR cooler model

4.6.3 EGR valve

Since the EGR valve is set to a specific level/position and not changed, the valve was calibrated to achieve the desired amount of EGR at a specific pressure difference over the EGR circuit. The valve is modeled as a single “orifice” and calibrated through changing orifice diameter.

4.6.4 Back pressure

The back pressure is set at the end environment. This is not the most correct way compared to the setup in reality but it avoids using a PID controller and reduces the simulation time significantly. No changes in the result was observed when comparing these two methods, which motivates the use of the simpler method.

4.6.5 Extra inlet tank

When running the model with EGR, it was discovered that burned gases escaped through the inlet environment called “Compressor”. This is due to fluctuations of mass flow in pipes and that the placement of the inlet environment was too close to the outlet and the mixing point of the EGR circuit. Since the composition is imposed in the inlet environment, it turned out that when burned gases escaped through the inlet environment during back flow, fresh air was inducted when the flow turned and went back in again. This resulted in a very low CO₂ concentration at the inlet side and made it difficult to calibrate the model and achieve results agreeing with the measured data.

To solve this problem, a tank/pipe (named buffer Tank) was placed between the mixing point of EGR and the inlet environment in the model, as can be seen in figure 4.11. This tank is supposed to act as a buffer to be able to handle the back flow during the engine cycle to avoid burned gases escaping through the inlet environment. To avoid that the tank affects other data like pressure and temperature, the tank was modeled frictionless and adiabatic. A so called “bellmouth” was also added both before and after the tank to avoid pressure drop between the tank boundaries.

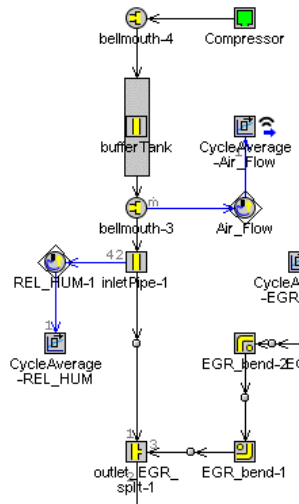


Figure 4.11 Schematics of the placement of the "bufferTank" to avoid burned gases escaping.

4.6.6 Calibration

Calibration of the EGR circuit was done through setting up DOE experiments and varying the factors mentioned below:

- Inlet gas tank heat transfer multiplier
- Cylinder temperature multiplier
- Exhaust valve lash
- Exhaust gas tank heat transfer multiplier
- EGR valve orifice diameter

The cylinder temperature multiplier is a multiplier that affects piston, cylinder wall and cylinder head temperature. The reason for varying a multiplier instead of each temperature individually is that all these temperatures showed the same behavior/response when doing a quick screening test of factors. When reducing the amount of experiments needed, these three factors were combined into one and represented as a multiplier. The original temperatures for the combustion chamber are listed in table 4.6 and are assumed values but kept within reasonable limits when compared to measured temperatures when running on diesel fuel.

Table 4.6 Original assumed combustion chamber temperatures before calibration.

Piston	600 K
Cylinder wall	400 K
Cylinder head	600 K

These factors have more or less effect on different responses but the primary target was to achieve good results for the CO₂ concentrations and the factor EGR valve orifice diameter that has major impact on this. To acquire as correct mass flows, and consequently trapped mass in the cylinder, as possible, the temperatures in the system need to be accurate. The reason is that a too high temperature at the inlet side of the system results in lower density of the gas and thus lower mass flow. An example of how a response is affected by different factors can be seen in figure 4.12. It can be seen that the EGR valve orifice diameter has a major effect but that cylinder temperature also has a noteworthy effect on the CO₂

concentration. It should also be stated that the figure only shows linear relationships between minimum and maximum values of a factor.

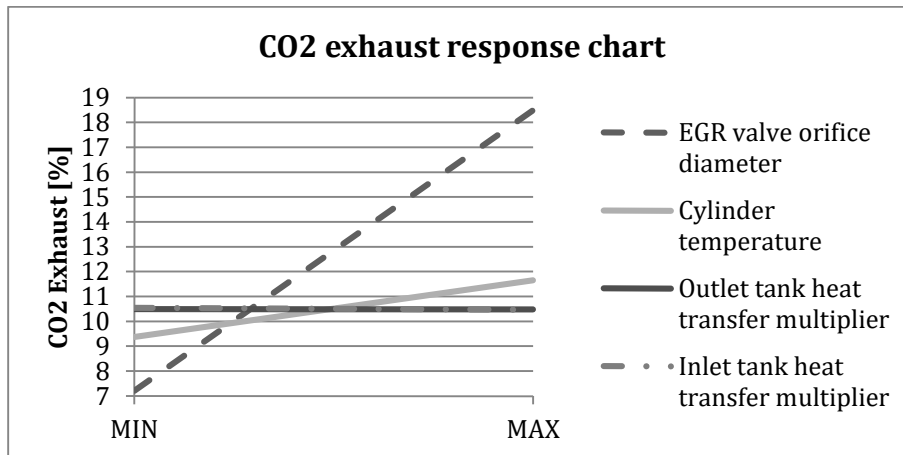


Figure 4.12 The main effects factors have on CO₂ concentration at the exhaust.

Two different load step numbers from one BNR were used to be optimized towards, BNR306#237 (B50) and BNR306#241 (C100). It would have been beneficial to have more load points to calibrate towards but since these two together consisted of about 1200 experiments and took more than 72 hours to simulate, a decision to calibrate towards these two load points only was taken.

4.7 Case 4: Predictive combustion model with EGR

In case four, case two and three were put together into a predictive model with EGR, which is the final and most complex model in this work. No major calibration was made for case four due to the earlier calibrations made for the previous cases.

4.7.1 Model validation

The combustion model used in case two is independently optimized for load points B50 and C100 according to section 4.5. This provides better accuracy for these two load points but makes the model unable to handle any transient or intermediate load points. If simulations at new load points are desired, they have to be calibrated with new multipliers for the DIPulse combustion model before they are added to the model.

To handle the effect of an arbitrary amount of EGR, while keeping break torque constant, the model was adapted to handle almost any amount of injected fuel. This was done through adding new modified injection rate profiles to cover various injected fuel amounts and thus amounts of EGR. The limits were chosen as the minimum to maximum injected mass of BNR306 for B50 and C100 respectively with 5 mg injected fuel step between each new injection rate profile. GT-Power will interpolate linearly between the intervals to find a profile that matches the requested input value.

4.7.2 Final model check

Since there is a delayed start of combustion, proven in the result section 5.4.2, additional simulations were done to see if one could compensate this with an advanced SOI. To study this and other effects, SOI was retarded 2 CAD and advanced 2 CAD and the result can be seen in section 5.4.3.

One main purpose with the model is to be able to handle different amounts of EGR. Therefore, it is of interest to see how the model responds when changing the EGR and how the results are affected by the change. Since the amount of EGR is not directly controlled but instead indirectly through setting the back pressure in relation to the charge pressure. This pressure difference, created by these two pressures, controls the amount of EGR. Charge pressure is set to 2400 mbar and 3000 mbar for B50 and C100 respectively. The back pressure is then stepwise increased with 50 mbar beginning at charge pressure and ending at an increment of 400 mbar for each load point. All other parameters are kept constant, including injected fuel mass.

5 Results

This chapter will present the results achieved during this work. It presents the results obtained for all four cases and including values for the different parameters used when calibrating the model.

5.1 Case 1: Without EGR and imposed combustion rate

In this case, no EGR was applied to the system and the combustion profile was imposed. The purpose with the case was to calibrate pressures and therefore, the results from pressure calibration in the system is presented. This includes matching the simulated and measured cylinder pressure and the fast inlet pressure sensor “P_int_K”.

5.1.1 Cylinder pressure calibration

In the cylinder pressure diagram, shown in figure 5.1, it is seen that during the compression stroke, the simulated pressure is a bit higher than the measured pressure up to about -10 CAD where fuel injection starts. After the fuel injection, the simulated pressure is instead lower than measured pressure. After peak pressure, the simulated cylinder pressure deviation from measured pressure is small.

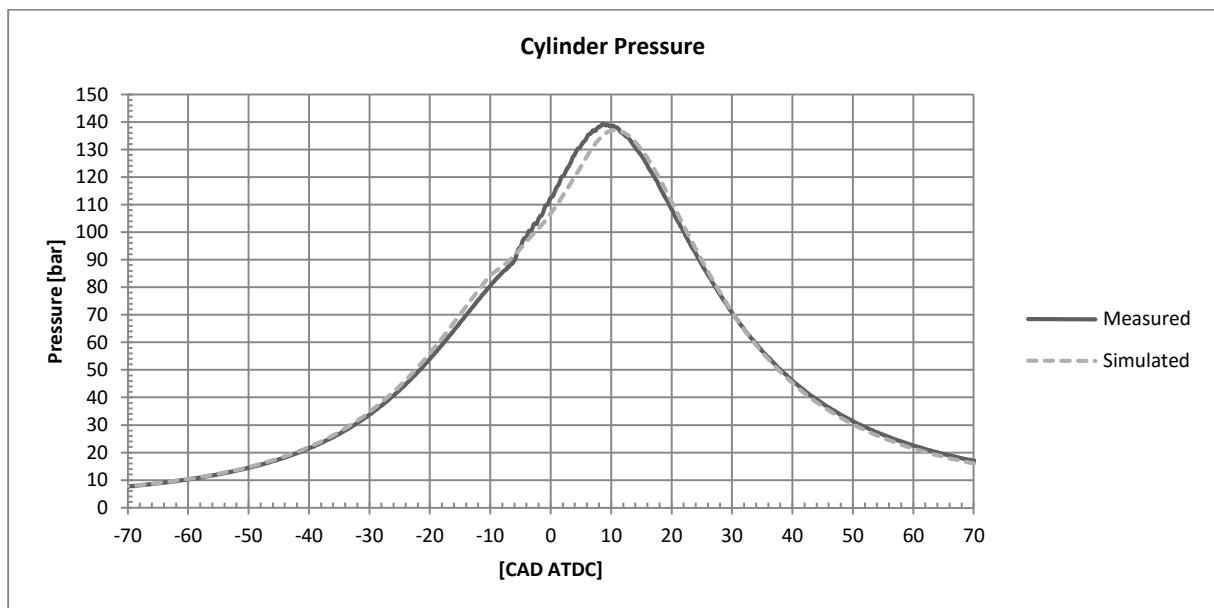


Figure 5.1 Cylinder pressure curve B50 without EGR (BNR306#250)

5.1.2 System pressure calibration

This section presents the results from the calibration of the fast pressure sensor “P_int_K”. The calibration procedure can be read in section 4.4.6 and 4.4.8.

The inlet gas tank was modeled both as a single volume and as multiple pipes with the aim to investigate how the pressure curves for the incoming flow changes with number of pipes and if the pulsations could agree better with the measured data.

The results, seen in figure 5.2, show that the pressure increases when number of pipes are increased. Although, a significant pressure drop during the intake stroke occurs when multiple pipes are used. Figure 5.2 only shows up to 1000 pipes but a case with 10 000 pipes was also simulated though no noteworthy difference was seen in the simulation compared to using 1000 pipes. However, the inlet tank was decided to be modeled as a single volume instead of multiple pipes due the effects on the pressure shown in figure 5.2.

The effect on the pressure measured with sensor “P_int_K” when modeling the inlet tank as a single volume is seen in figure 5.3. It can be seen that “Simulated original” and “Measured” are better correlated even without any calibration compared to when the tank is modeled as multiple pipes.

When changing parameters according to section 4.4.8, a better consistency between measured and simulated pressure was obtained, which is also shown in figure 5.3. The main focus during the calibration was to achieve good accuracy between IVO and IVC, where the pressure affects the inducted mass to the cylinder the most.

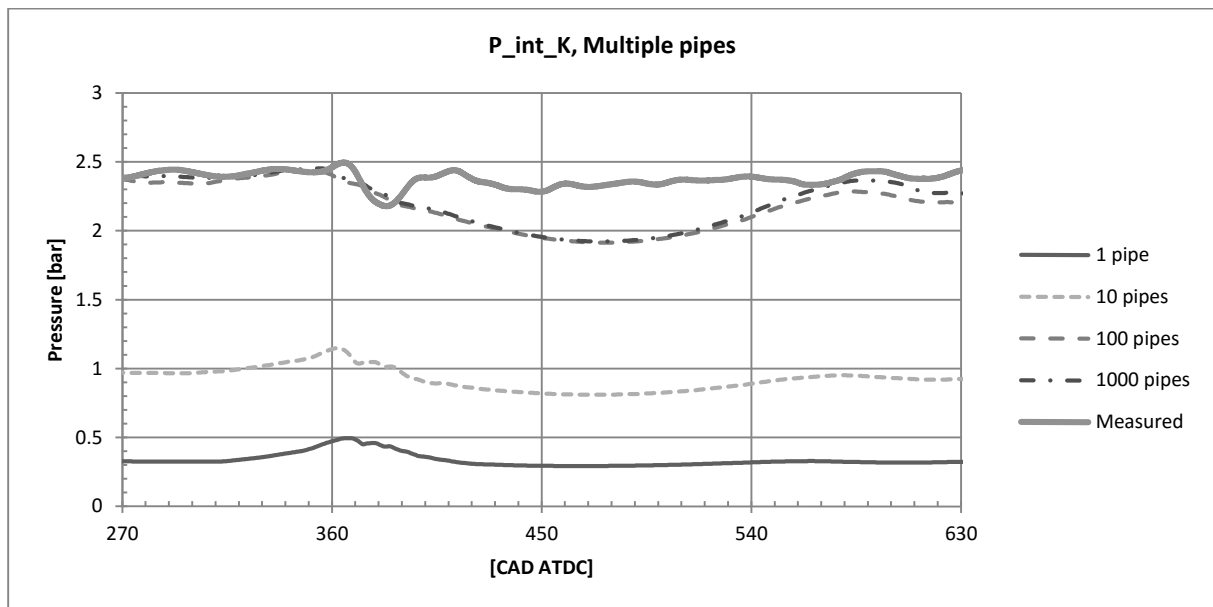


Figure 5.2 Changes in pressure in P_int_K sensor, 1 to 1000 pipes (BNR306#250)

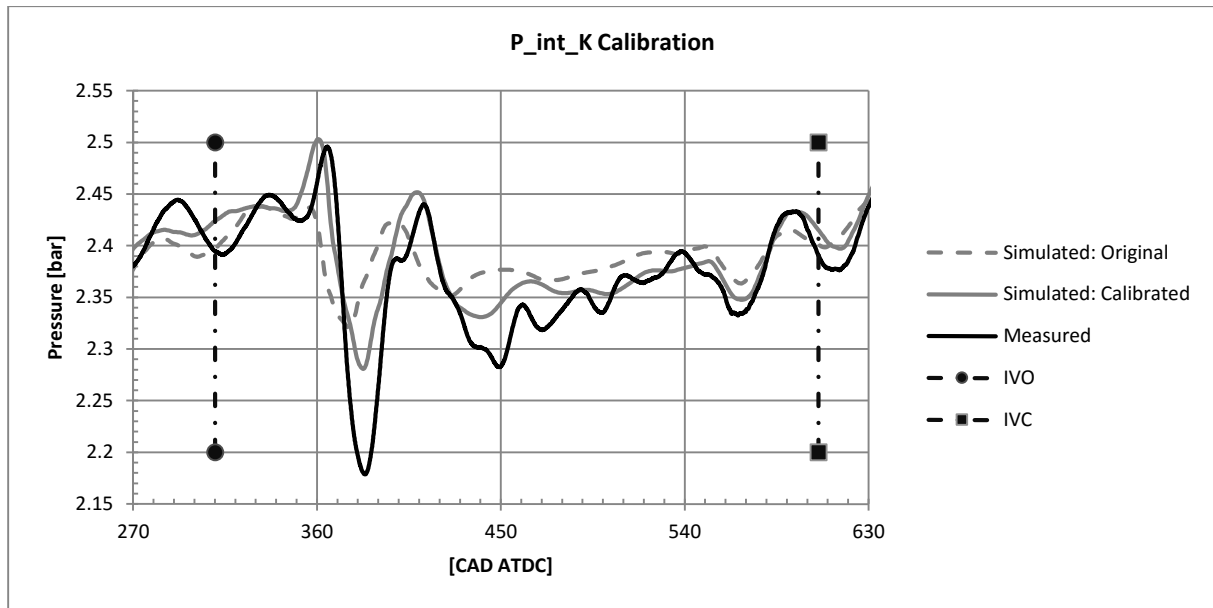


Figure 5.3 Before and after calibration of P_{int_K} sensor pressure compared with measured data (BNR305#250)

5.2 Case 2: Predictive combustion without EGR

This section presents the results and effects achieved when varying different parameters in the calibration model. The results have mainly been analyzed through comparing the predicted rate of heat release curve with the apparent rate of heat release curve and the predicted cylinder pressure with the measured cylinder pressure.

5.2.1 DIPulse multipliers

Starting from the optimized DIPulse multipliers listed in table 5.2, one B50 case (BNR306#236) using the diesel piston was chosen to investigate the effect of the multipliers one at a time according to figure 5.4. More detailed figures are available for both B50 and C100 and can be seen in figure 9.6 to figure 9.13 in appendix A - 4.

Varying the entrainment multiplier affects the entire combustion process. When the premixed combustion spike increases, the diffusion combustion rate decreases correspondingly in amplitude, since the amount of fuel injected is constant for all cases. Decreasing the entrainment rate also reduces the slope of the premixed combustion.

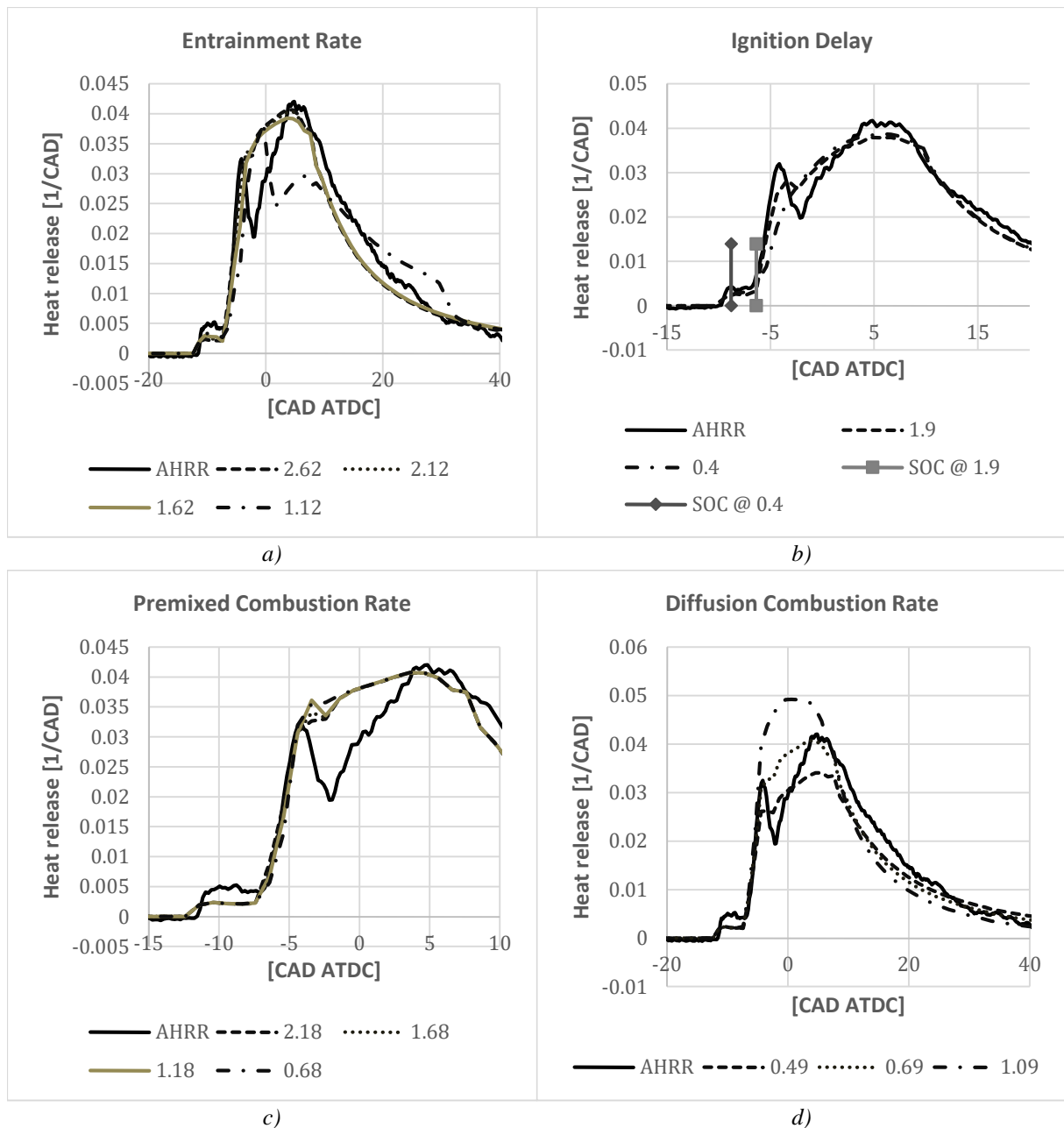


Figure 5.4 Effect of varying combustion multipliers on normalized heat release for B50. AHRR is the apparent heat release rate calculated from measured cylinder pressure. a) Entrainment rate, b) Ignition delay, c) Premixed combustion rate, d) Diffusion combustion rate

The ignition delay multiplier adjusts the start of combustion and the initial rate of heat release. A longer ignition delay causes a more pronounced premixed combustion and a steeper slope. The effect on the ignition delay when lowering the ignition delay multiplier can be seen in table 5.1. Lowering the ignition delay multiplier results in an ignition delay closer to that of measured data but reduces the heat released in the premixed combustion as seen in figure 5.4.

Table 5.1 Ignition delay multiplier's effect on corresponding ignition delay for B50 (BNR306#236)

Ignition Delay Multiplier	Ignition Delay [CAD]
1.9	3.52
1.4	2.78
Measured data	2.50

The premixed combustion rate multiplier on the other hand only affects the premixed combustion peak's amplitude and slightly the slope of the premixed combustion. It can thus be seen in the figure that the multiplier is having effect only during the premixed combustion phase without consequently affecting the diffusion rate combustion.

The diffusion combustion rate multiplier acts on both the diffusion combustion phase and the premixed combustion phase. There is a relationship between the premixed and the diffusion combustion rate's amplitude, which means that increasing the diffusion combustion rate also results in increasing the premixed combustion rate as seen in figure 5.4. However, at the highest value of the multiplier, no distinction can be seen between the premixed combustion and the diffusion combustion. A more rapid diffusion combustion rate results in a quicker decline of the late combustion.

The values of the multipliers obtained after the optimization using the DIPulse calibration Excel sheet is seen in table 5.2 and table 5.3. The tables are divided according to the two different pistons used in the model, the diesel and DME piston. The multipliers differ between the two load points B50 and C100 and also within B50 with and without EGR.

Table 5.2 Optimized values for DIPulse multipliers using the $\phi 92$ diesel piston

DIPulse Multipliers:	B50 no EGR	B50 EGR	C100 EGR
Entrainment Rate	2.800	2.618	2.800
Ignition Delay	1.428	1.895	1.812
Premixed Combustion Rate	2.176	2.181	2.069
Diffusion Combustion Rate	0.550	0.690	0.714

Table 5.3 Optimized values for DIPulse multipliers using the $\phi 88$ -REC DME piston

DIPulse Multipliers:	B50 EGR	C100 EGR
Entrainment Rate	2.554	2.275
Ignition Delay	1.954	1.700
Premixed Combustion Rate	2.297	2.155
Diffusion Combustion Rate	0.697	0.779

5.2.2 Pressure adjustments during the compression stroke

Calibration of pressure during the compression stroke of the cycle can be done through either adjusting the compression ratio or adjusting the compression stiffness in the system. Two different load points were used for this analysis, B50 (BNR306#236) and C100 (BNR306#240). A summary of different graphs showing the effect of varying the compression ratio and the compression stiffness can be seen in figure 5.5. The legend entry in

the figure is organized according to {Load point, Compression ratio [-], Compression stiffness [N/mm]} where “ign” in compression stiffness is equal to an infinite stiff system. A summary of the combination between the compression stiffness and the compression ratio can be seen in table 5.4.

Changing the stiffness and the compression ratio affects the calculated pressure in different ways. Both the low compression combination and the low stiffness combination, listed in table 5.4, give approximately the same deviation when comparing with the measured cylinder pressure during the compression stroke, as can be seen in figure 5.5 c) and d). However, both still give better resemblance top measured cylinder pressure than the theoretical value listed in table 5.4.

Table 5.4 Combinations of compression ratio and compression stiffness

	Compression ratio [-]	Compression stiffness [N/mm]
Theoretical	15.1	ign (infinite)
Low compression	14.6	ign (infinite)
Low stiffness	15.1	200'000

The low stiffness combination have more effect on the cylinder pressure when pressure increases, as seen in figure 5.5 a) and b). Even though both have an accurate cylinder compression pressure, the low stiffness combination gives lowest peak pressure of all combinations. This effect is even more noticeable for C100 where the measured cylinder pressure overall is much higher.

In figure 5.5 e) and f), the AHRR calculated from measured cylinder pressure can be seen for B50 and C100 respectively. The curves show only a period before and after start of combustion and how the heat release is affected by changes in compression ratio and stiffness. It can be seen that the theoretical values result in a too high cylinder pressure, which is seen as a negative heat release. On the other hand, the low stiffness combination results in too low pressure and is instead compensated with a positive heat release rate despite that it occurs before the start of combustion. The best match is the low compression combination that is neutral until start of combustion. In addition, this combination had good accuracy with the compression pressure and peak pressure. Hence, this combination was therefore chosen to continue with further in the modeling process.

Keep in mind that the results shown in figure 5.5 presents the combustion model that has been optimized for a compression ratio of 15.1 with a stiffness set to “ign”. Additional simulations with three different compression ratios were done with the combustion model that had been optimized for a compression ratio of 14.6, which can be seen in appendix B - 1. However, the results from these simulations do not change the conclusion of compression ratio chosen.

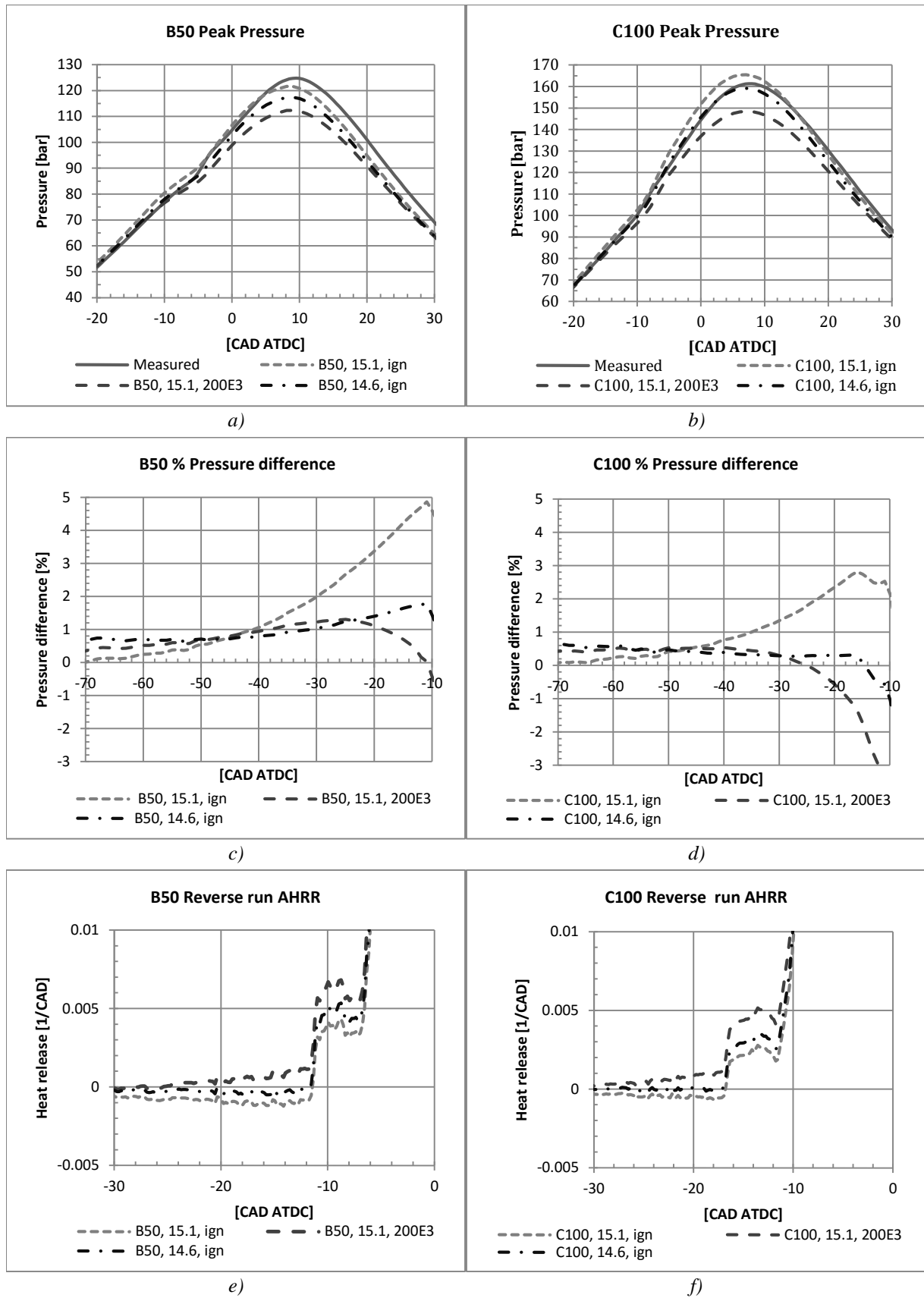


Figure 5.5: a) & b) are cylinder pressure, c) & d) are a close-up of percentage difference in pressure during compression, e) & f) are a close-up of AHRR at SOC. Combustion model optimized for compression ratio 15.1. SOI for B50 and C100 is -9.9 and -15 CAD ATDC respectively.

5.2.3 Nozzle hole diameter and discharge coefficient

The nozzle hole diameter and the discharge coefficient can be used as calibration parameters in the model. They affect the velocity of the injected fuel, if the fuel mass rate is kept constant, and thus changes the premixed combustion rate and consequently the diffusion combustion rate. This effect is illustrated in figure 5.6 where both the nozzle discharge coefficient and the nozzle hole diameter is lowered simultaneously and it can be seen that a better result is achieved.

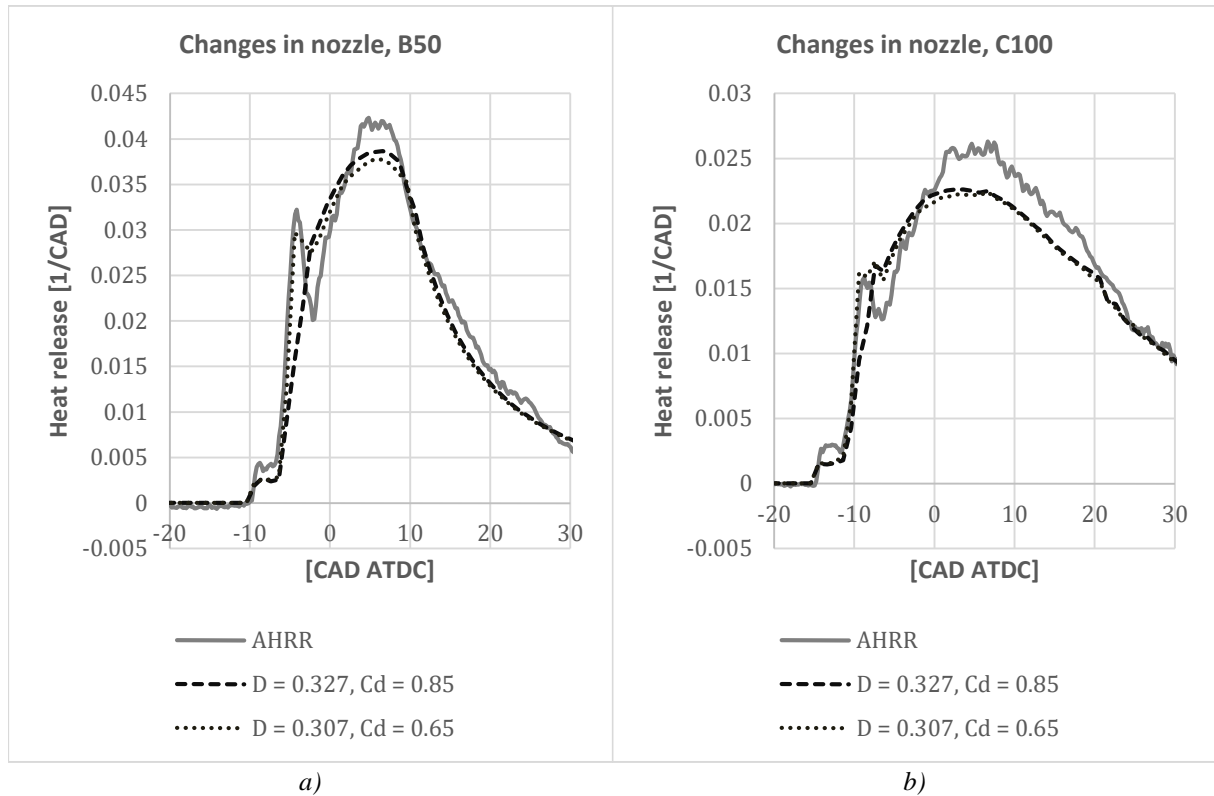


Figure 5.6 Changes in nozzle parameters for a) B50, BNR306#236 and b) C100, BNR306#240. D is nozzle diameter in mm, C_d is the discharge coefficient.

5.2.4 Convection multiplier

The convection multiplier is used to make adjustments in the convective heat transfer in the cylinder. The effect of changing the convection multiplier on the RoHR is small and therefore not presented but it has some effect on the pressure. More information about the convective in-cylinder heat transfer can be read in section 2.6.2.

In figure 5.7 a) and b), that show the relative difference between the predicted and measured cylinder pressure, it can be seen that the difference increases during the power/expansion stroke for B50, around 60 to 70 CAD ATDC. However, when looking at the absolute difference instead, that can be seen in figure 5.8, the largest difference occurs around 10 to 30 CAD ATDC for both B50 and C100, which is where the maximum cylinder pressure occurs. It can also be seen that the convection multiplier has the largest effect on the power/expansion stroke rather than the compression stroke.

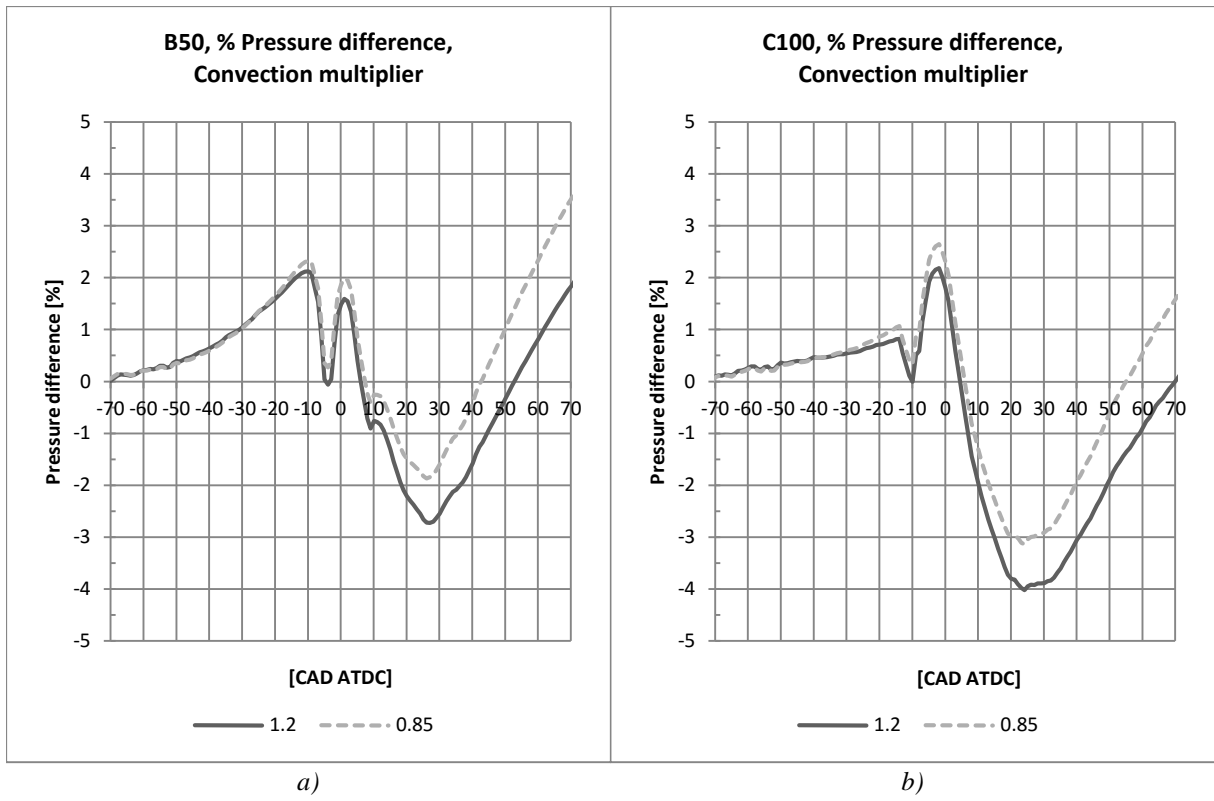


Figure 5.7 Percentage difference in cylinder pressure when changing convection multiplier compared with measured data, a) BNR306#236 and b) BNR306#240.

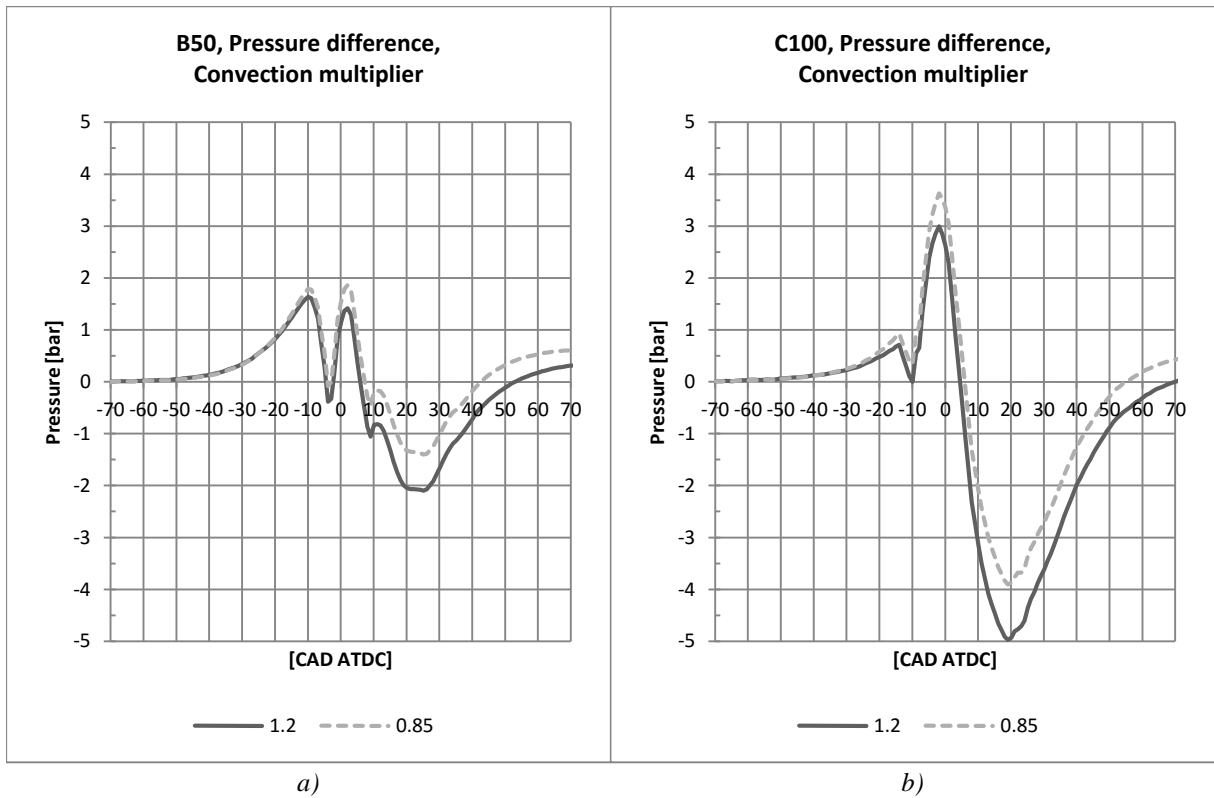


Figure 5.8 Difference in cylinder pressure for B50 and C100 when varying convection multiplier. Measured data, a) BNR306#236 and b) BNR306#240.

5.2.5 LHV multiplier

The results of the LHV multiplier achieved from the calibration model is seen in figure 5.9. It can be seen that the LHV multipliers fall within the recommended limits of $\pm 5\%$ for all tested step numbers from BNR306.

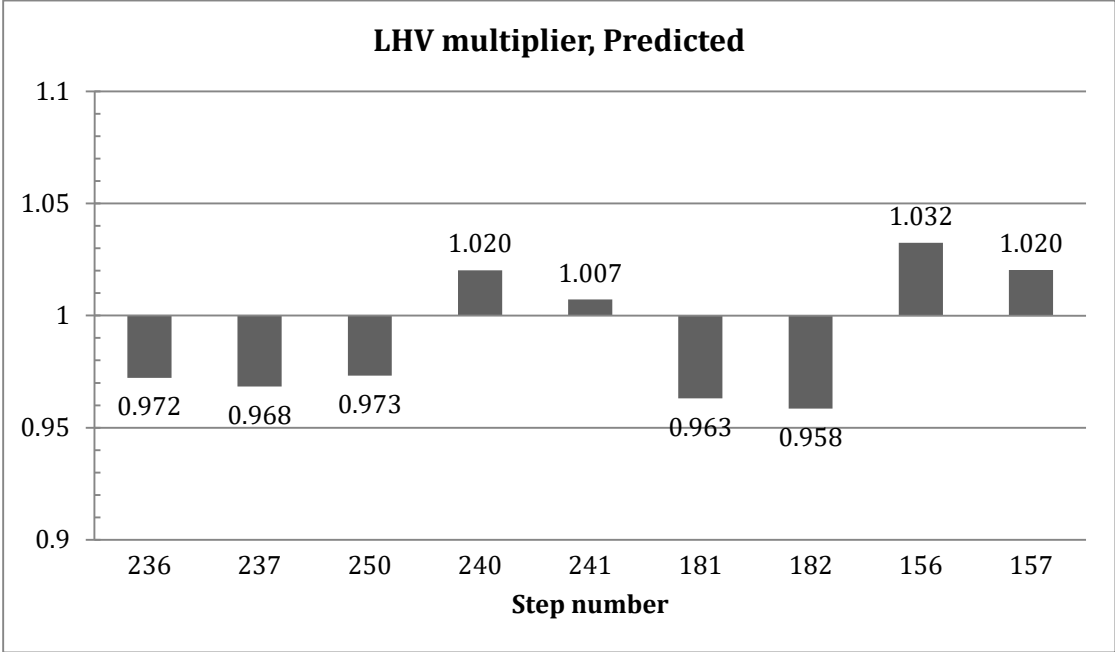


Figure 5.9 LHV multiplier, Predicted. Step numbers from BNR306.

5.2.6 Sensitivity analysis of injection rate curves

In order to investigate the sensitivity of the injection rate curves, the B50 load point BNR306#236 was chosen and its injection rate curve was modified in three different ways. The changes caused by modifying the injection rate curve will be presented through rate of heat release plots.

Figure 5.10 shows the original injection rate profile that has been used as a reference when comparing the results. All plots, figure 5.10 to figure 5.13, show the predicted and apparent rate of heat release including the original and the modified injection rate profiles.

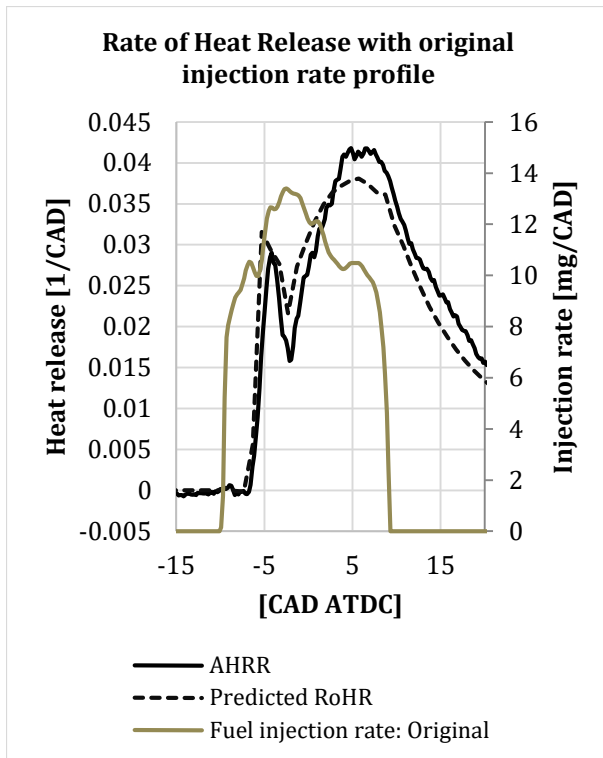


Figure 5.10 Predicted and apparent rate of heat release with original injection rate profile

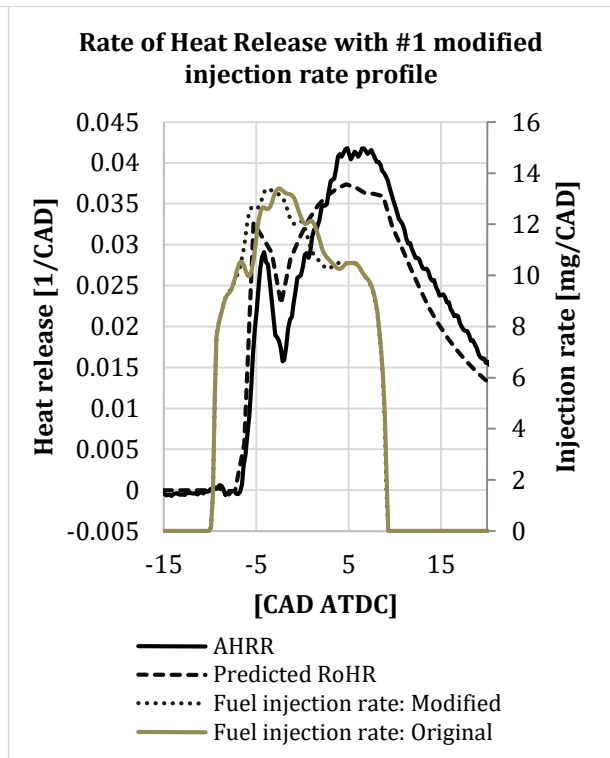


Figure 5.11 Predicted and apparent rate of heat release with the first modified injection rate profile

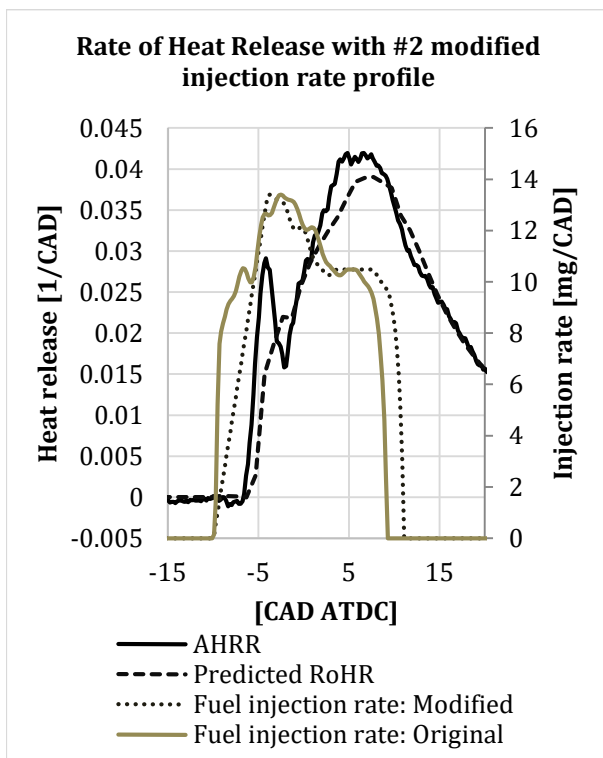


Figure 5.12 Predicted and apparent rate of heat release with the second modified injection rate profile

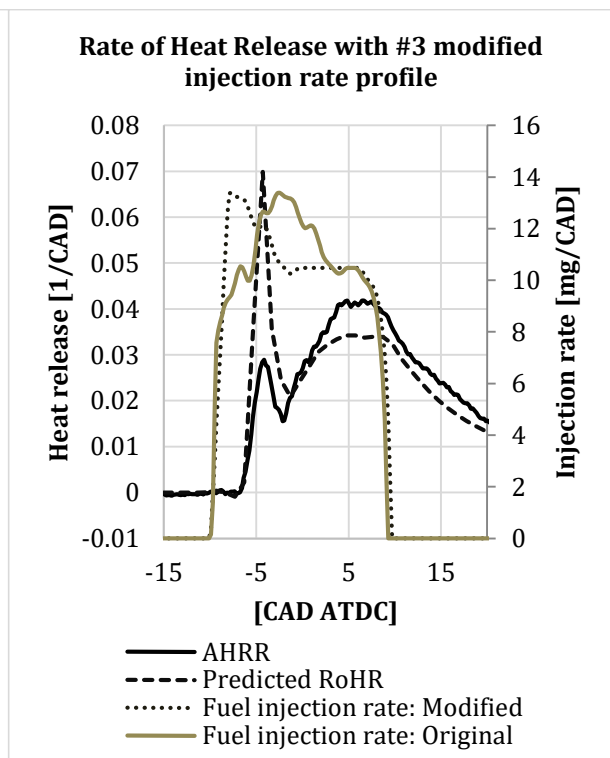


Figure 5.13 Predicted and apparent rate of heat release with the third modified injection rate profile

In figure 5.11 the first maxima in the injection rate curve is cut and part of the curve is shifted to the left, resulting in an earlier maxima of the fuel injection rate and a slight shift of the premixed combustion peak to the left.

The second modified injection rate curve, seen in figure 5.12, has been significantly modified through cutting off the first top and replacing it with a straight diagonal line starting from the same point as the original injection rate curve. This results in a less rapid initial combustion rate and vanished premixed combustion peak, which was not the case for the original curve and the first modified injection rate curves. It can thus be seen that the transition from the premixed combustion phase to the diffusion combustion phase is smooth with no dip in the heat release between the phases.

In figure 5.13, the upward injection rate slope is much steeper, which means that more fuel is injected in shorter time. This leads to an increased premixed combustion rate and a significantly higher premixed combustion peak. Consequently, the diffusion combustion peak becomes significantly lower.

5.2.7 Enthalpy in liquid fuel

In order to investigate what causes the initial heat release that starts shortly after SOI, the enthalpy in the liquid DME fuel object was modified.

This was done through changing the constants a_1 , a_2 and a_3 from their initial original values according to table 5.5 and it resulted in disappearance of the initial heat release, which is seen in figure 5.14. More about how the enthalpy in the liquid fuel object is calculated can be read in section 4.3.

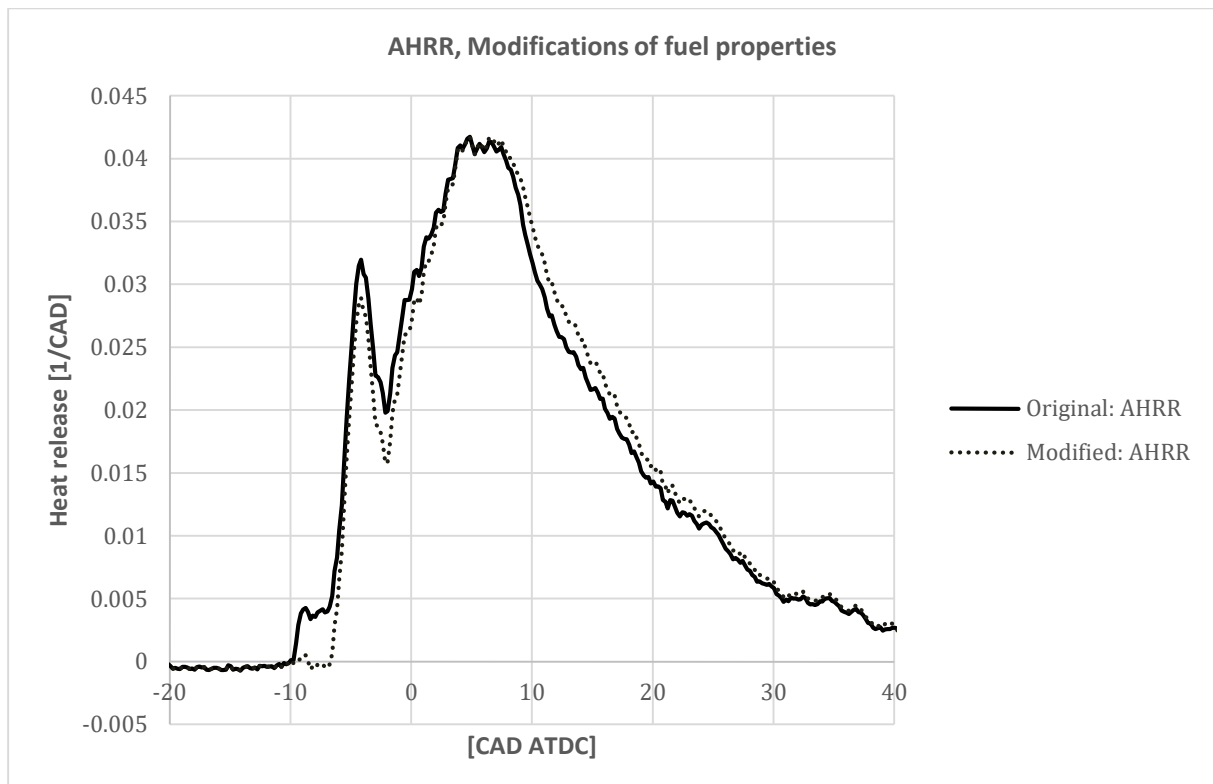


Figure 5.14 The effect of changing the enthalpy in the liquid DME fuel

Table 5.5 Modification of enthalpy in liquid fuel

Constant	Original value	Modified value
a1	2447	1000
a2	2.1245	0
a3	0.00567	0

However, this was only a test and the changed values for the constants should not be used for the full model where other calculation methods are used. More about this can be read in the discussion section 6.3.2.

5.3 Case 3: Imposed combustion profile with EGR

This section will present the results of the EGR circuit calibration through comparing simulated results with measured data for various sensors.

A summary of the results from the EGR calibration can be seen in table 5.7 as a percent difference between simulated and measured values and the factors used to achieve these results can be seen in table 5.6. As mentioned in section 4.6.5, the EGR system is calibrated towards BNR306 #237 and #241. For BNR308, a new EGR valve orifice diameter needs to be calibrated. However, new calibrations for the combustion multipliers or valve lashes are not necessary.

Table 5.6 Factors used for optimal result of BNR306

EGR valve orifice diameter, [mm]	13.04
Cylinder temperature multiplier, [-]	1.109
Inlet tank heat transfer multiplier, [-]	1
Outlet tank heat transfer multiplier, [-]	1.31
Exhaust valve lash, [mm]	0.3367

Regarding the results shown in table 5.7, it should be noted that the load step number #250 is run without EGR, hence low values on EGR rates and CO₂ concentration in to the cylinder makes the percentage difference very high but can be neglect since the absolute difference is much lower. This also applies to “T_EGR_exh_in” since this temperature is in the EGR circuit. Additionally, some other distinctions can be made from the table:

- EGR (mass rate) has better accuracy than EGR (CO₂)
- EGR (CO₂) is generally underestimated
- Air flow rate is more accurate for B50 than for C100 (not true for #250 which is without EGR)
- Temperatures at inlet side of B50 has lower accuracy than for C100

Table 5.7 Percent difference of simulated case 3 data compared to measured data of BNR 306

Load Point	B50	B50	B50	C100	C100
Load step number	250	237	236	241	240
EGR (mass)	551.7%	-2.4%	-1.5%	-1.1%	-1.6%
EGR (CO2)	169.0%	-10.6%	-10.1%	-9.8%	-11.2%
CO2_IN	158.1%	-4.1%	-2.2%	-8.0%	-6.8%
CO2P (exhaust)	-3.3%	7.1%	8.7%	2.7%	5.3%
Brake Torque	2.2%	0.0%	-0.1%	2.9%	3.9%
Maximum Pressure	2.9%	-2.4%	-2.6%	-1.2%	-1.2%
Air Flow Rate	10.7%	-0.8%	-1.4%	5.6%	5.2%
T_IN_EN	-0.3%	7.8%	8.3%	-0.9%	0.0%
T_int	-5.7%	3.7%	5.6%	-2.3%	-1.1%
T_EXH	-5.5%	1.1%	2.2%	-1.9%	-0.5%
T_EGR_exh_in	17.3%	1.1%	2.8%	-1.8%	1.6%

5.4 Case 4: Predictive combustion with EGR

A summary of the results when running the predictive combustion model from case 2 combined with the EGR circuit from case 3 are presented in table 5.8. It shows the relative difference between measured and simulated values for variation in load as well as piston. The results in terms of percent deviation are also presented as root mean square (RMS) error for each category in figure 5.15.

As mentioned in section 5.3, when looking at load step number #250, too much weight should not be put to the results dependent on EGR. Therefore, the values for this step number is excluded in calculations of the RMS error in figure 5.15.

It can be concluded that the values, when comparing the diesel piston, are very similar for this case to that of case 3.

Table 5.8 Percent difference of simulated case 4 data compared to measured data of BNR 306

Load point	B50	B50	B50	C100	C100	B50	B50	C100	C100
Step number	236	237	250	240	231	181	182	156	157
Piston	Diesel	Diesel	Diesel	Diesel	Diesel	DME	DME	DME	DME
EGR (mass rate)	-2.3%	-3.1%	548.1%	-1.1%	-2.0%	-7.7%	-5.0%	-4.4%	-5.0%
EGR (CO2)	-11.0%	-11.1%	79.1%	-10.9%	-10.4%	-15.2%	-13.3%	-12.9%	-13.4%
CO2_IN	-5.2%	-6.3%	70.3%	-7.6%	-10.7%	-10.0%	-6.7%	-12.2%	-13.7%
CO2P (exhaust)	6.2%	5.3%	-3.9%	3.5%	0.0%	6.1%	7.9%	1.8%	0.0%
Brake Torque	-2.2%	-1.7%	2.2%	0.0%	0.7%	-1.7%	-2.2%	2.1%	2.1%
Peak pressure	-0.8%	0.0%	1.4%	0.0%	1.2%	0.8%	0.0%	1.8%	2.5%
Air Flow Rate	0.0%	0.0%	11.2%	4.7%	6.1%	0.8%	-3.2%	7.8%	8.2%
T_IN_EN	9.0%	8.8%	1.3%	8.8%	0.0%	-2.9%	9.3%	-1.1%	-1.1%
T_int	6.3%	4.4%	-3.8%	7.9%	-1.4%	-4.1%	7.9%	-2.8%	-2.7%
T_EXH	8.1%	7.1%	0.8%	4.9%	1.7%	4.5%	6.6%	2.0%	0.7%
T_EGR_exh_in	7.0%	5.4%	18.8%	5.3%	0.4%	5.0%	5.9%	1.2%	0.0%

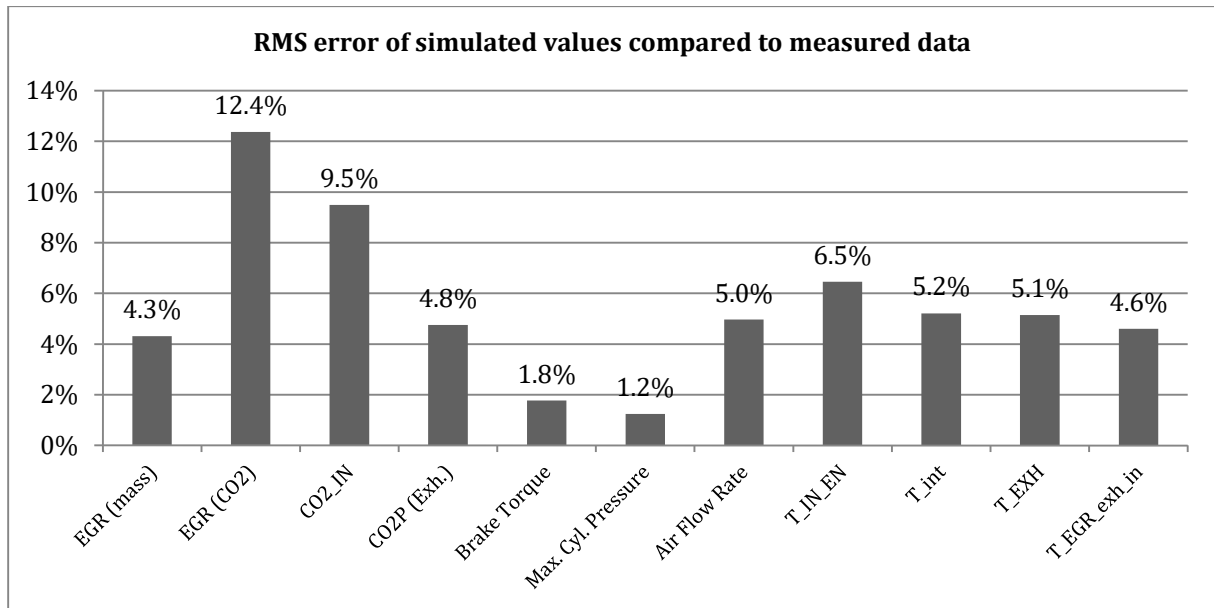


Figure 5.15 RMS error for listed BNR306 cases, except BNR306#250.

5.4.1 Cylinder pressure

The predicted cylinder pressure is an effect of predicted heat release, gas composition, compression ratio, fuel injection rate and so forth. In figure 5.16 and figure 5.17, the cylinder pressure for B50 and C100 are shown. The figures are zoomed around the peak pressure since the largest deviations are found there. See appendix A - 5 for additional diagrams.

For B50, the pressure is over predicted by a small amount during the compression stroke and right after SOC, as can be seen as an increase of the slope (at about -5 CAD) after the dip in the pressure curve. The peak pressure is well correlated and over 10 CAD ATDC, the predicted pressure is a bit lower during the power/expansion stroke.

C100 on the other hand, resulted in well matched pressure during the compression stroke until SOC where it starts deviate and over predicts the pressure. The pressure after 10 CAD ATDC during the power/expansion stroke follows the measured cylinder pressure curve well.

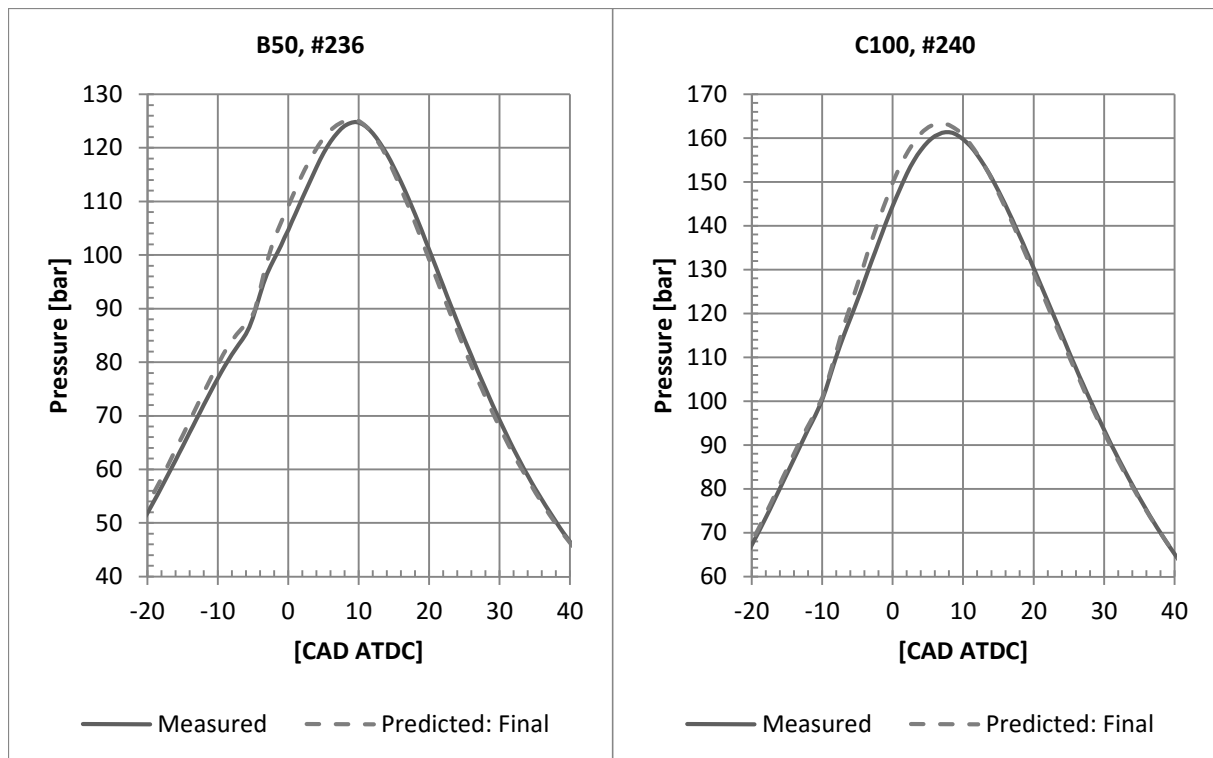


Figure 5.16 Cylinder pressure of load point B50 compared with measured pressure from BNR306#236 and prediction from calibration model (case 2).

Figure 5.17 Cylinder pressure of load point C100 compared with measured pressure from BNR306#240 and prediction from calibration model (case 2).

5.4.2 Rate of heat release

In figure 5.18, the rate of heat release is shown for both the calibration model (case 2) and the final model (case 4). There are three different rate of heat release curves obtained from the calibration model that uses different assumptions. Two of them use simplified assumptions, such as assuming that the fuel is instantly heated to the same temperature as the surrounding gases and the third one uses other assumptions and calculation methods, such as containing an ignition delay model. The curves are:

- “Calibration: AHRR” is the AHRR curve calculated from measured cylinder pressure with simplified assumptions.
- “Calibration: RoHR simplified” is the predicted rate of heat release calculated from burn rate that uses the same assumptions as the curve calculated from cylinder pressure, which makes the two heat release rates comparable.
- “Calibration: RoHR” is the predicted rate of heat release that contains the ignition delay model.
- “Final: RoHR” is the predicted rate of heat release that is achieved in the final model (case 4) and has the ignition delay model.

The heat release rates from the calibration model that use the simplified assumptions have a shorter ignition delay than the rate of heat release curves that has an ignition delay model, as seen in figure 5.18. It can be seen that the RoHR is shifted to the right and the amplitude of the premixed combustion has increased. This indicates that the ignition delay has increased and a summary of ignition delay for some load points are listed in table 5.9. The table shows

that the ignition delay increases with increased amount of EGR and that C100 has shorter ignition delay than B50 for an equal amount of EGR.

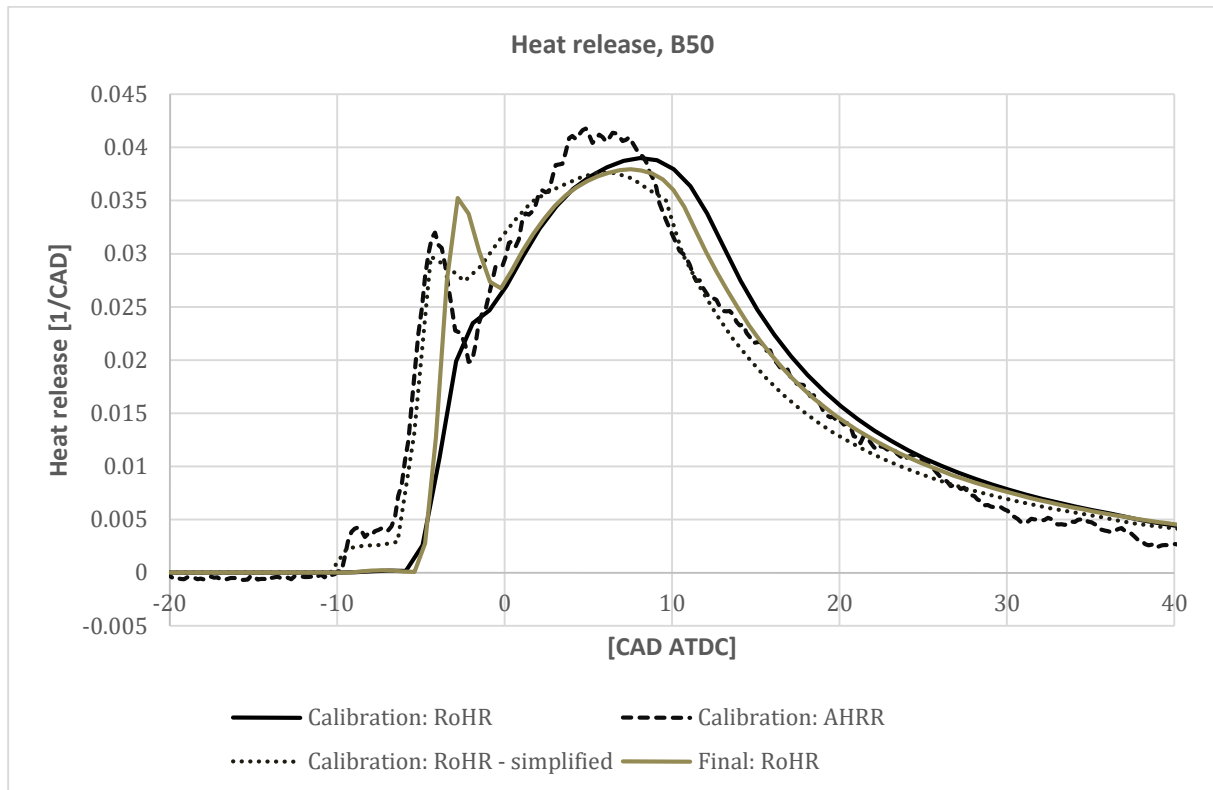


Figure 5.18 Heat release calculated with different models and assumptions. Measured data that AHRR is based on: BNR306#236.

Table 5.9 Summary of simulated data of fuel injection and ignition in case 4, BNR306.

Load point	B50	B50	B50	C100	C100	B50	B50	C100	C100
Step number	236	237	250	240	231	181	182	156	157
Angle at Start of Injection [CAD]	-9.9	-9.9	-9.9	-15	-15	-10	-10	-15.1	-15.1
Angle at End of Injection [CAD]	9.24	9.08	7.67	25.9	25.1	9.15	8.77	25.4	24.9
Injection duration [CAD]	19.1	19	17.6	40.9	40.1	19.1	18.8	40.5	40
Injected Mass per Cycle [mg/cycle]	201	199	185	335	328	201	197	333	328
Angle at SOC [CAD]	-5.66	-5.69	-6.87	-10.8	-10.9	-5.71	-5.66	-11	-11
Ignition delay [CAD]	4.24	4.21	3.03	4.18	4.11	4.29	4.34	4.11	4.09

5.4.3 Final model validation

To validate the final model and see that it responds as expected, some parameters have been changed and the responses have been studied.

Since there is a delayed start of combustion, as mentioned in section 5.4.2, SOI was shifted by ± 2 CAD to investigate its effect on the rate of heat release and ignition delay. The results are seen as RoHR in figure 5.19 and as cylinder pressure in figure 5.20. When SOI for B50 is advanced to -11.9 CAD instead of -9.9 CAD, SOC becomes more consistent with the AHRR that is calculated from measured cylinder pressure. Consequently, a much higher premixed combustion peak is achieved, which results in a higher pressure. The increased premixed combustion is due to an increased ignition delay according to table 5.10.

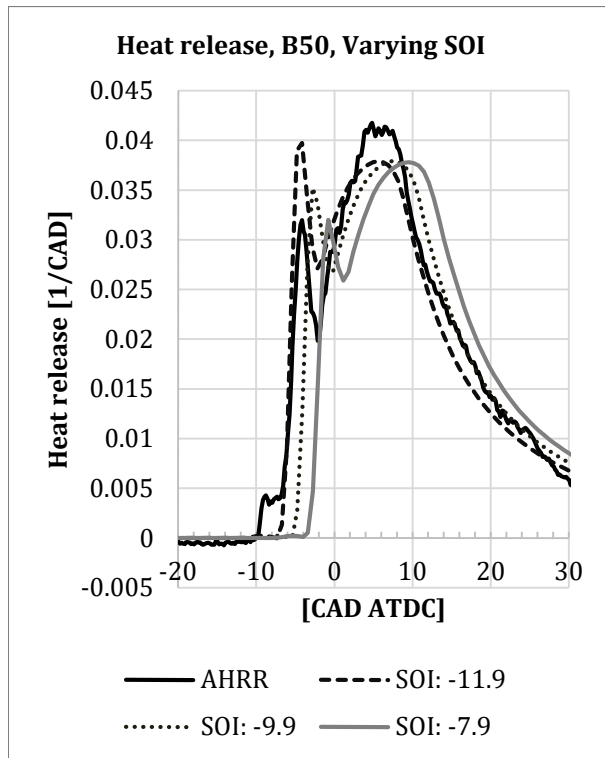


Figure 5.19 RoHR of B50 when varying SOI. AHRR calculated from measured cylinder pressure (BNR306#236)

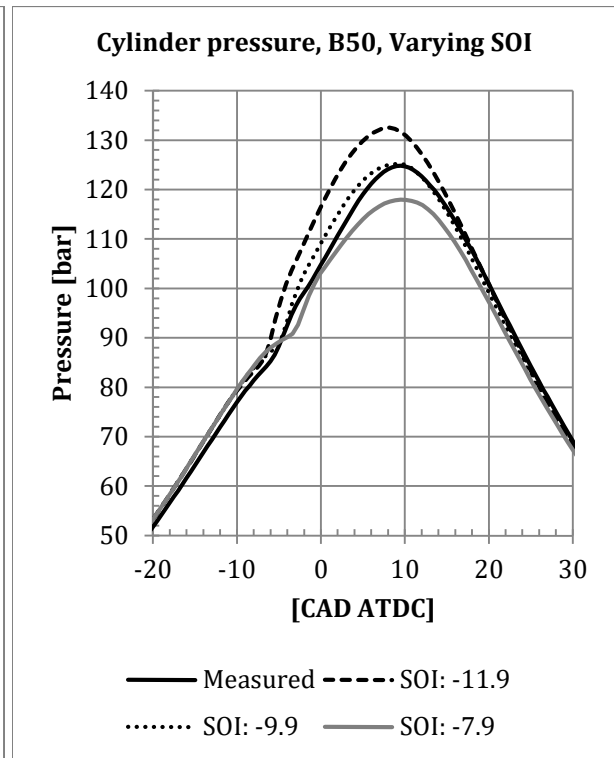


Figure 5.20 The effect of SOI on cylinder pressure, B50.

Table 5.10 Summary of ignition delay when varying SOI, BNR306 step number #236 & #240.

Step number	236	236	236	240	240	240
Load Point	B50	B50	B50	C100	C100	C100
Angle at Start of Injection [deg]	-11.9	-9.9	-7.9	-17	-15	-13
Combustion Start [deg]	-7.38	-5.66	-3.88	-12.5	-10.9	-9.18
Ignition delay [deg]	4.52	4.24	4.02	4.52	4.14	3.82

The results achieved when changing the pressure difference over the EGR circuit is seen in figure 5.21 for both load point B50 and C100. The figure shows the amount of EGR based on both CO₂ concentration and mass fractions. Mass based EGR have higher values than CO₂ based and the EGR for B50 are higher than those for C100 at the same pressure difference. Mass based EGR for equal pressure between backpressure and charge pressure (zero pressure difference) becomes negative. This is due to reverse flow in the EGR circuit (fresh air going through EGR circuit and not through cylinder).

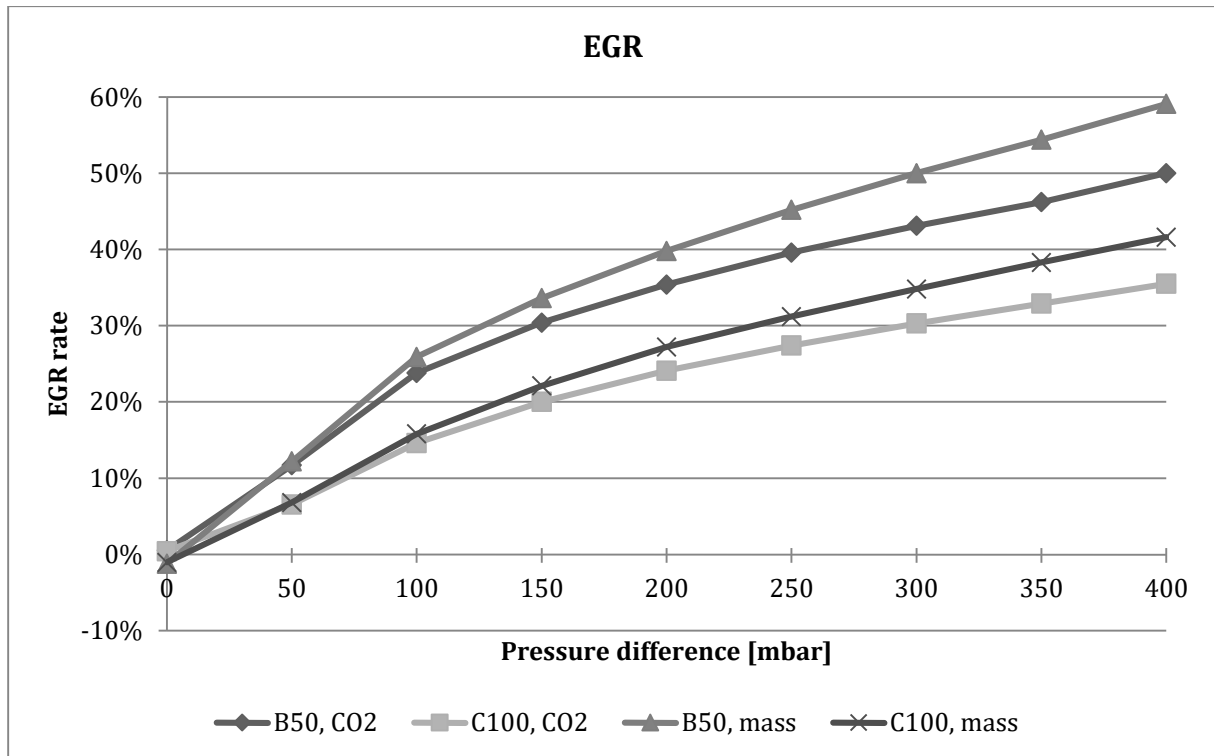


Figure 5.21 Changes in EGR amounts as a function of the pressure difference over the EGR circuit. Amount of EGR is based either on CO₂ concentration or mass flow.

Hereafter when EGR is mentioned, it is based on CO₂ concentration since negative amount can be achieved when using mass based EGR. CO₂ based EGR is also beneficial since it can be directly measured in real engine tests. Since it is of interest to see how different parameters are affected by the amount of EGR, and not the back pressure, the results in figure 5.21 are plotted over EGR instead.

In figure 5.22, the CO₂ concentration at the intake and exhaust are seen and their values increases with increased amount of EGR. The CO₂ concentrations at the exhaust are higher than at the intake and CO₂ the concentrations for C100 are higher than for B50.

The ignition delay presented in figure 5.23 shows an increasing trend both for B50 and for C100 when the EGR increases. The “stepwise” increase in C100 is not realistic and is due to too few decimals in the results achieved from GT-Power. Hence, a trend-line is put in place for C100 to simplify the comparison with B50.

The break torque, showed in figure 5.24 is decreasing with increasing EGR for both B50 and C100. Figure 5.25 shows maximum cylinder temperature during one cycle. “Mean temperature” is the mean temperature of the content in the cylinder. “Burned zone temperature” is the temperature in the zone where combustion takes place. It is seen in the figure that these temperatures decrease with increased amount of EGR, which is expected.

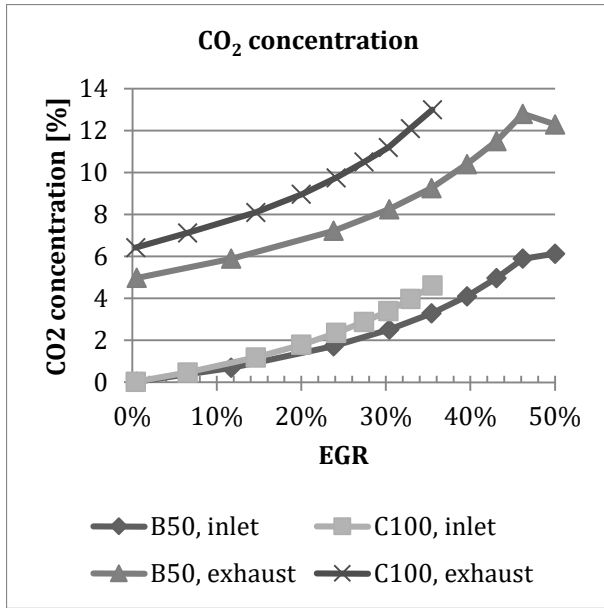


Figure 5.22 CO₂ concentration in exhaust and inlet for B50 and C100.

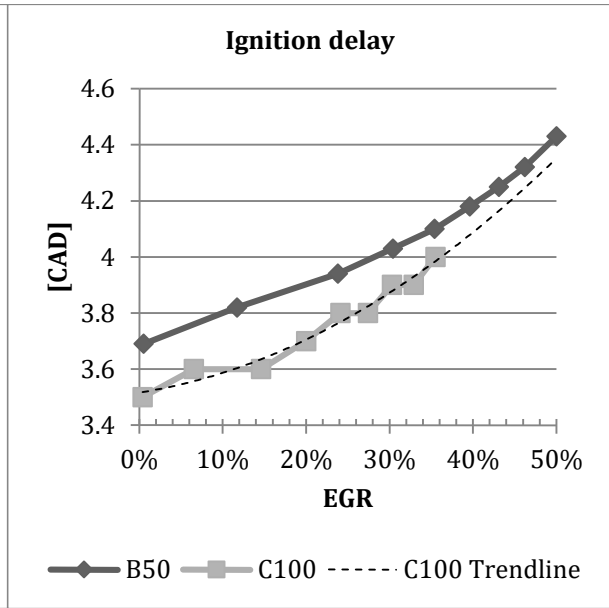


Figure 5.23 Ignition delay for B50 and C100 over increasing EGR.

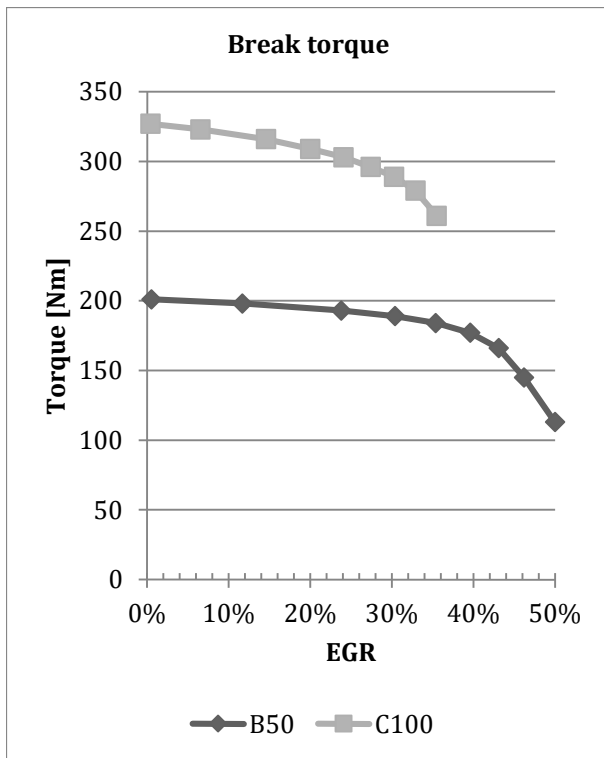


Figure 5.24 Break torque for B50 and C100 over increasing EGR.

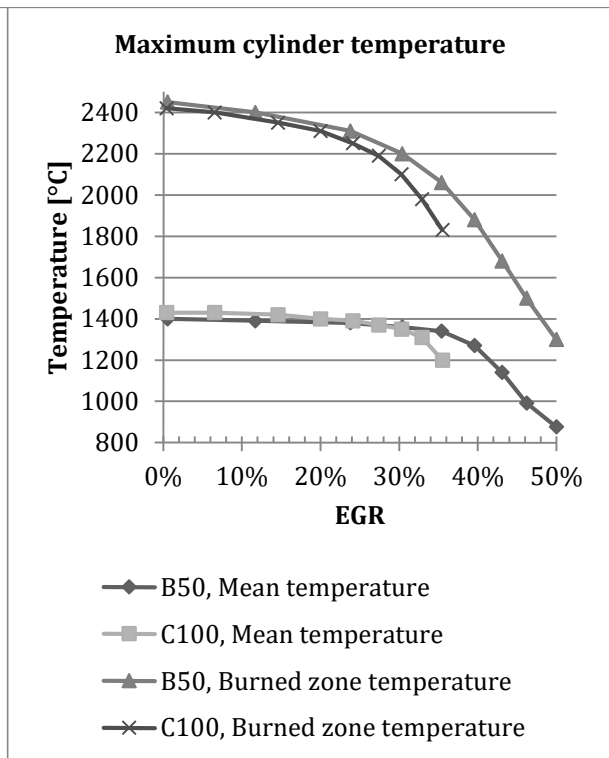


Figure 5.25 Maximum cylinder temperature for B50 and C100 over increasing EGR.

In figure 5.26, the exhaust temperatures are shown and as a reference, experimental exhaust temperature for A50 cases in BNR305 are given. A second degree polynomial trend-line is fitted for the measured data to be able to see the shape better. It is also seen that C100 have generally higher temperature than B50 and B50 have higher temperature than measured A50. Temperatures also increase with increased EGR.

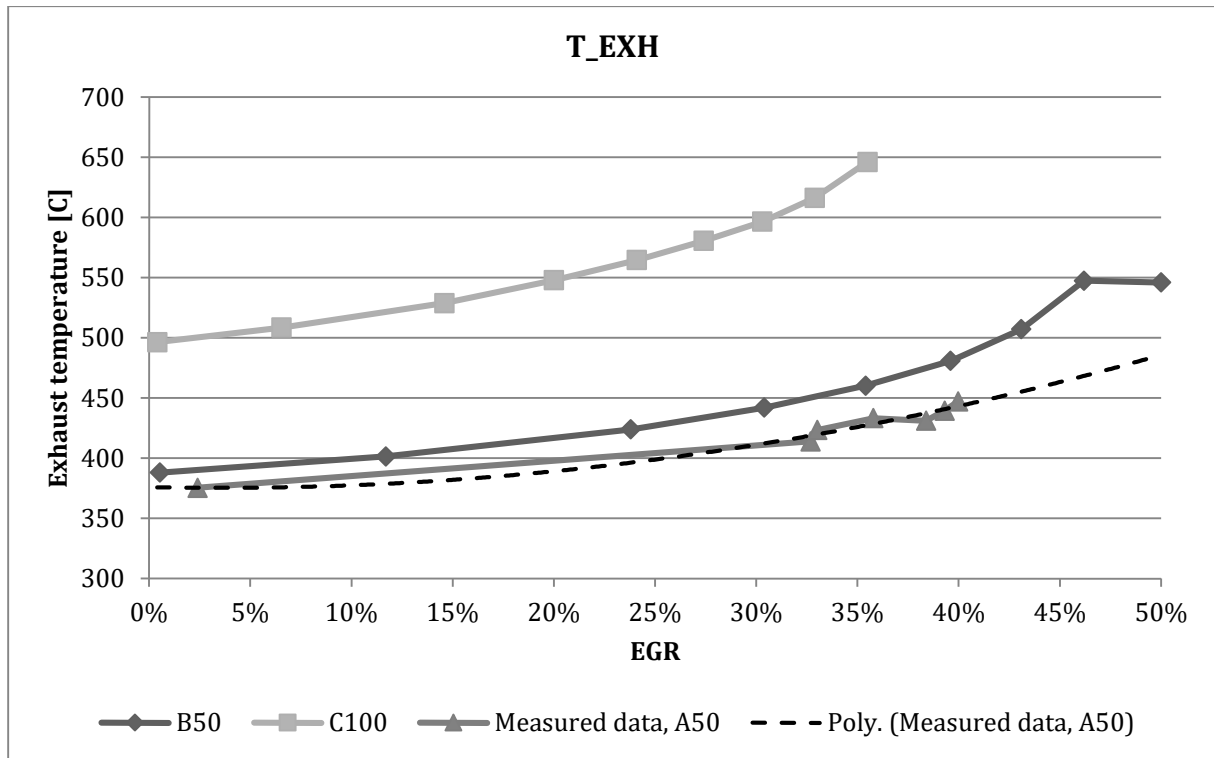


Figure 5.26 Exhaust temperature for B50 and C100 plotted over increasing EGR, compared with measured data from A50 in BNR305.

In figure 5.26 and figure 5.22 an abrupt change in the trend for B50 can be seen, at the high EGR amounts, and affects both exhaust temperature and CO₂ concentrations. This change is due to an air to fuel ratio lower than the stoichiometric air to fuel ratio and is a direct result of the high amount of EGR used. Hence, there is not enough oxygen in the combustion chamber for a complete combustion of the injected fuel.

6 Discussion

This chapter will include a general discussion about the results achieved and more specific discussion of certain areas like the EGR circuit and the predictive combustion model DIPulse.

6.1 EGR circuit

The EGR can be controlled using different methods. However, in this engine and in this model, it is controlled through adjusting the back pressure. This creates a pressure difference between the exhaust and inlet side of the engine, which acts as the driving force of the EGR. Other parameters that affects the EGR mass flow is the pressure drop across the EGR cooler and the pressure drop across the EGR valve.

The EGR valve is manually actuated and can be set from fully open to fully closed and all positions in-between. This can cause problems because the position is not very accurate and a small difference in position has a large effect on the pressure drop over the valve, therefore affecting the calibration of the system significantly. With different sets of measured data, different positions of the valve might have been used. The valve is modeled as a reduced hole diameter and thus needs to be calibrated and adjusted with each set of measured data to provide accurate results.

6.2 Calibration of EGR circuit

When calibrating the non-predictive combustion model with EGR, it is difficult to know which parameters to optimize. Since there are two different ways of calibrating the EGR, one in terms of CO₂ concentration and one in terms of mass flow, there are at least two distinct ways of calibrating, according to equation (6.1) and (6.2).

$$EGR_{Mass}[\%] = \frac{\dot{m}_{EGR}}{\dot{m}_{fresh\ air} + \dot{m}_{EGR} + \dot{m}_{fuel\ injected}} \cdot 100 \quad (6.1)$$

$$EGR_{CO_2}[\%] = \frac{CO_2\ into\ cylinder\ [\%]}{CO_2\ out\ from\ cylinder\ [\%]} \cdot 100 \quad (6.2)$$

When calibrating the EGR based on the mass rate in the system, the EGR_{mass} parameter calculated by GT-Power can be used to achieve a correct relationship between the flows and thereafter use the fresh air flow into the system. When calibrating the EGR based on CO₂, one can use the concentrations of CO₂ in and out from the cylinder directly and thereby get the EGR indirectly.

The calibration is preferably done through setting up DOE analyses and changing selected factors that are then optimized so that the parameters (responses) correlate with measured data. However, the responses are based on a fitted surface using the least square method. This means that the optimization is not exact since the predicted values from the DOE analysis differ from the simulated and the simulated values in turn differ from reality.

When calibrating the system, it is difficult to obtain CO₂ concentrations that are consistent with measured data at the same time as the fresh air flow into the system is correct. This can depend on the variations in measured data since CO₂ concentrations have a standard deviation

of 0.27 percent units at a concentration of 5.17 % as can be seen in figure 6.1. The figure shows that when trying to run the engine at similar loads with similar settings, various results are achieved. To be able to compare the deviation with the simulated RMS error, the standard deviation of 0.27 is divided with 5.17 to get the ratio of the standard deviation. The comparison is shown in figure 6.2 and it can be clearly seen that the simulated RMS error is within the limits of the standard deviation from the measurements.

Even though the errors in the simulated CO₂ concentrations are high, the EGR amount based on the CO₂ concentration is also high and the simulated error is still within the limits of the deviation from measured data, as seen in figure 6.2. Hence, it is difficult to calibrate the EGR circuit more accurately.

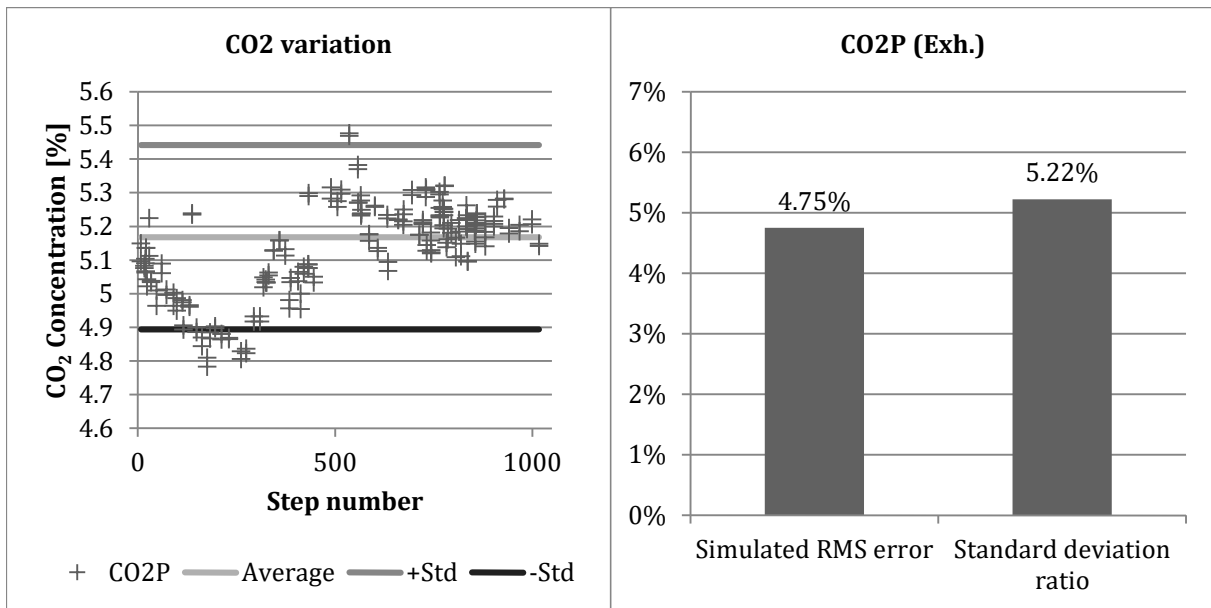


Figure 6.1 Standard deviation in CO₂ measurement at exhaust for BNR306, load point B50 with SOI of -15 CAD ATDC

Figure 6.2 Error of CO₂ concentration in exhaust. Simulated RMS error in relation to measured and the ratio of standard deviation to measured average.

6.3 Predictive combustion model (DIPulse)

The results from the calibration of the predictive combustion model DIPulse (case 2) are discussed in this section.

6.3.1 The convection and LHV multiplier

The convection multiplier affects the maximum cylinder pressure mostly, which can be expected since it is set to a constant value and higher pressure and temperature increases the heat transfer through the cylinder for constant wall temperatures and convection multiplier.

The cylinder pressure could be even better correlated through using a profile angle array for the convection multiplier in the heat transfer object during the compression and power stroke. However, this was not prioritized in this work since the cylinder pressure is quite well matched already.

The LHV multiplier is within the limit for all step numbers. Since deviation in the LHV multiplier depends on various things that can originate from both model errors and errors in measured data and the multipliers lie within the recommended limits, further work have not been done to improve the LHV multiplier.

6.3.2 Matching the RoHR curves in the calibration model

The effect of the entrainment rate multiplier is that the heat release from the premixed combustion rate is less rapid when lowering the multiplier, which is expected since it modifies the entrainment of the gases to the fuel spray. Increasing the entrainment rate increases the amount of fuel that can be evaporated in a shorter time and thus, the combustible mixture present at the SOC will increase. The larger amount of combustible mixture that is available at SOC, the rapider and larger the heat release from the premixed combustion will be. Increased entrainment rate will also result in a quicker mixing of the injected fuel and the surrounding gases after SOC since it is a fixed value and thereby, increasing the diffusion combustion rate.

The ignition delay multiplier has the expected effect with a larger premixed combustion when increasing the ignition delay multiplier. The SOC using the optimized multiplier values deviate from those achieved from measured data, which can be adjusted using the multiplier. However, when lowering the multiplier to achieve a better match with the measured data, the premixed combustion rate decreases and thus resulting in a poorer match between the AHRR calculated from measured cylinder pressure and the predicted heat release rate.

Another way to get around the problem with the mismatch of SOC in the model with that of measured data, is to advance the SOI, which can be seen in section 5.4.3. The SOI needs to be advanced approximately 2 CAD relative to measured SOI to achieve a better correlated SOC. It should be stated that this results in prolonged ignition delay, and thus result in an ignition delay that deviates even more from the measured data. However, the premixed combustion rate, SOC, end of the premixed combustion and start of diffusion combustion phase will be better matched between the simulated and predicted rate of heat release curves.

The diffusion combustion rate multiplier affects the diffusion combustion phase and leads to less distinction between the premixed combustion and the diffusion combustion when increasing the multiplier. This is expected since a larger portion of diffusion combustion reduces the portion of premixed combustion (at constant fuel mass/energy release). Increasing the portion of diffusion combustion leads to increased pressure and temperature in the cylinder, which in turn leads to quicker vaporization of the fuel when injected into the cylinder. Quicker evaporation results in a less distinctive dip between the premixed combustion and the diffusion combustion due to shorter ignition delay and consequently less premixed combustion.

6.3.3 Enthalpy in the liquid fuel

The enthalpy in the liquid DME fuel object was modified and the results showed that the initial heat release, which occurred in all the rate of heat release plots when using the calibration model, disappeared when the constants used to calculate the enthalpy were lowered.

The reason for this is that the calibration model lacks a fuel heat-up model and assumes that the fuel is instantly heated to the same temperature as the surrounding gases in the cylinder.

The energy required for this instantaneous temperature increase of the fuel is over predicted and results in a pressure fall that becomes too low compared to the measured cylinder pressure, which is a consequence of the heat loss in the cylinder. The pressure loss has to be compensated through adding heat release when the fuel is injected to be able to match the predicted cylinder pressure with the measured cylinder pressure and is thus the cause to the initial heat release.

It can therefore be concluded that the initial heat release is only present due to assumptions in the model and does not exist in reality or in the full predictive model that has an ignition delay model, where other assumptions and calculations are used. The enthalpy of the fuel should therefore not be modified in the final model, which is why the original fuel constants are kept.

6.3.4 Sensitivity analysis of injection rate curves

It can be concluded that the fuel injection rate profile has a major impact on the combustion when using DIPulse as have been shown in section 5.2.6. It is not as significant difference between the original case and the first modified injection rate as it is between the original curve and the second and third modified injection rates. This is likely coherent with the extent of modification on the modified injection rates. The modifications on the second and third injection rates may seem a bit extreme, but they prove that the model is sensitive for the shape of the injection rates. The rate of heat release and the injection rate profiles are compared in figure 6.3 and figure 6.4.

When the injection rate increases rapidly from the SOI, which corresponds to a steep initial slope in the injection rate profile, it has a direct effect on the premixed combustion. The effect is apparent when looking at the third modified injection rate curve and this is due to more injected fuel in a shorter time period and longer penetration of the fuel jet into the air. An increased amount of fuel available at SOC results in increased heat release from premixed combustion.

An increase of the fuel's injection rate is coherent with higher injection pressure, which affects the atomization and breakup of the fuel spray droplets. Consequently, it leads to increased heat transfer area between the surrounding gas and the fuel, which results in increased evaporation rate. The third modified injection rate curve has an initial high injection rate, which causes high evaporation rate and a greater amount of combustible mixture present at start of combustion causing the high premixed combustion peak.

The second modified injection rate curve on the other hand is less steep and leads to less fuel injected for the same crank angle degree and hence also slower evaporation rate of the fuel before start of combustion, which is why the premixed peak seems to have vanished. It also affects the ignition delay, which is prolonged by approximately one crank angle degree compared to the other cases as seen in table 6.1. A larger portion of the fuel is burned during the diffusion combustion phase, which results in a higher heat release peak. This behavior also has other effects such as higher peak cylinder pressure and increased NO_x formation due to higher cylinder temperature.

Table 6.1 Ignition delay for the different injection curves

Injection curve applied	Ignition Delay [CAD]
Original	3.41
#1, modified	3.41
#2, modified	4.42
#3, modified	3.89

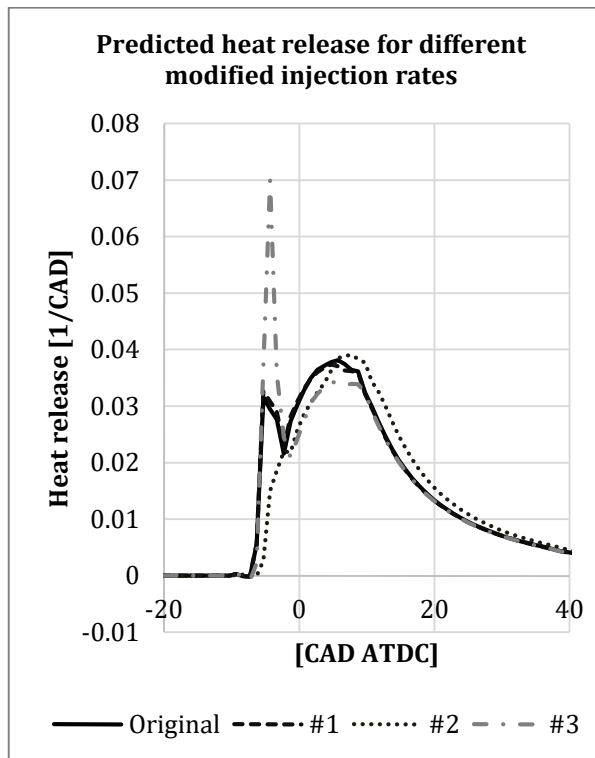


Figure 6.3 Predicted AHRR for different modified injection rate profiles

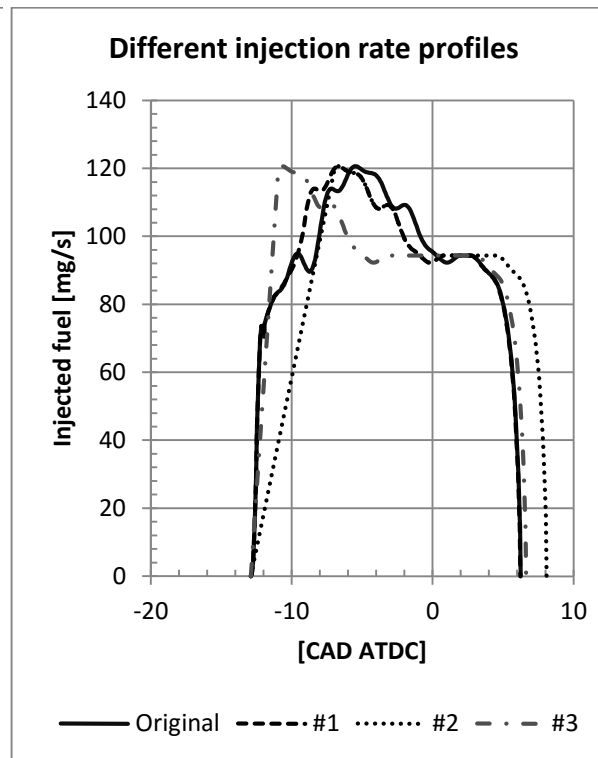


Figure 6.4 Modified injection rates in comparison to "original"

It has been proven that the fuel injection rate curves is an important input parameter when using the predictive combustion model DIPulse in GT-Power. Controlling the fuel's injection rate is important when running physical engines as well, which means that the results are somehow reflecting reality. Although, it is difficult to evaluate to what extent the effects achieved when modifying the injection rate profiles correlate with reality since neither the original nor the modified injection rate profiles are experimentally validated.

The injection rate curves used in this work are simulated with an accuracy that is difficult to estimate. Various assumptions have been made when the fuel injection rates were simulated and because it is complex to measure and achieve accurate injection rate curves from engine runs, the curves are not yet validated. It should also be mentioned that the injection duration is not adapted to the measured data and it has not been investigated what difference it would make if it was adjusted. It may lead to higher amplitude for some cases and lower amplitude for other, but this is left to be studied in future work.

6.4 Final model results and behavior

In previous discussion in section 6.2, it was shown that the results of CO₂ concentration, even though high error, were within the limits of deviation from measured data.

In section 5.4.2, it is shown that there is an increased ignition delay and that it could be affected by different parameters of which some are in-cylinder temperature, pressure and gas composition (amount of EGR). However, since B50 without EGR is also affected by the increased ignition delay it is safe to assume that the increased delay is not due to large amounts of EGR. However, comparing temperature and pressure in the final model (case 4) with those from the calibration model (case 3), both are higher in the final model which should result in lowered ignition delay but that is not the case. As of now, the reason behind the increased ignition delay is unknown.

Reflecting back at section 5.4.3 Final model, generally no odd behavior can be noticed and the model behaves as expected. However, one will expect that the accuracy of the prediction will decrease the further out from the calibrated EGR levels one goes. That is, the combustion multipliers calibrated for B50 and no EGR will most likely be more accurate at an interval between 0 – 10% EGR than those calibrated for an EGR level of 30 – 40 %. One could choose to have calibrated combustion multipliers for a much wider range of EGR, however the accuracy of predictions is expected to decrease for the whole range.

6.5 Sources of errors

During this work, many assumptions and simplification had to be made that sometime was due to lack of data or time. Here, some of the most probable sources of errors are presented.

- Mostly external geometrical measurements of the engine were made.
 - This could affect the total volume in the system.
 - Contractions and expansions in the system may not be modeled properly.
- Inaccurate EGR valve opening position.
 - This could have been changed in between measurement campaigns.
- Deviation in CO₂ measurement data.
 - Since the amount of EGR is calibrated towards CO₂ concentration this affects the accuracy of mass flow in the system.
- Few fuel injection rate simulations.
 - The predictive combustion model DIPulse is sensitive towards inaccuracy in injection rates. Manual modifications of injection rates had to be made which is not the most accurate way to proceed.
- Fuel injection rate simulations not verified towards experimental data.
 - As above, DIPulse is sensitive towards injection rates. As no verification is made one cannot say how accurate the simulations are.

7 Conclusion

Fossil fuels have been dominating the transport sector during the past century and due to environmental concerns, the interest of alternative fuels has increased. DME is a suitable alternative for diesel fuel in compression ignition engines which has potential to be CO₂ neutral. However, the combustion process needs to be optimized with the help of CFD analysis. For this analysis, accurate boundary conditions are needed.

This work has focused on creating a GT-Power model of a single cylinder research engine, that is run on the alternative fuel DME. The purpose is to produce accurate boundary data for the combustion chamber so that the CFD analysis of the combustion process of DME can be performed.

The outcome of this work is a GT-Power model of a single-cylinder research engine, with a predictive combustion model (DIPulse) calibrated for DME. The model is valid and separately calibrated at two load points, B50 and C100. In other words, it cannot handle any transitions or intermediate load points. However, it is capable to handle various amounts of EGR and injected fuel mass at the two load points.

The predicted RoHR achieved from simulations show an increased ignition delay in comparison with AHRR, which is calculated from measured cylinder pressure. This delay is independent on the amount of EGR and the reason behind this increased ignition delay is at present unknown.

Even though the final model shows relatively high RMS errors, 9.5% for CO₂ concentration at the intake side of the system and 4.8% at the exhaust side of the system, it is shown that the CO₂ concentration at exhaust is within the variation of measured lab data. Hence, it is reasonable to assume that it is difficult to achieve higher accuracy with present data.

Due to DIPulse's need for accurate injection rates, it is recommended to simulate new and more injection rate profiles for the aimed rail pressure and different injected fuel masses if one wants to improve the model's accuracy and avoid a probable source of error. Another option is to modify the present injection rates so that the injection duration is similar to measured lab data, since the present injection rates can deviate in injection duration up to 10% in comparison to measured lab data. However, the latter option may introduce other forms of errors due to changes in injection rate amplitude that is most likely needed.

The predicted cylinder pressure curve and measured cylinder pressure curve can, as a complement, be analyzed in a stand-alone heat release analyzing tool. That would make it possible to analyze and compare the two resulting AHRRs based on the same assumptions and investigate where SOC occur when using another software.

8 References

- AMF, 2015. *Dimethyl ether (DME)*. [Online]
Available at: http://www.iea-amf.org/content/fuel_information/dme
[Accessed 13 September 2015].
- BioDME, 2015. *Work packages*. [Online]
Available at: <http://www.biodme.eu/work-packages>
[Accessed 29 May 2015].
- DieselNet, 2015. *Standards: Emission Test Cycles: ESC*. [Online]
Available at: <https://www.dieselnet.com>
[Accessed 18 09 2015].
- European Commission, Joint Research Centre, 2014. *Well-To-Wheels analysis of future automotive fuels and powertrains in the European context*, Luxembourg: Publications Office of the European Union.
- Gable, C. & Gable, S., 2015. *What is Cetane?*. [Online]
Available at: <http://alternativefuels.about.com/od/researchdevelopment/a/cetane.htm>
[Accessed 13 September 2015].
- Gamma Technologies, 2014a. *GT-SUITE, Engine Performance Application Manual, Version 7.4*, Westmont, IL: s.n.
- Gamma Technologies, 2014b. *GT-SUITE, Flow Theory Manual, Version 7.4*, Westmont, IL: s.n.
- Gamma Technologies, 2015. *Predictive Diesel Combustion Modeling*, s.l.: s.n.
- Greszler, A., 2013. *DME from Natural Gas or Biomass: A Better Fuel Alternative*, s.l.: s.n.
- Heywood, J. B., 1988. *Internal Combustion Engine Fundamentals*. Singapore: McGraw-Hill.
- Hohenberg, G., 1980. *Advanced Approaches for Heat Transfer Calculations*, s.l.: Society of Automotive Engineers.
- Ho, T., James, C. M. & Jeffrey, B. S., 2004. *Thermodynamic Properties of Dimethyl Ether - An Alternative Fuel for Compression-Ignition Engines*, Detroit: SAE International.
- Khair, M. K. & Jääskeläinen, H., 2010. *Combustion in Diesel Engines*. [Online]
Available at: https://www.dieselnet.com/tech/diesel_comb.php
[Accessed 6 October 2015].
- Khair, M. K. & Jääskeläinen, H., 2013. *Diesel Fuel Injection*, s.l.: s.n.
- Maurya, R. K., Agarwal, A. K. & Pal, D. D., 2013. Digital signal processing of cylinder pressure data for combustion diagnostics of HCCI engine. *Mechanical Systems and Signal Processing*, 36(1), pp. 95-109.
- Mingfa, Y., Zunqing, Z., Sidu, X. & Maoling, F., 2003. *Experimental Study on the Combustion Process of Dimethyl Ether (DME)*, Pittsburgh: SAE International.

Mittermaier, H., 1996. *AVL Single Cylinder high BMEP Test Engine for lubricant, emissions and fuel research with VOLVO 2.0 L top work*, s.l.: AVL.

Mollenhauer, K. & Tschoeke, H., 2010. *Handbook of Diesel Engines*. London, New York: Springer.

Salsing, H., 2011. *DME Combustion in Heavy Duty Engines*, Gothenburg: Chalmers Reproservice.

Semelsberger, T. A., Borup, L. R. & Greene, L. H., 2005. Dimethyl ether (DME) as an alternative fuel. *Journal of Power Sources*.

Strandhede, J., 2013. *Volvo Lastvagnar breddar sitt utbud för alternativa bränslen i Nordamerika*. [Online]

Available at: <http://www.volvotrucks.com/dealers-vtc/sv-se/RejmesTransportfordon/newsmedia/pressreleases/Pages/pressreleases.aspx?pubid=15904> [Accessed 14 September 2015].

Teng, H., McCandleless, J. & Schneyer, J., 2002. *Viscosity and Lubricity of (Liquid) Dimethyl Ether - An Alternative Fuel for Compression-Ignition Engines*, Detroit: SAE International.

United Nations Framework Convention On Climate Change, 2014. *Glossary of climate change acronyms*. [Online]

Available at: http://unfccc.int/essential_background/glossary/items/3666.php [Accessed 16 September 2015].

Volvo Truck Cooperation, 2015. *Alternative fuels - The way forward*, s.l.: s.n.

www.tpub.com, 2015. *Four-Stroke Cycle Diesel Engine*. [Online]

Available at: <http://www.tpub.com/eqopbas/3.htm> [Accessed 19 May 2015].

9 Appendices

Appendix A Plots and Tables

- A - 1 Describing different BNR and Load step number**
- A - 2 Calibration model objects and parameters**
- A - 3 Varying Compression ratios**
- A - 4 Effect of varying DI-Pulse multipliers**
- A - 5 CO₂ concentration sensitivity**
- A - 6 Injection and combustion events**
- A - 7 Pressure and Heat Release curves from final model (case 4)**

Appendix B Drawings and Schematics

- B - 1 Drawings and external measurements**
- B - 2 Showing GT-Power case circuits**

Appendix A Plots and Tables

A - 1 Describing different BNR and Load step number

Table 9.1 Parameters for BNR 306

Load step number	Load point	NOx Level [g/kWh]	EGR (CO2 based) [%]	Charge Pressure, [mbar]	Back Pressure, [mbar]	Relative Humidity, [%]	Engine Speed, [RPM]	Injected fuel mass, [mg]	Fuel injection timing, [CAD]	Piston
250	B50	10	0.3	2410.7	2399.5	5.72	1498	184.6	-9.9	Ø92-Diesel
237	B50	0.3	40.7	2399.9	2608.0	5.72	1497	199.3	-9.9	Ø92-Diesel
236	B50	0.24	42.0	2399.8	2624.0	5.72	1497	200.9	-9.9	Ø92-Diesel
241	C100	0.3	33.7	3004.3	3302.0	7.15	1796	328.4	-15	Ø92-Diesel
240	C100	0.24	34.9	3005.0	3317.0	7.15	1796	335.0	-15	Ø92-Diesel
181	B50	0.24	44.1	2399.6	2626.5	5.72	1500	201.1	-10	Ø88-REC DME
182	B50	0.3	42.7	2399.5	2617.0	5.72	1499	197.2	-10	Ø88-REC DME
156	C100	0.25	34.8	3001.5	3300.0	7.15	1797	332.8	-15.1	Ø88-REC DME
157	C100	0.3	34.3	3002.3	3290.5	7.15	1798	327.5	-15.1	Ø88-REC DME

Table 9.2 Parameters for BNR 308

Load step number	Charge Pressure, [mbar]	Back Pressure, [mbar]	Relative Humidity, [%]	Engine Speed, [RPM]	Injected fuel mass, [mg]	Fuel injection timing, [CAD]	Fuel Injection duration, [CAD]
304	2407	2535.8	5.72	1500	200.14	-13	21
305	2406	2539.5	5.72	1500	200.74	-13	21
306	2705.9	2875.9	6.44	1500	197.5	-13	21
307	2706	2871	6.44	1500	198.6	-13	21
283	3011.9	3192.7	7.15	1799	334.99	-15	36.5
284	3010.9	3185.7	7.15	1800	333.4	-15	36.5
285	3011.7	3180	7.15	1800	327.8	-15	36.5
286	3011	3193	7.15	1800	326.25	-18	36.5
287	3009.6	3198	7.15	1801	327.3	-18	36.5
288	3010.3	3195.4	7.15	1801	327.92	-18	36.5
289	3011.3	3190	7.15	1801	326.8	-18	36.5

A - 2 Calibration model objects and parameters

Table 9.3 Data specified in calibration model

Main object	Parameter	Unit
InjProfileConn	Injected mass	[mg/cycle]
	Injection profiles	[bar/mass, CAD ATDC]
EngCylinder	Start of Injection	[CAD]
	Injected Fluid Temperature	[°C]
	Injection nozzle geometry	[mm/no unit]
	Injection profiles	[mg, CAD]
	Swirl, tumble turbulence	[-]
EngCylinder, EngCylCombDIPulse	Multipliers	Entrainment rate [-] Ignition delay [-] Premixed combustion rate [-] Diffusion combustion rate [-]
EngCylinder, EngBurnRate	Start of Combustion	CAD ATDC
	EngBurnExhMeasure	HC [PPM] CO [PPM] NO [PPM]
	Measured Cylinder Pressure	[CAD ATDC, bar]



Figure 9.1 System circuit for case 2

A - 3 Varying Compression ratios

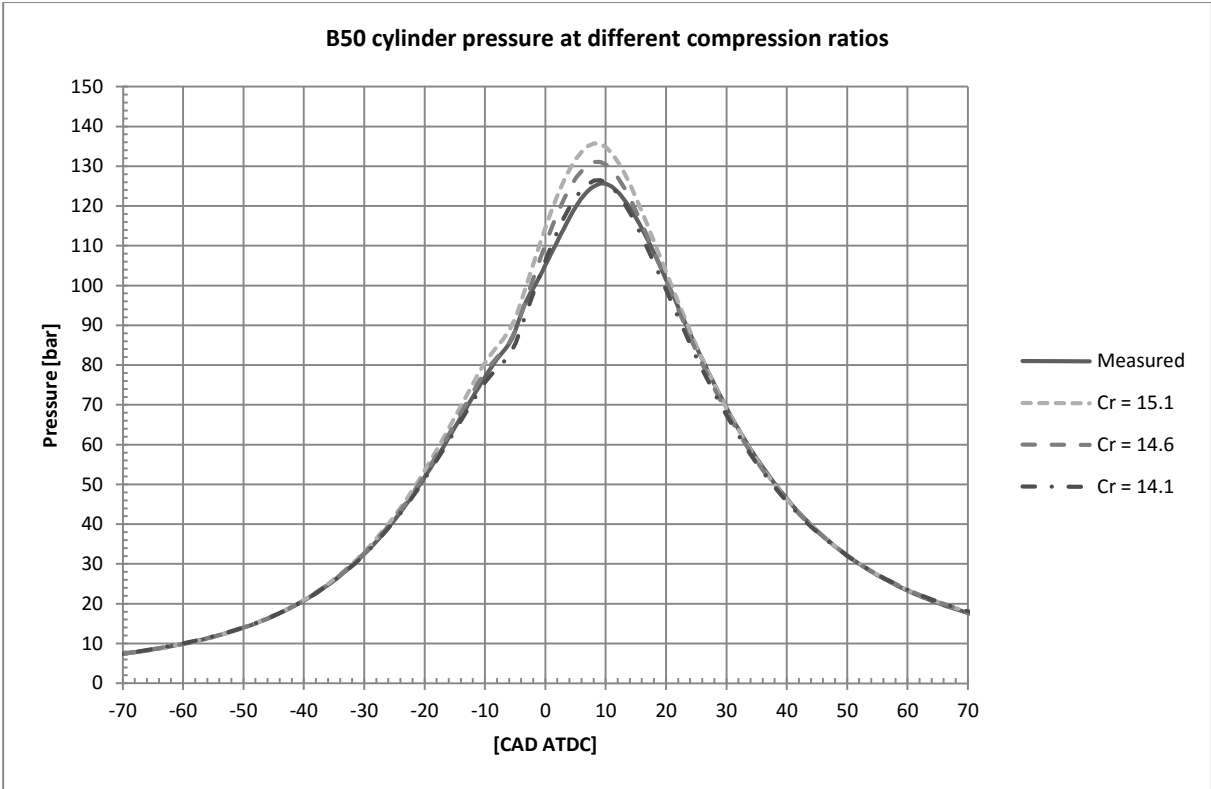


Figure 9.2 B50 cylinder pressure at different compression ratios. Measured data BNR306#237.

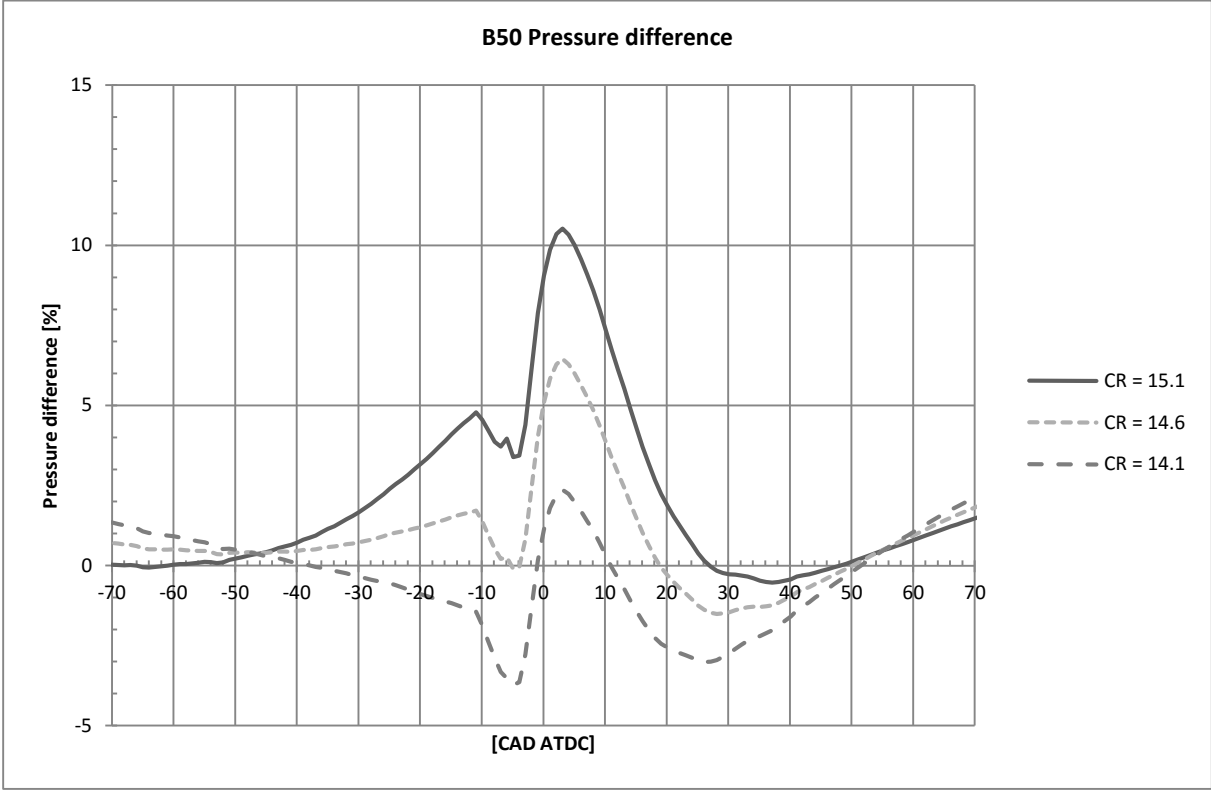


Figure 9.3 B50 percent difference in cylinder pressure for different compression ratios. Data compared to BNR306#237

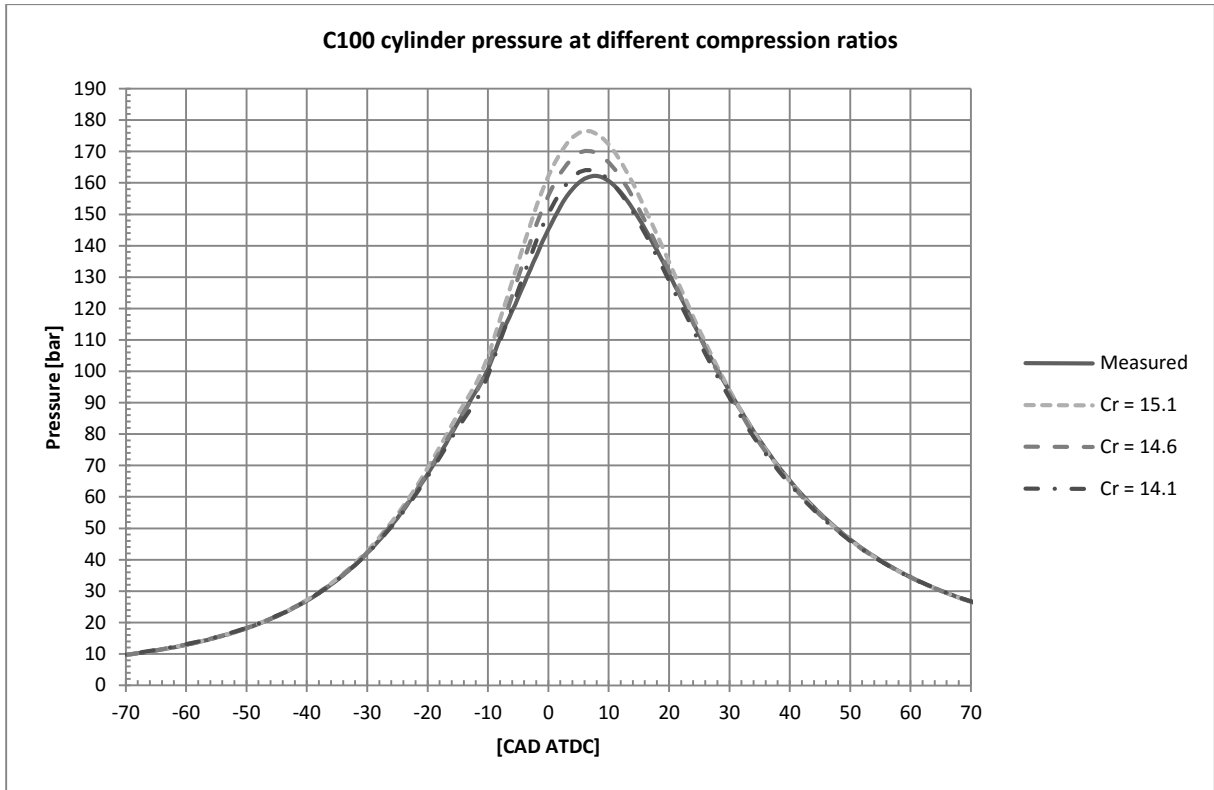


Figure 9.4 C100 cylinder pressure at different compression ratios. Measured data BNR306#241.

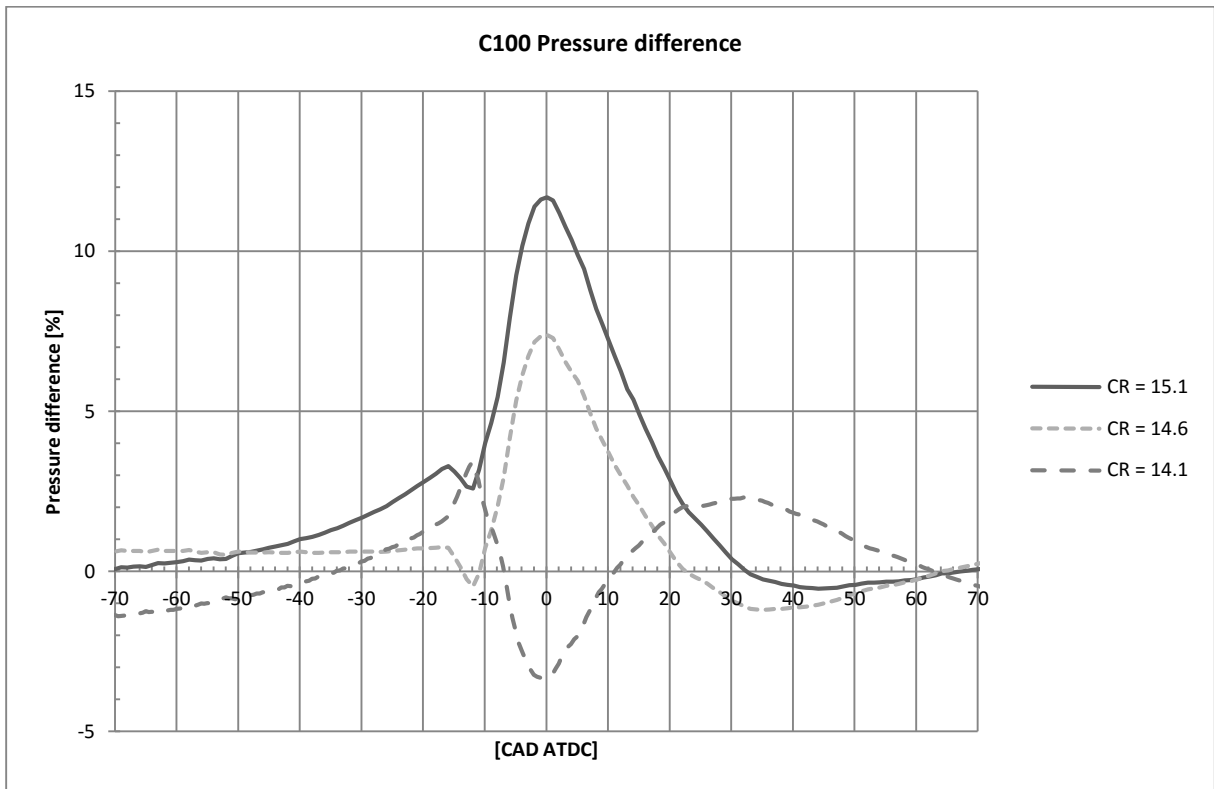


Figure 9.5 C100 percent difference in cylinder pressure for different compression ratios. Data compared to BNR306#241

A - 4 Effect of varying DI-Pulse multipliers

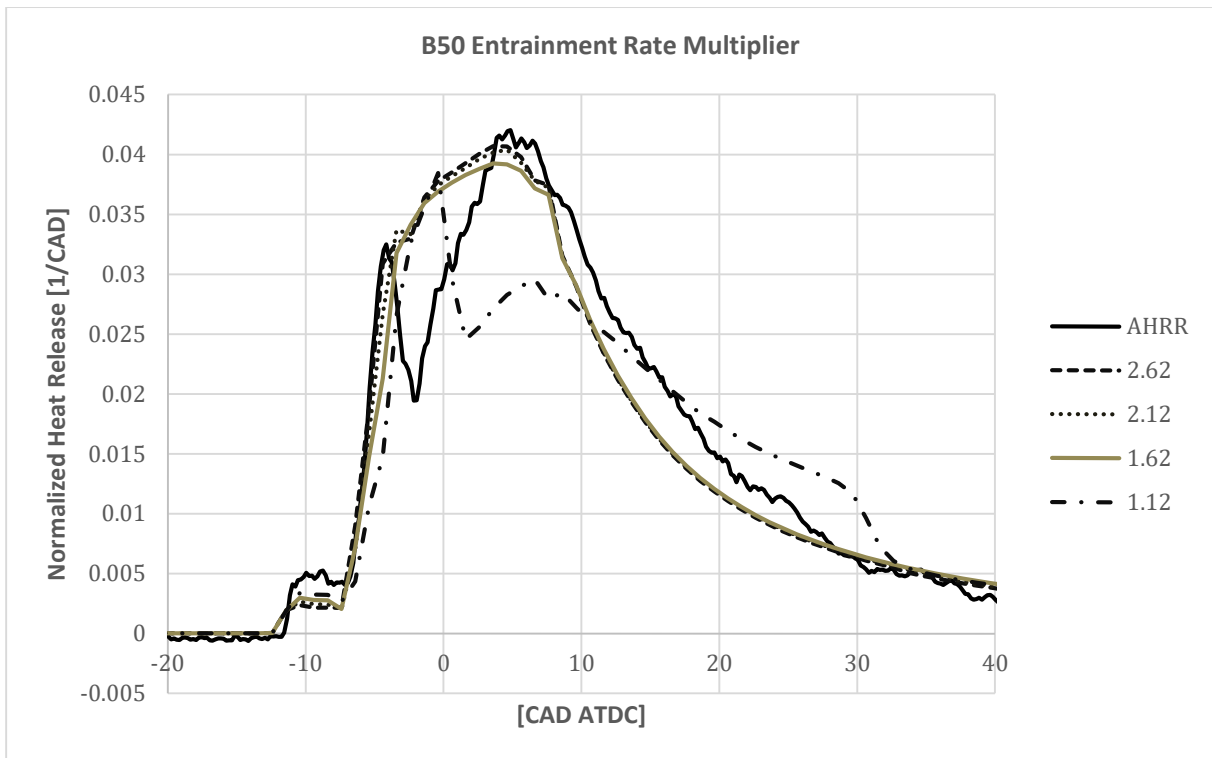


Figure 9.6 Entrainment Rate Multipliers, B50

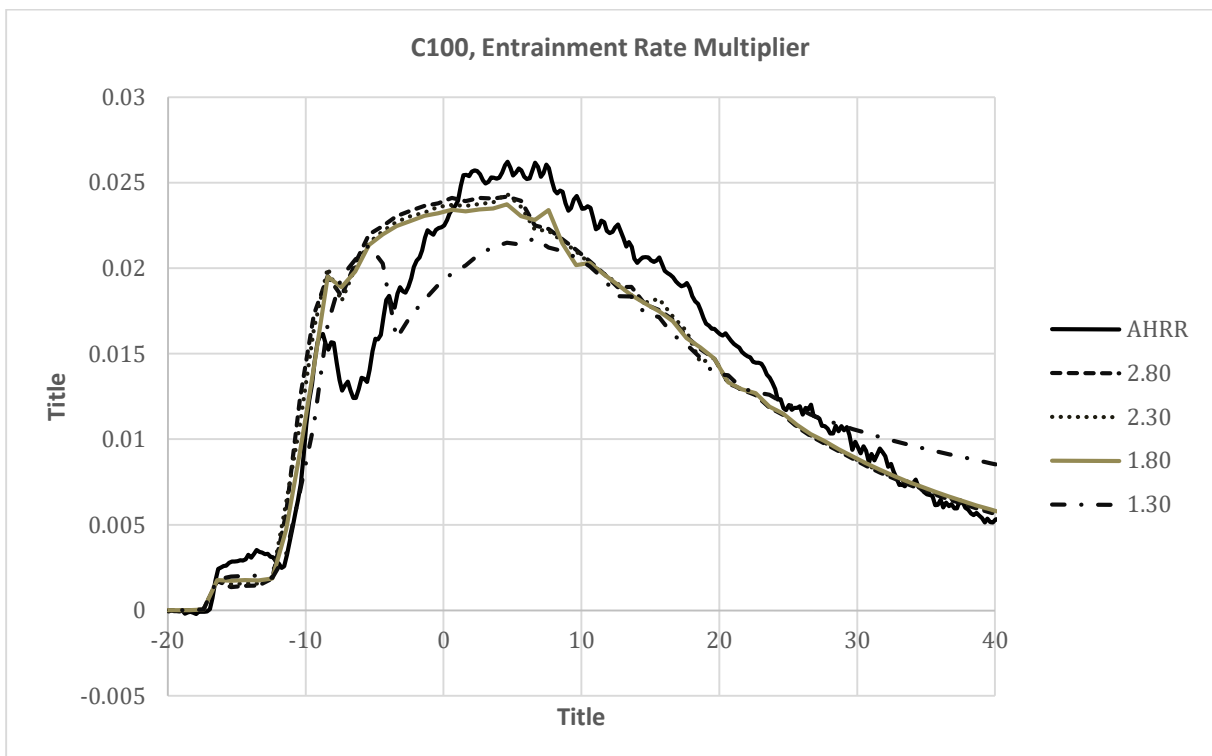


Figure 9.7 Entrainment Rate Multipliers, C100

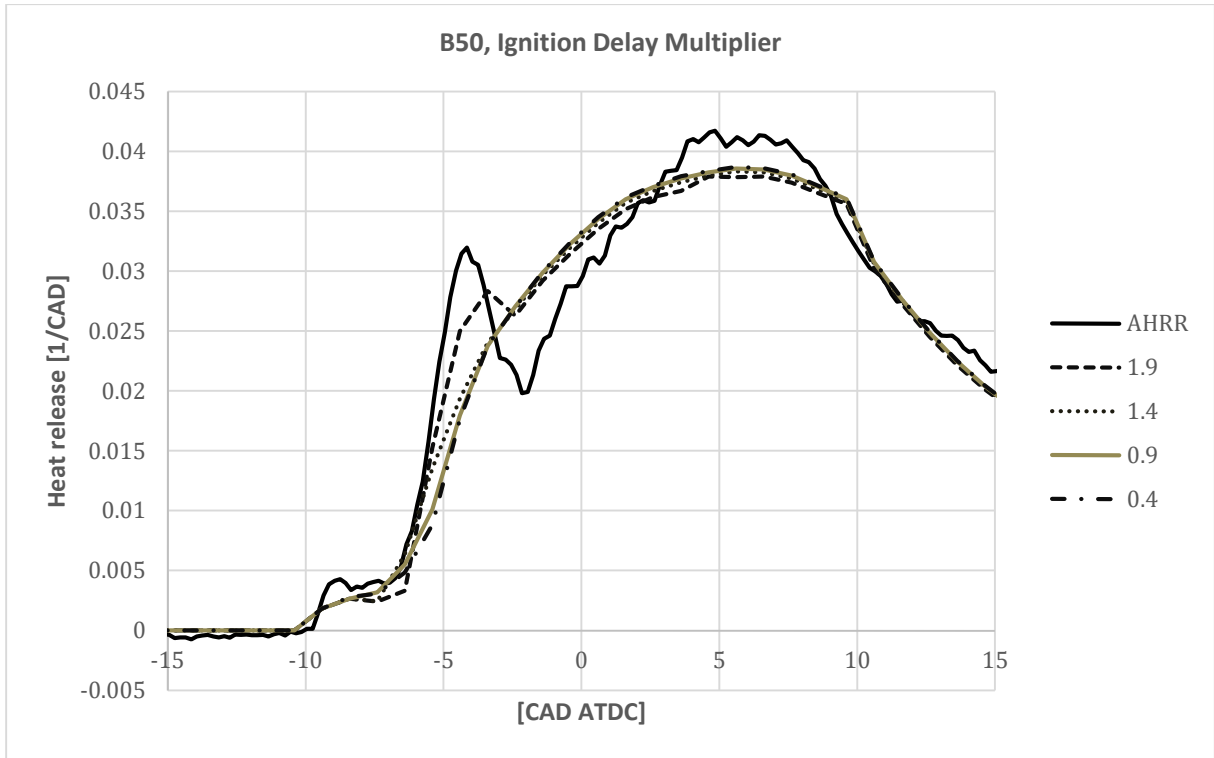


Figure 9.8 Ignition Delay Multipliers, B50

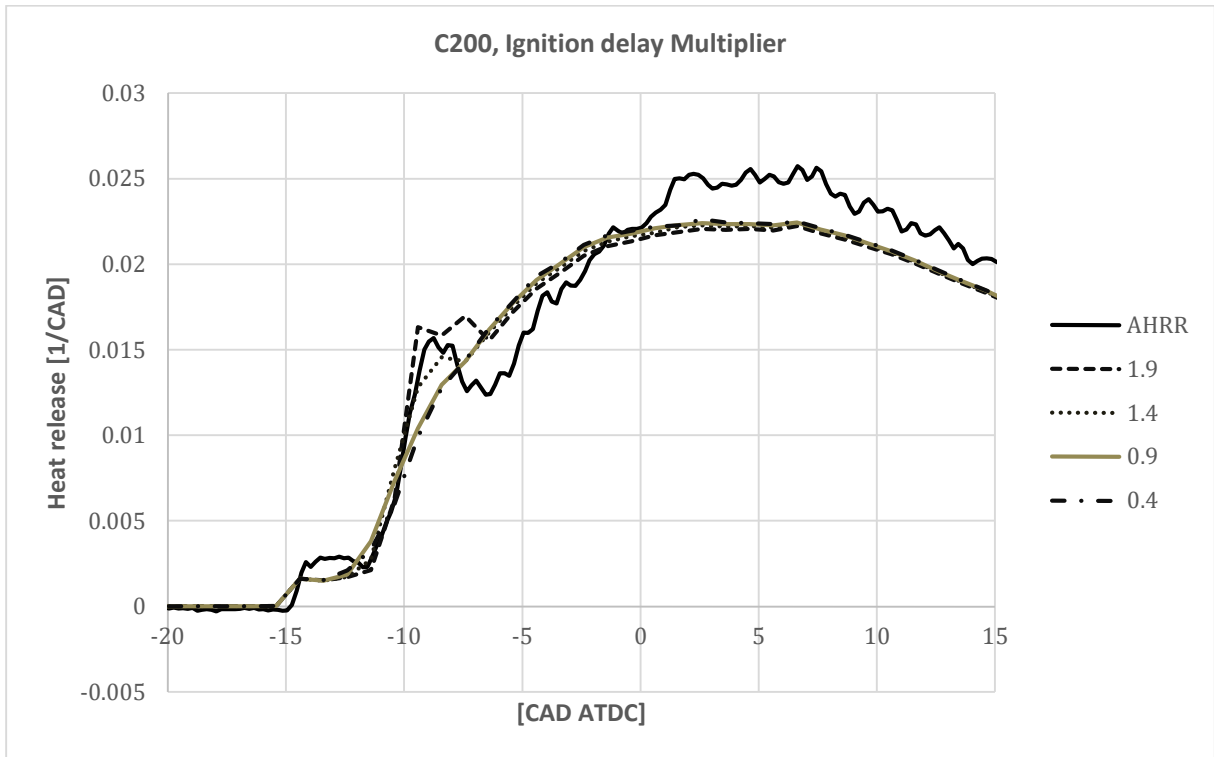


Figure 9.9 Ignition Delay Multipliers, C100

Table 9.4 Ignition delay for different ignition delay multipliers

Ignition Delay Multiplier	Ignition Delay B50, Step no 236 [CAD]	Ignition Delay C100 NO _x =0.24 [CAD]
1.9	3.52	4.00
1.4	2.78	3.40
0.9	1.97	2.60
0.4	1.10	1.69
Measurement data	2.50	3.40

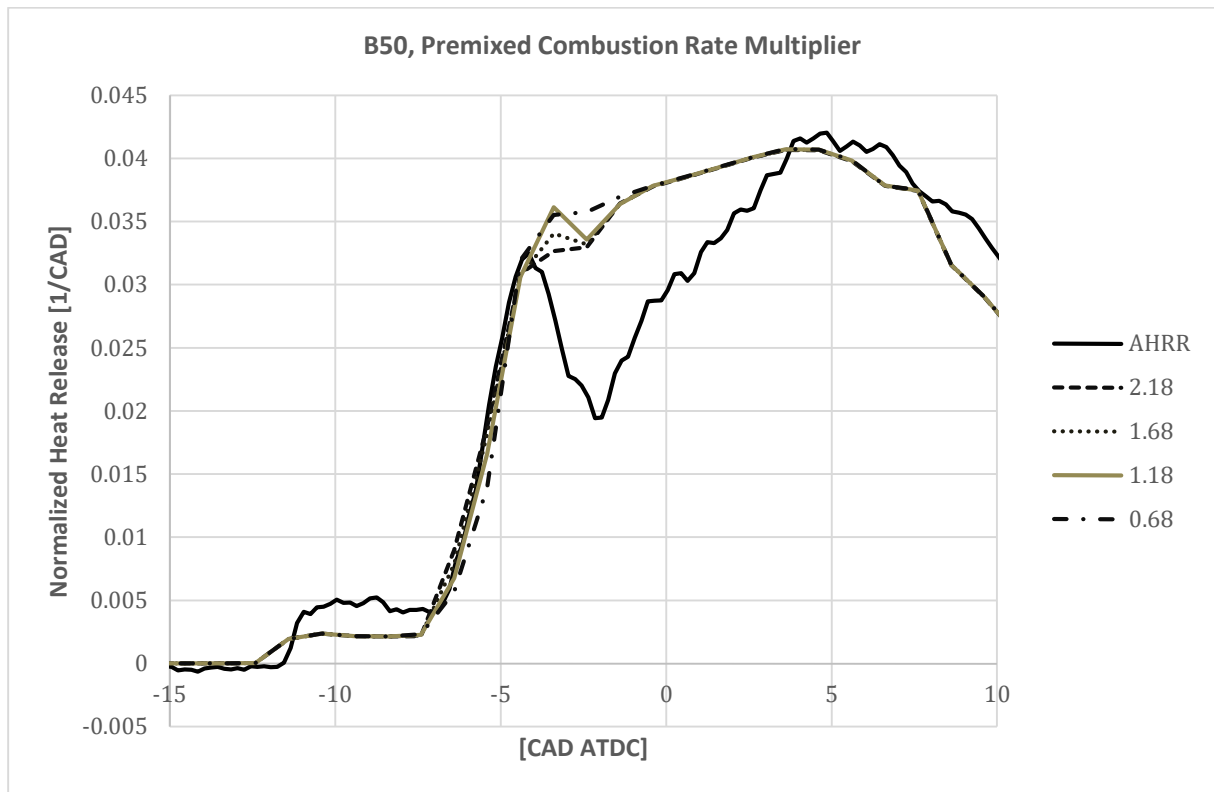


Figure 9.10 Premixed Combustion Rate Multiplier, B50

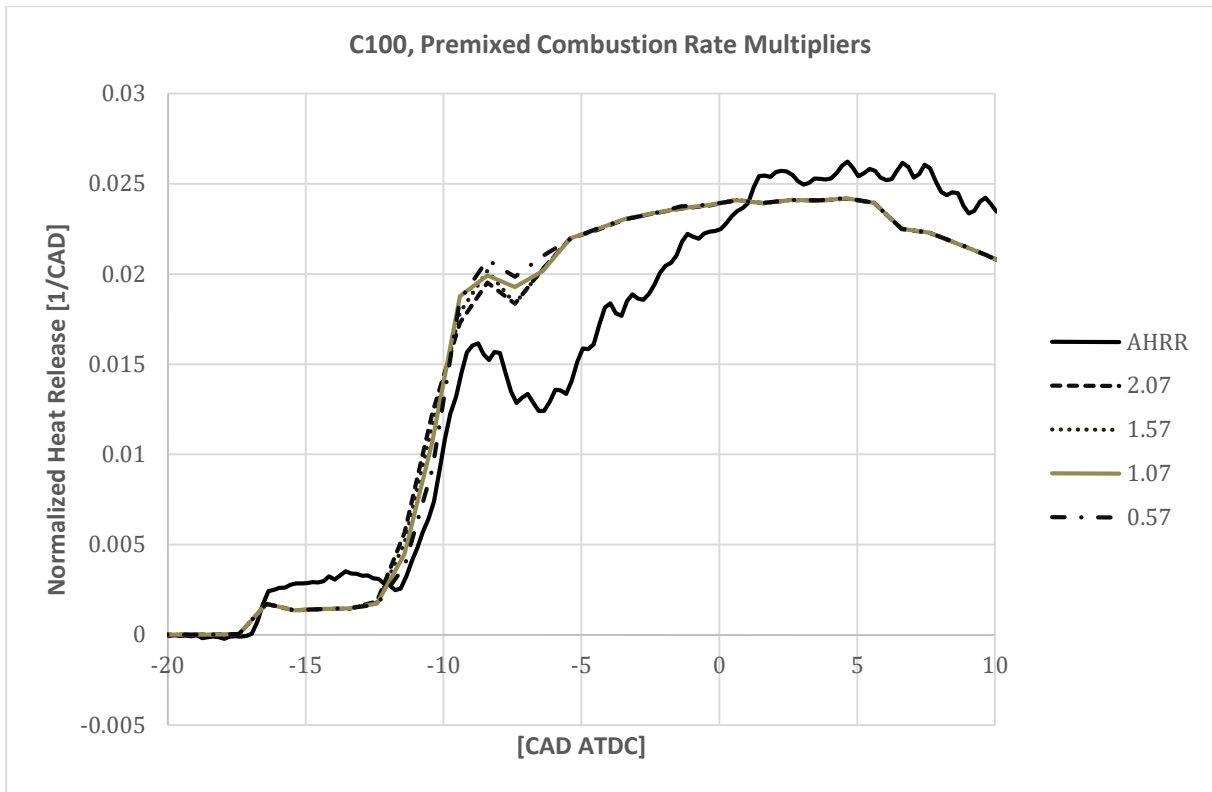


Figure 9.11 Premixed Combustion Rate Multiplier, C100

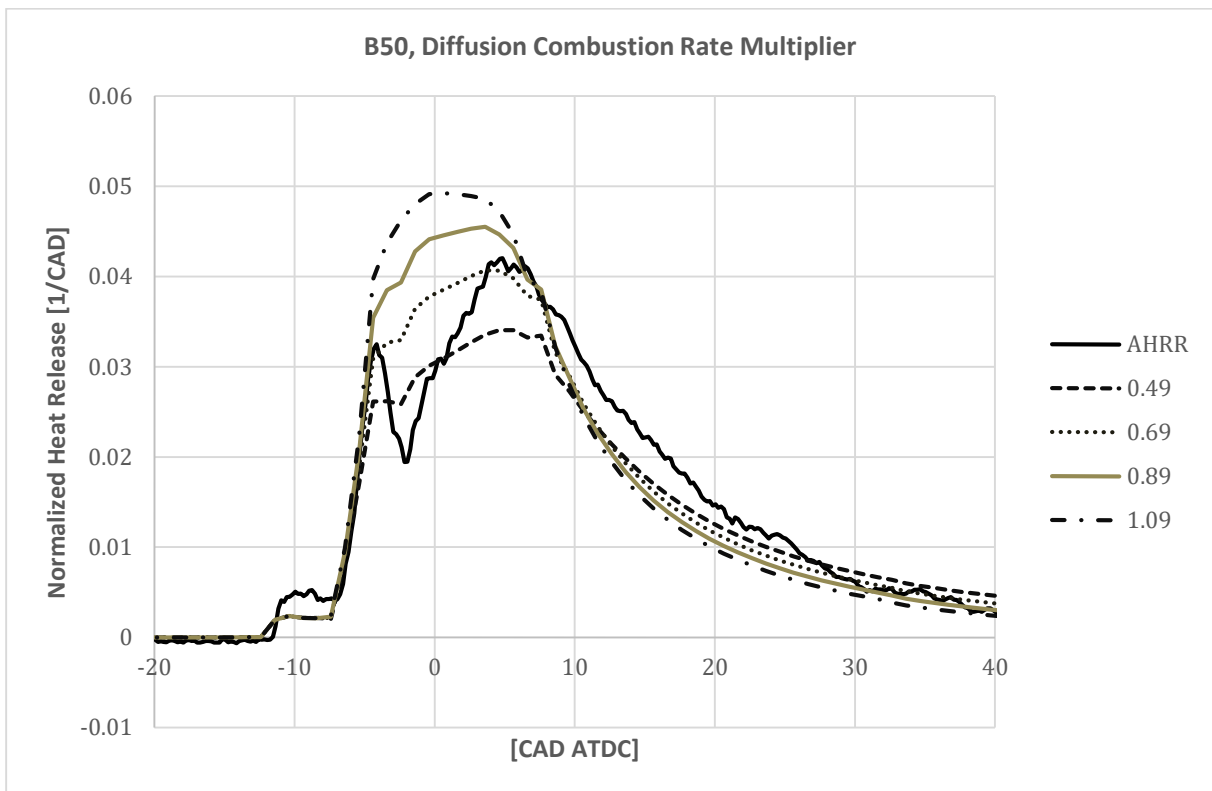


Figure 9.12 Diffusion Combustion Rate Multiplier, B50

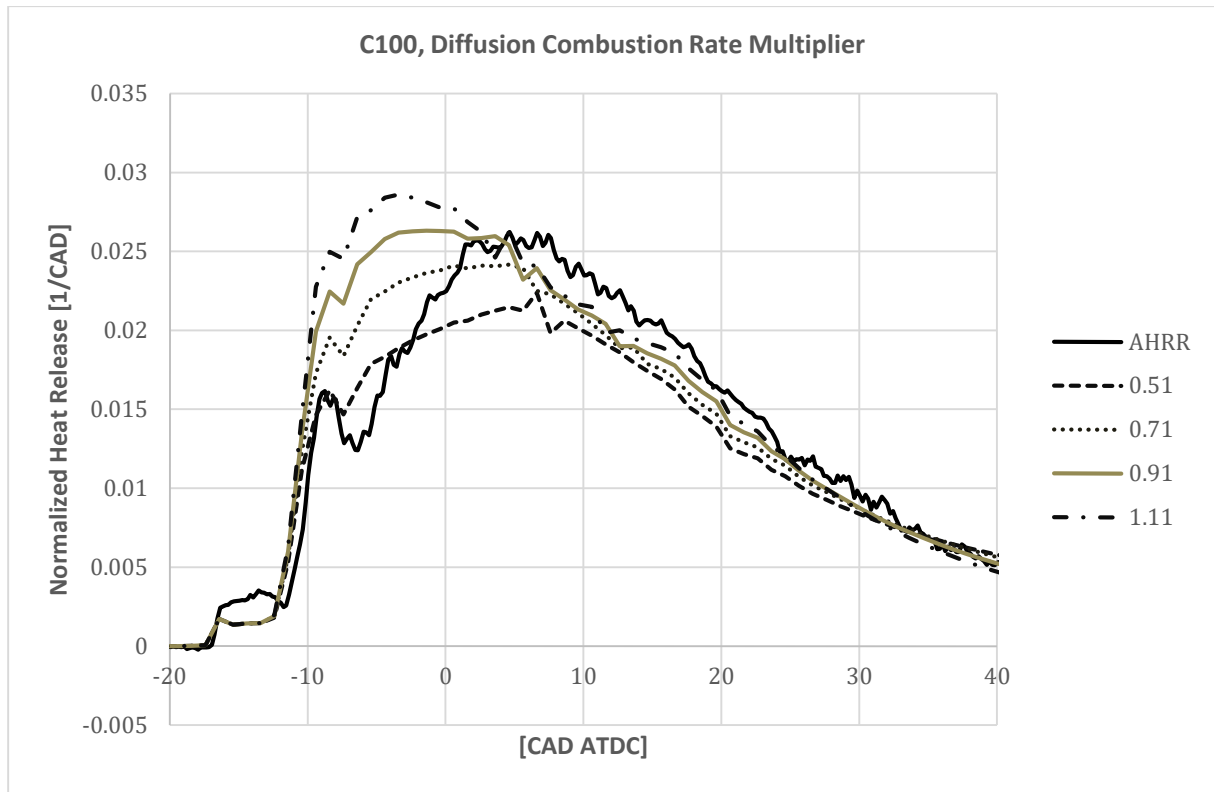


Figure 9.13 Diffusion Combustion Rate Multiplier, C100

A - 5 CO₂ concentration sensitivity

Since an EGR circuit is a feedback system it is important to set a lower limit of the amount of time simulated before checking convergence and have a low convergence setting. The lower limit is important due to the time it takes for certain part in the system to respond to changes. The convergence criterion is specified in absolute percentage units and is therefore not scaled with measured CO₂ concentration. To study the effect of convergence criteria on CO₂ concentration and CO₂ based EGR, several simulations with different convergence criteria were run. The results can vary significantly depending on the convergence criteria chosen, see figure 9.14 and figure 9.15. Hence, as a result of the CO₂ concentration variation the amount of EGR, based on CO₂ concentration, changes as can be seen in figure 9.16. It is important to keep in mind that computational time increases with lower value of convergence.

All simulations run converged, except the one with the narrowest criteria of 1E-5 percentage units where it reached the upper limit of the allowed simulation time (150 seconds).

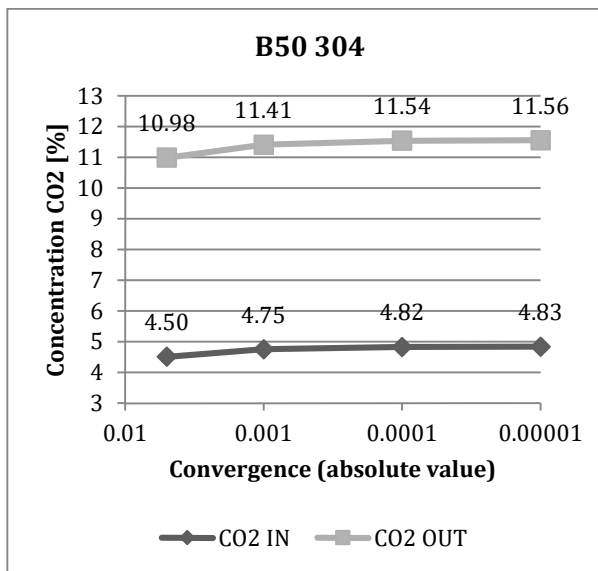


Figure 9.14 CO₂ concentrations in B50 BNR308#304

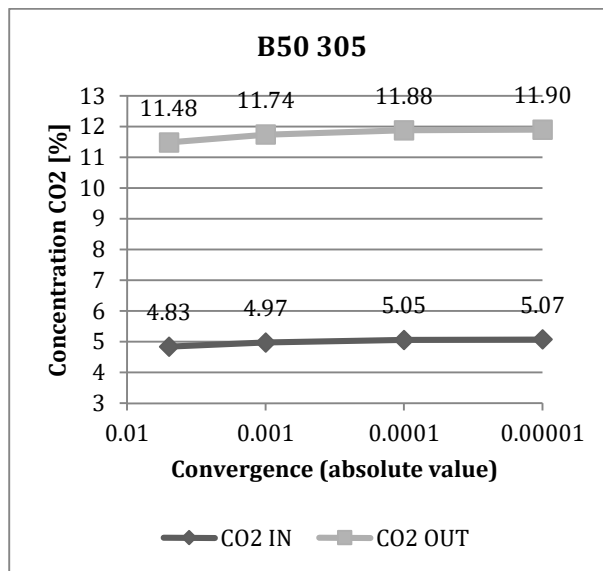


Figure 9.15 CO₂ concentrations in B50 BNR308#305

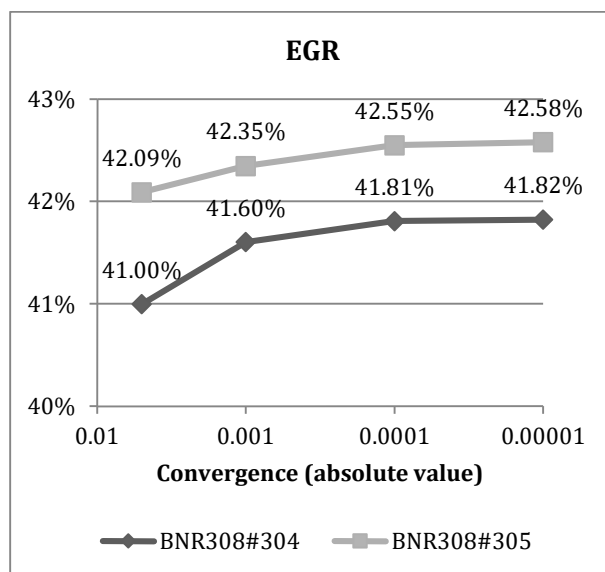


Figure 9.16 EGR rates of B50 BNR308 #304 & #305

A - 6 Injection and combustion events

The data in table 9.5 are gathered from AHRR calculated by OSIRIS and the fast pressure sensor “P_injl”. The ignition delay is calculated based on SOC and SOI whereas the injection duration is the difference between EOI and SOI.

Table 9.5 Measured injection and combustion events, BNR 306

Step no	Load Point	Piston	SOC [CAD ATDC]	SOI [CAD ATDC]	EOI [CAD ATDC]	Ignition delay [CAD]	Injection duration [CAD]
236	B50	ø92 Diesel	-7.4	-9.9	11.5	2.5	21.4
237	B50	ø92 Diesel	-7.4	-9.9	11.6	2.5	21.5
250	B50	ø92 Diesel	-8.1	-9.9	10.2	1.8	20.1
240	C100	ø92 Diesel	-11.6	-15.0	25.2	3.4	40.2
241	C100	ø92 Diesel	-11.7	-15.0	24.0	3.3	39.0
181	B50	Ø88-REC DME	-7.4	-10	11.3	2.6	21.3
182	B50	Ø88-REC DME	-7.5	-10	11.1	2.5	21.1
156	C100	Ø88-REC DME	-11.6	-15.1	24	3.5	39.1
157	C100	Ø88-REC DME	-11.6	-15.1	23.6	3.5	38.7

Table 9.6 Difference between simulated and measured injection duration for all load points

Step number	Load Point	Piston	Injection duration difference between simulated and measured [%]
236	B50	ø92 Diesel	10.7
237	B50	ø92 Diesel	11.6
250	B50	ø92 Diesel	12.9
240	C100	ø92 Diesel	-1.5
241	C100	ø92 Diesel	-2.8
181	B50	Ø88-REC DME	-10.3
182	B50	Ø88-REC DME	-10.9
156	C100	Ø88-REC DME	3.6
157	C100	Ø88-REC DME	3.4

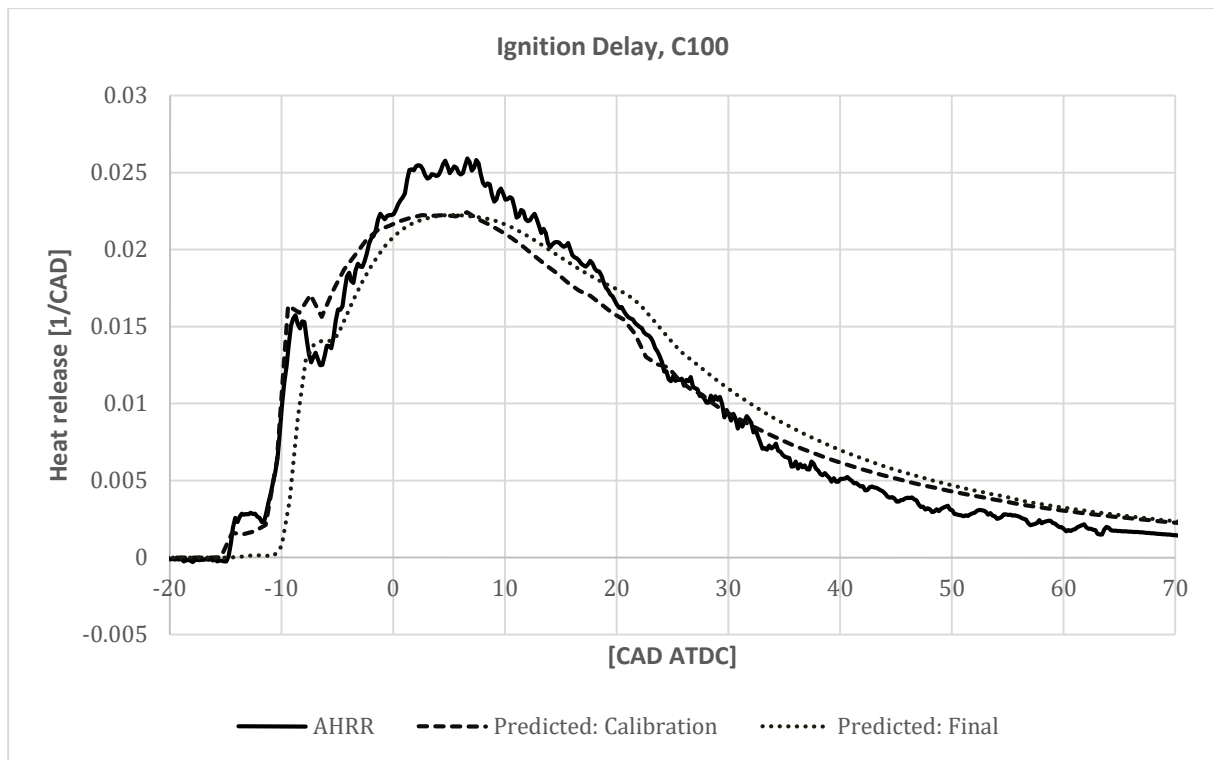


Figure 9.17 Heat release showing the effect of the ignition delay model. "Predicted: Final" has an ignition delay model. AHRR is calculated from measured cylinder pressure data BNR306#240.

A - 7 Pressure and Heat Release curves from final model (case 4)

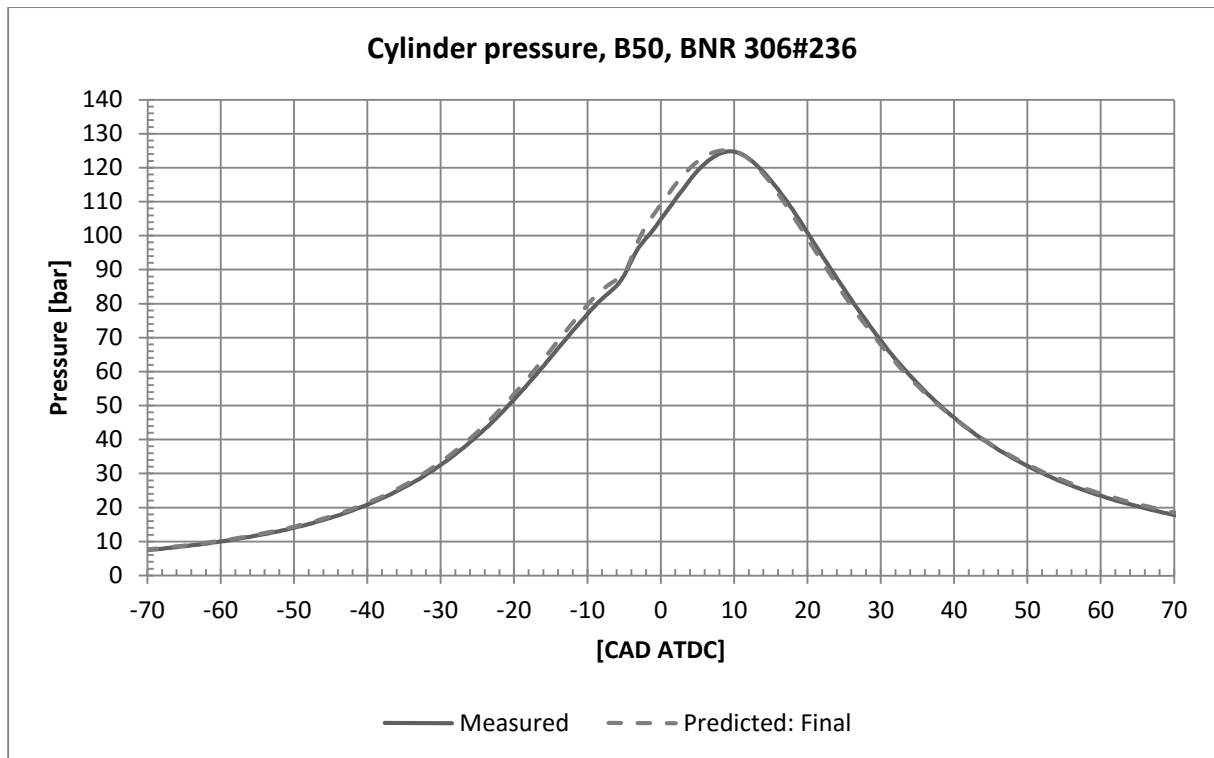


Figure 9.18 Cylinder pressure of load point B50 compared with measured pressure from BNR306#236.

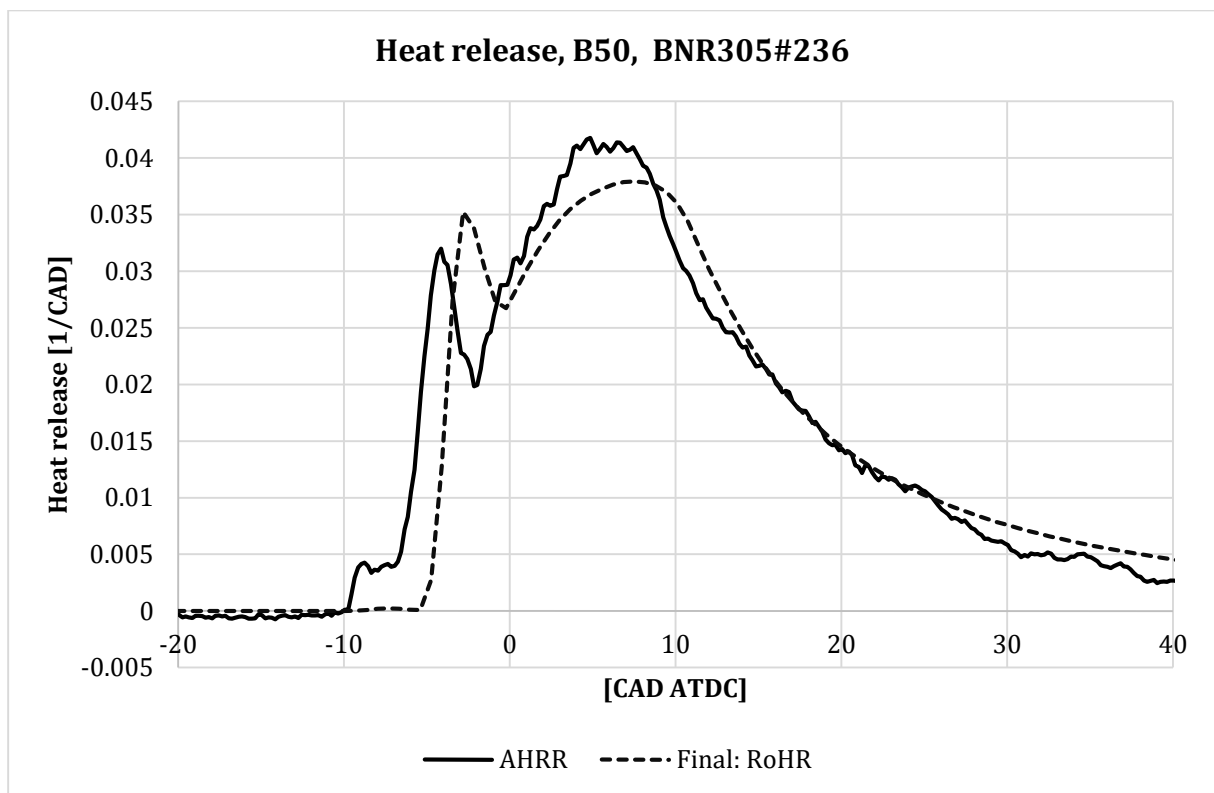


Figure 9.19 Heat release from load point B50 compared with calculated AHRR based on measured cylinder pressure from BNR306#236.

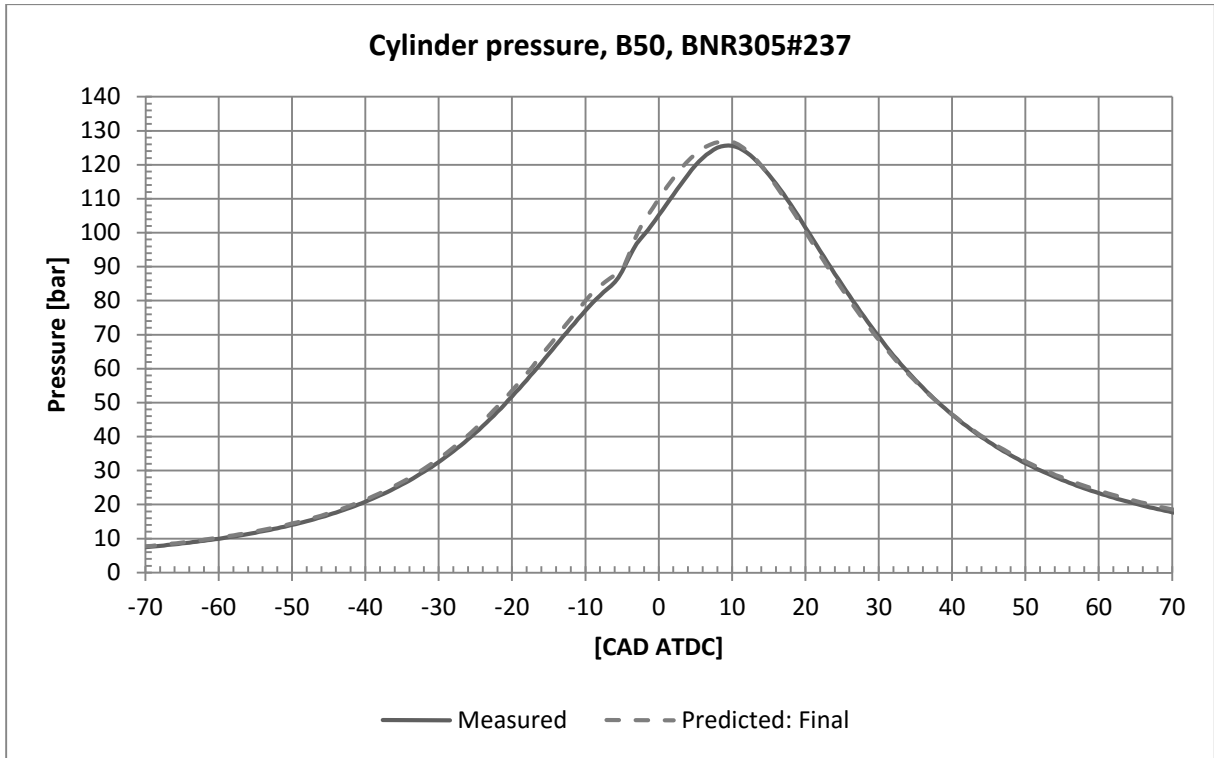


Figure 9.20 Cylinder pressure of load point B50 compared with measured pressure from BNR306#237.

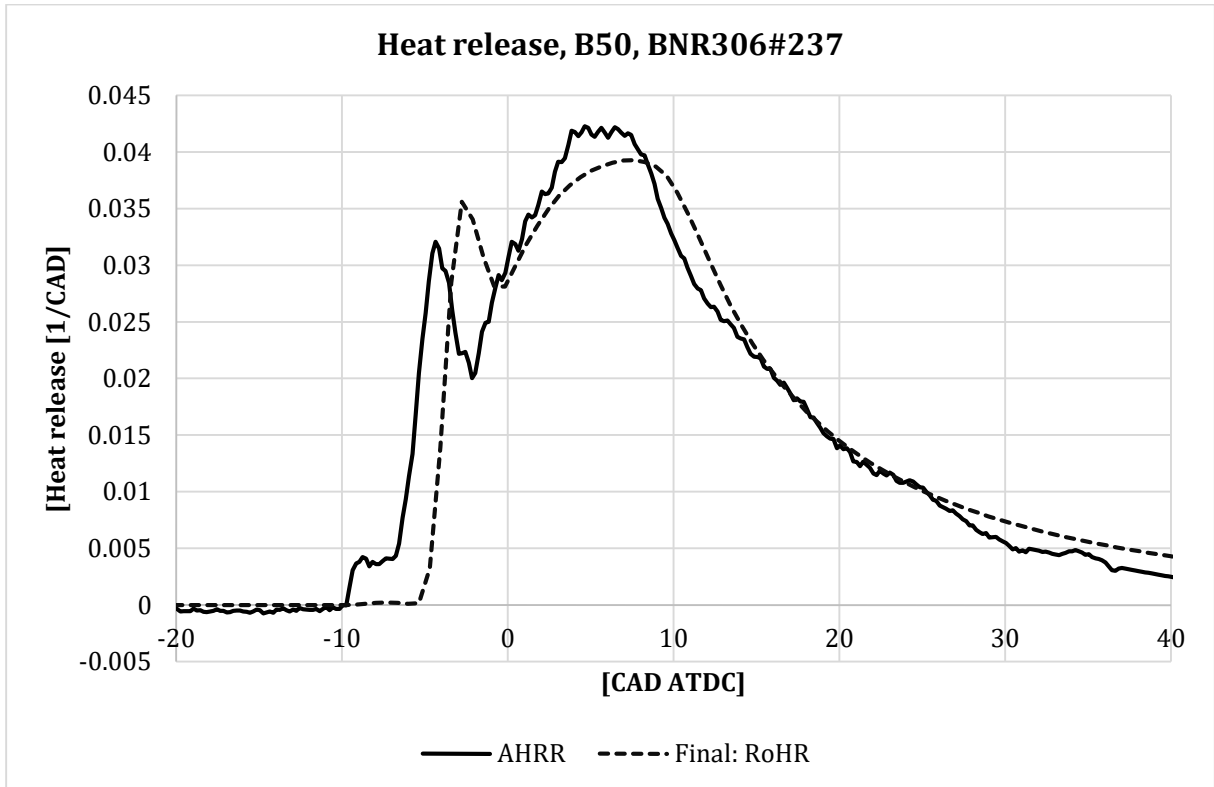


Figure 9.21 Heat release from load point B50 compared with calculated AHRR based on measured cylinder pressure from BNR306#237.

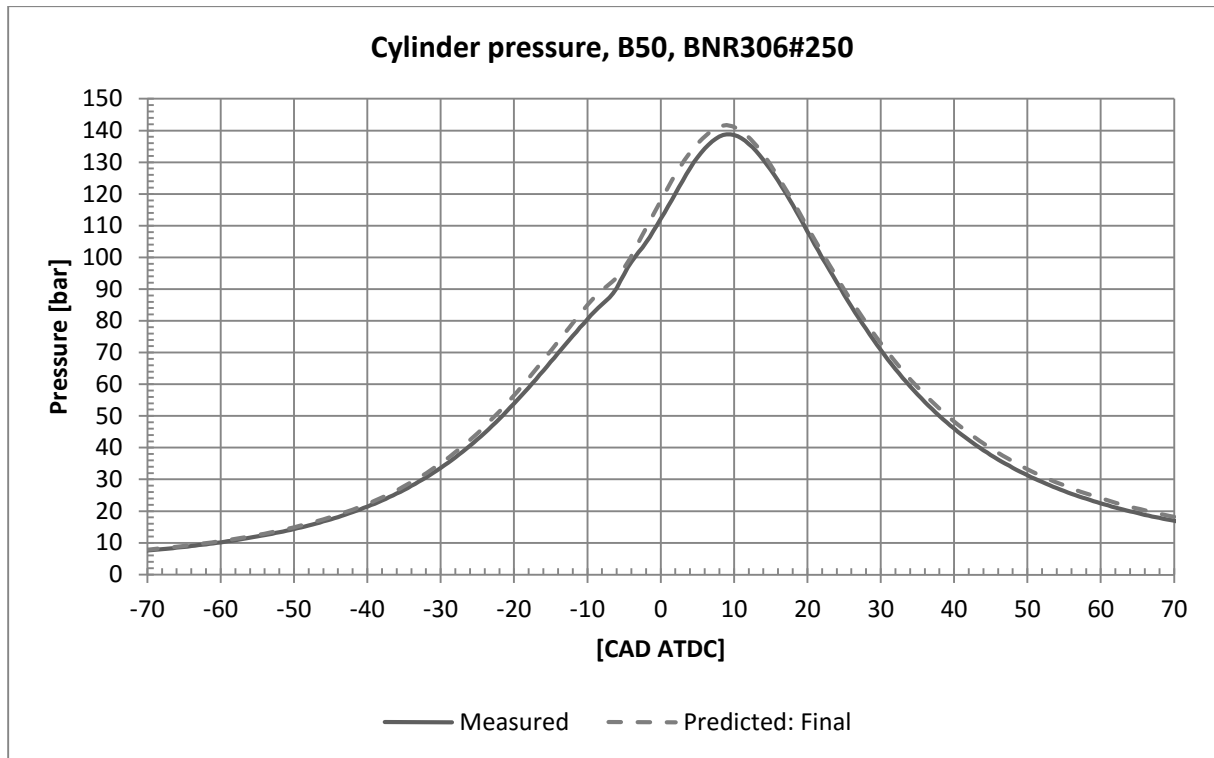


Figure 9.22 Cylinder pressure of load point B50 compared with measured pressure from BNR306#250.

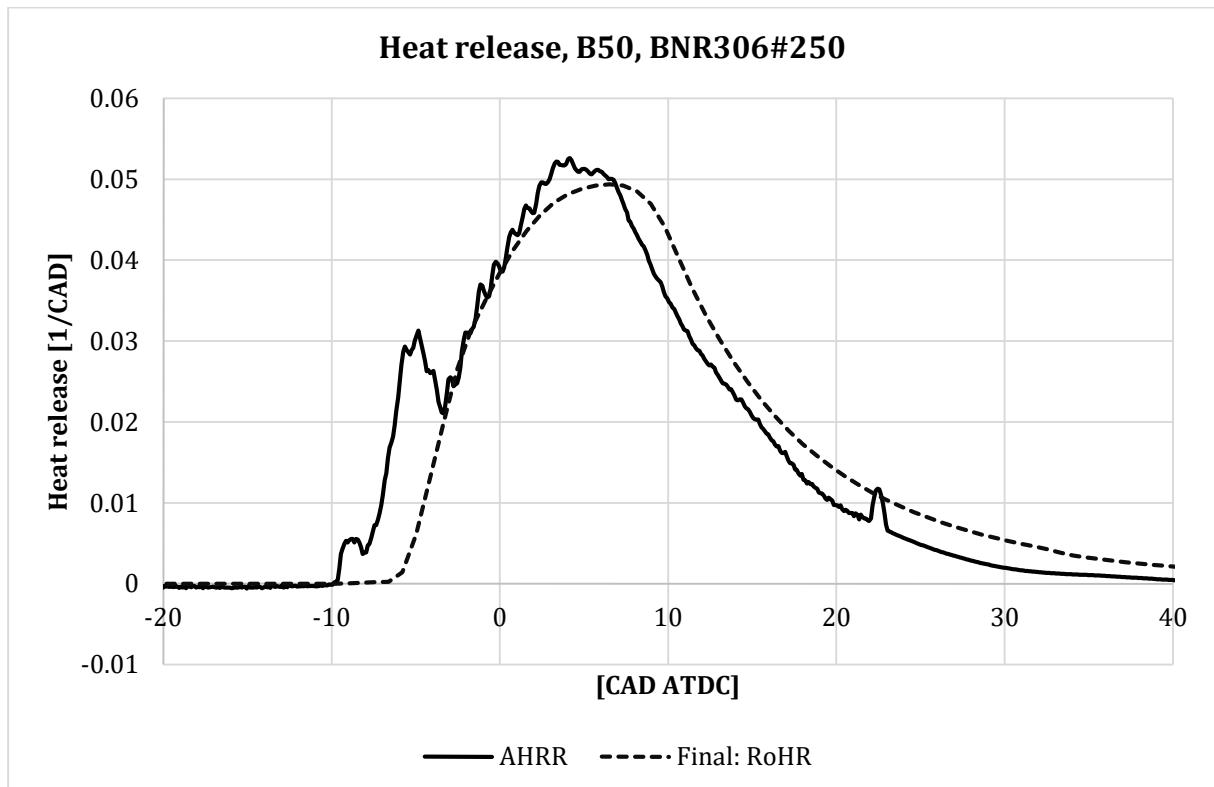


Figure 9.23 Heat release from load point B50 compared with calculated AHRR based on measured cylinder pressure from BNR306#250.

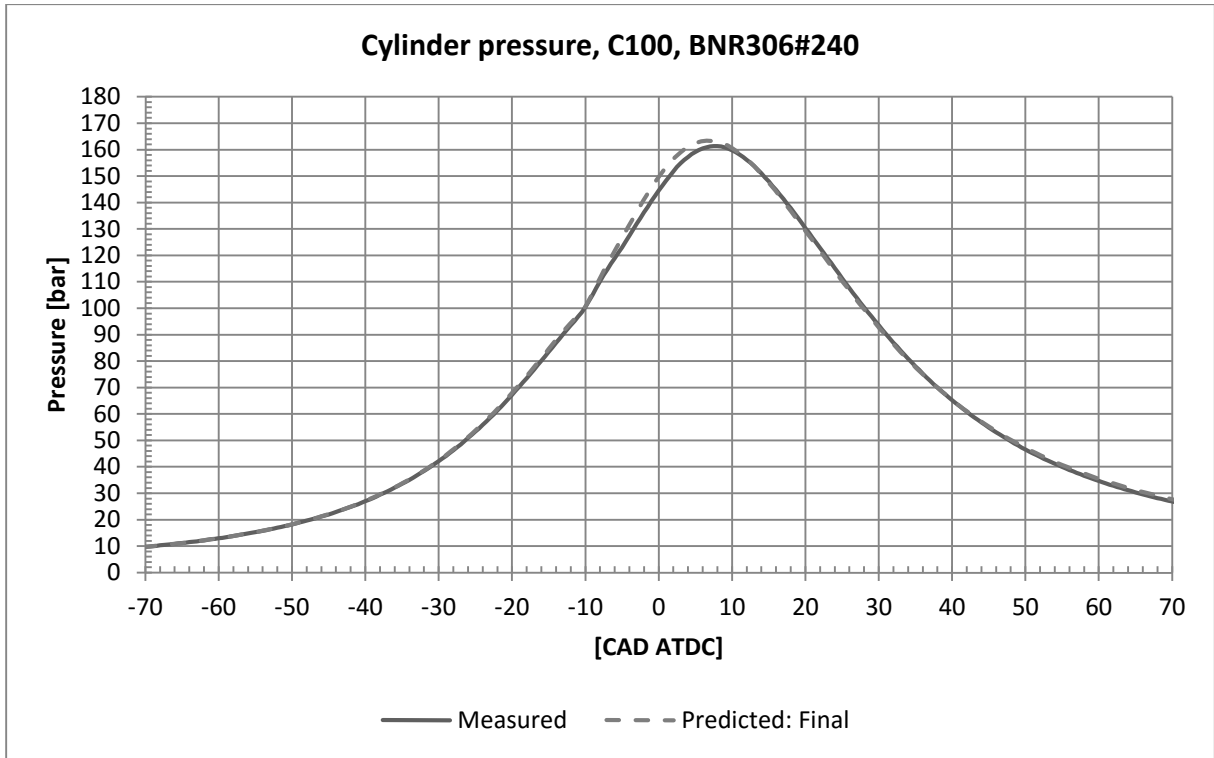


Figure 9.24 Cylinder pressure of load point C100 compared with measured pressure from BNR306#240.

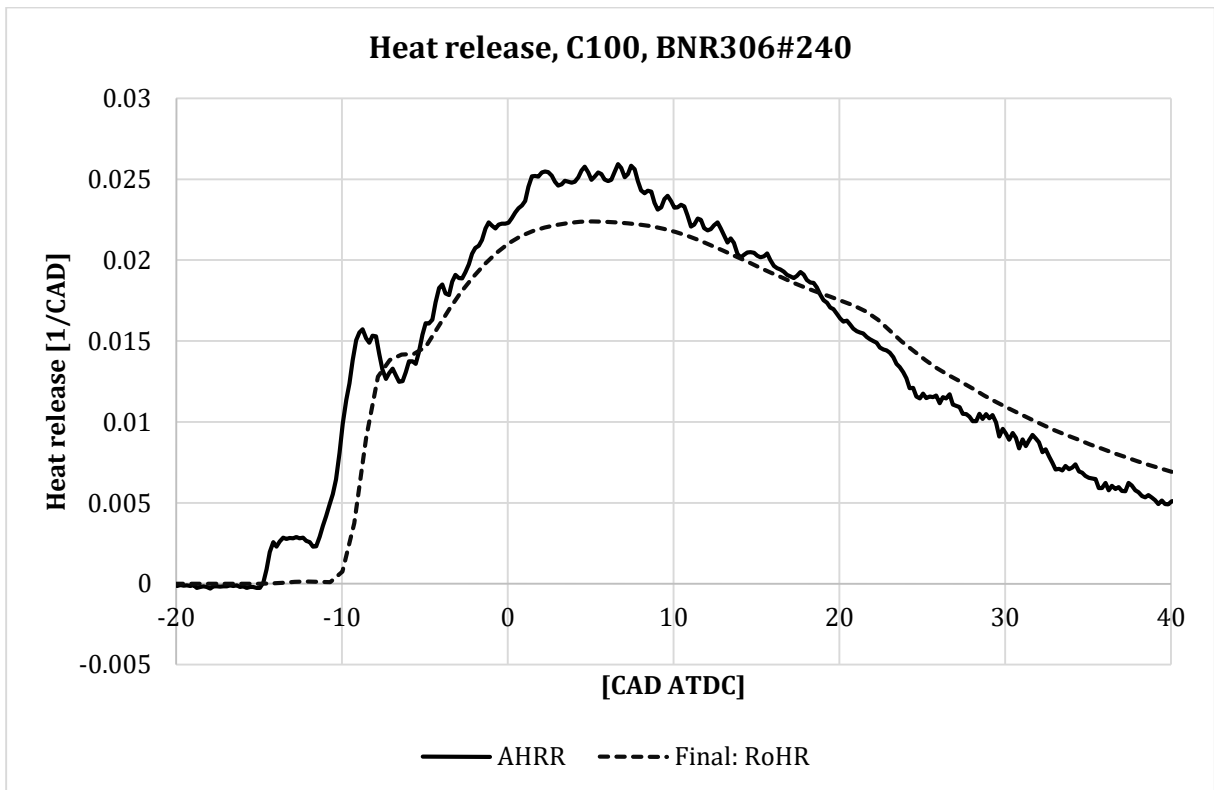


Figure 9.25 Heat release from load point C100 compared with calculated AHRR based on measured cylinder pressure from BNR306#240.

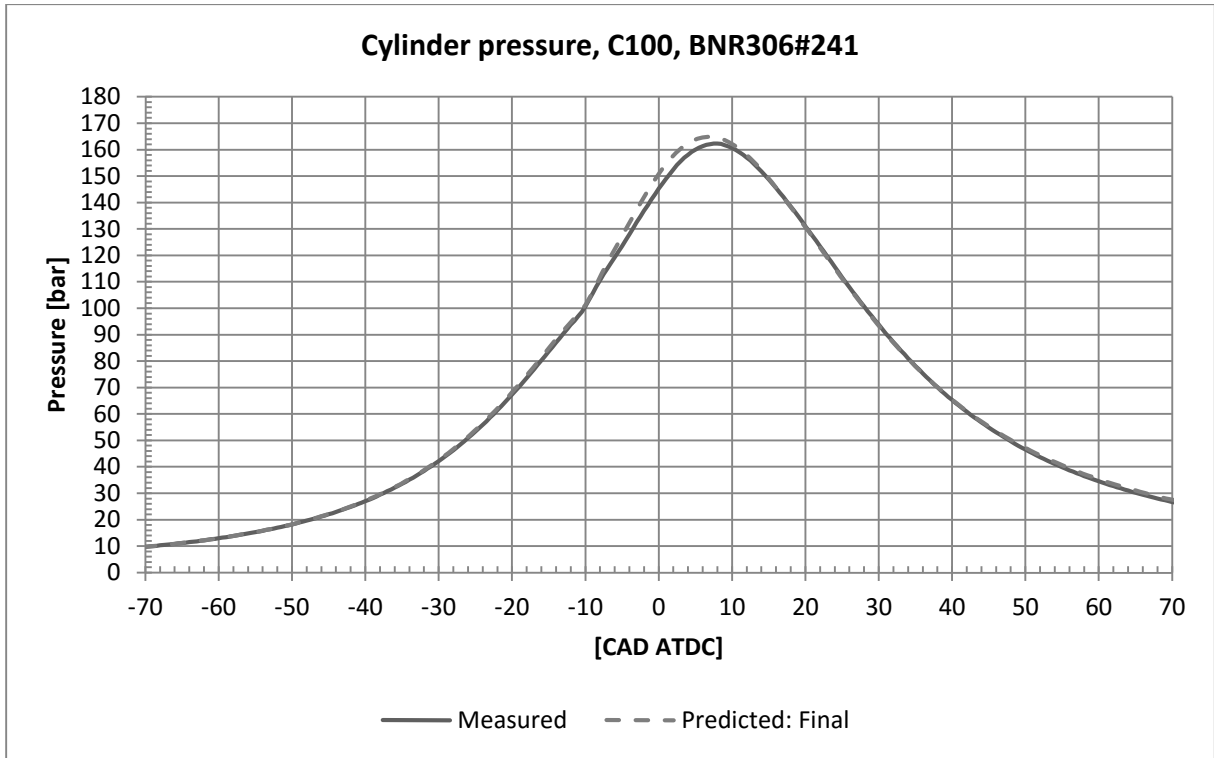


Figure 9.26 Cylinder pressure of load point C100 compared with measured pressure from BNR306#241.

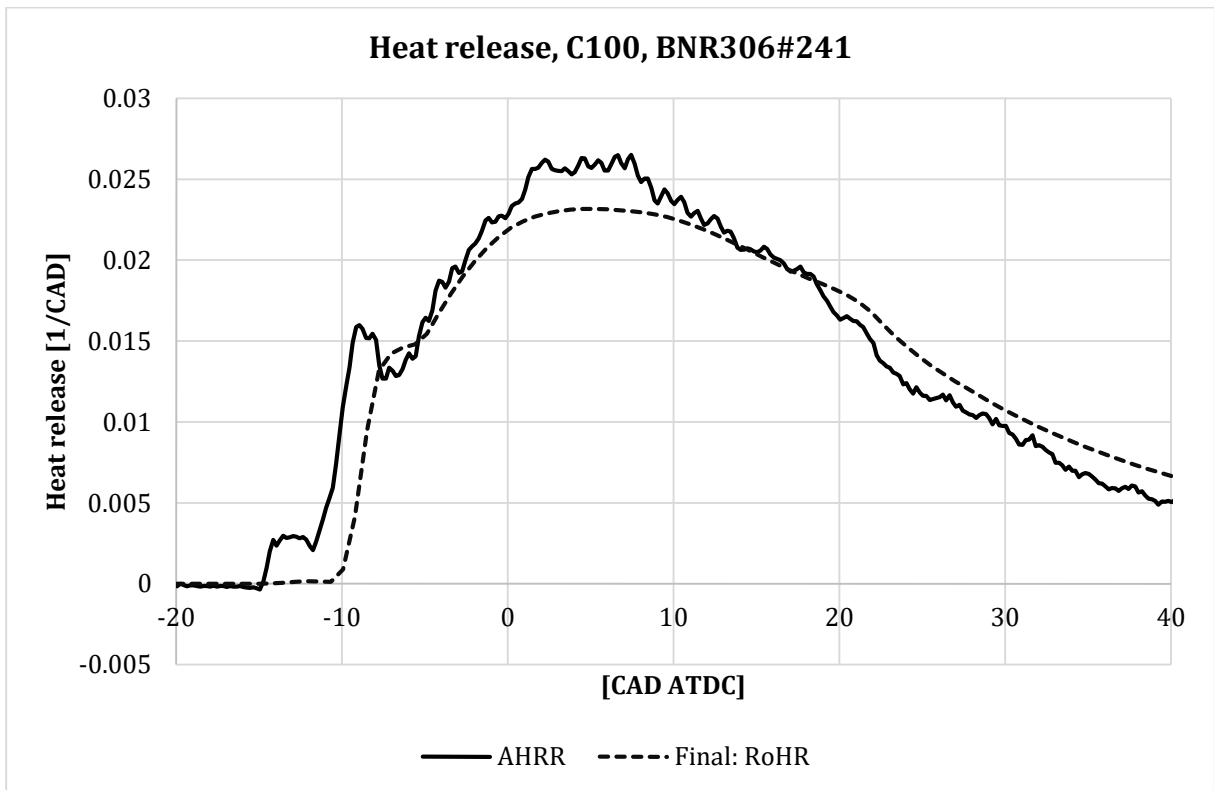


Figure 9.27 Heat release from load point C100 compared with calculated AHRR based on measured cylinder pressure from BNR306#241.

Appendix B Drawings and Schematics

B - 1 Drawings and external measurements

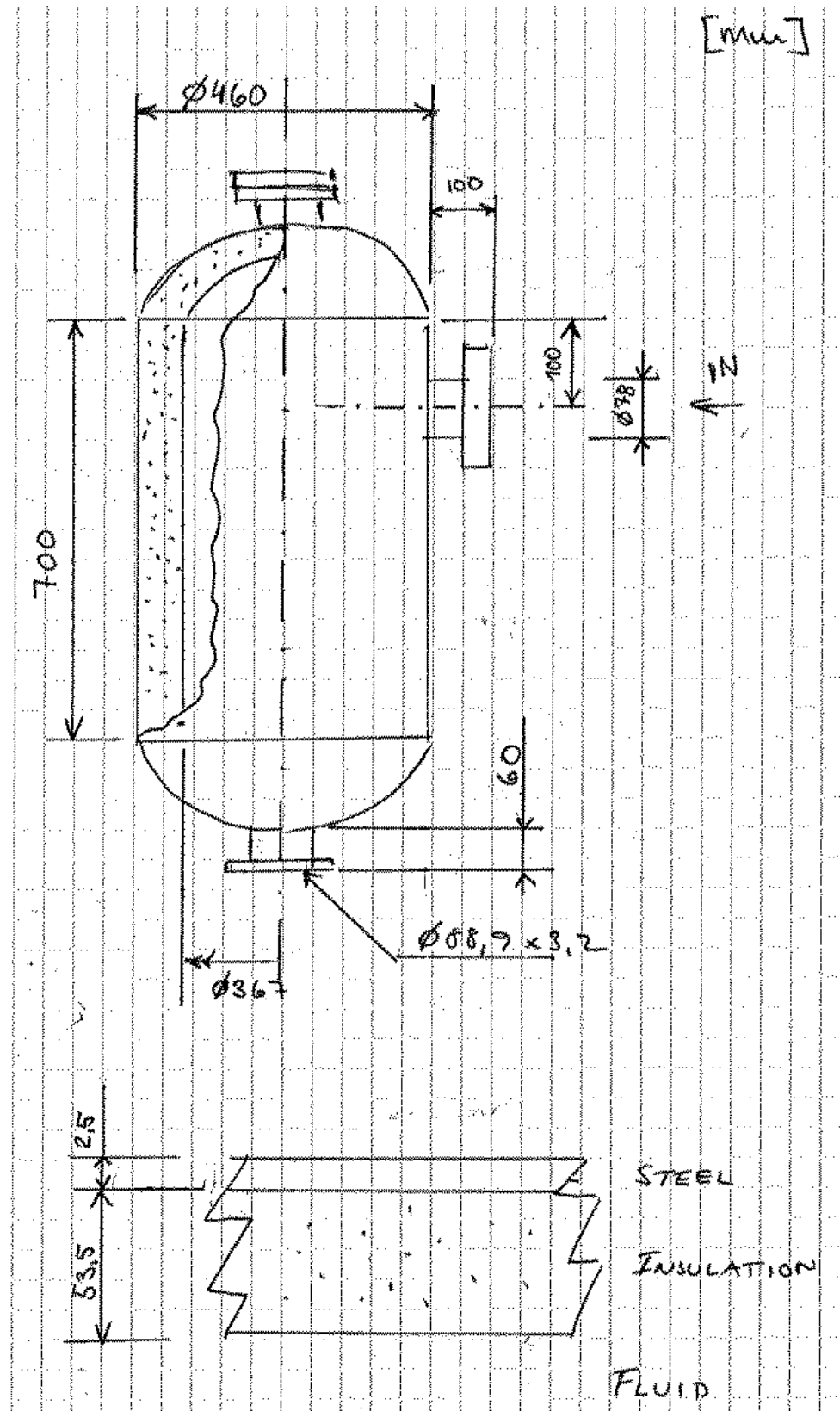


Figure 9.28 Drawing: exhaust tank

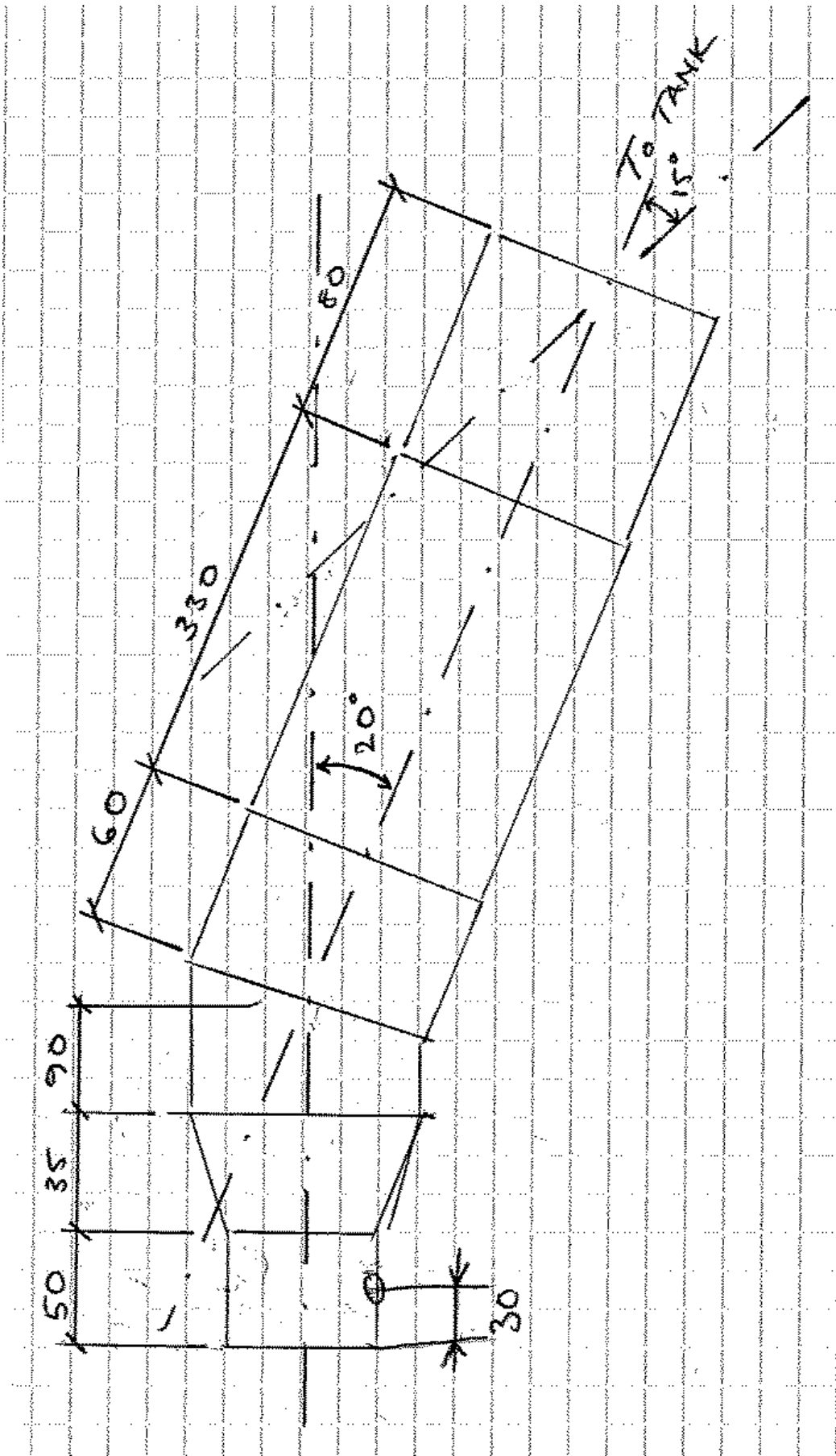


Figure 9.29 Drawing: exhaust pipe

DN 100 / 114,3 DIN 2633 PN 16 L 22,8

BF42 70 969 XA (H)

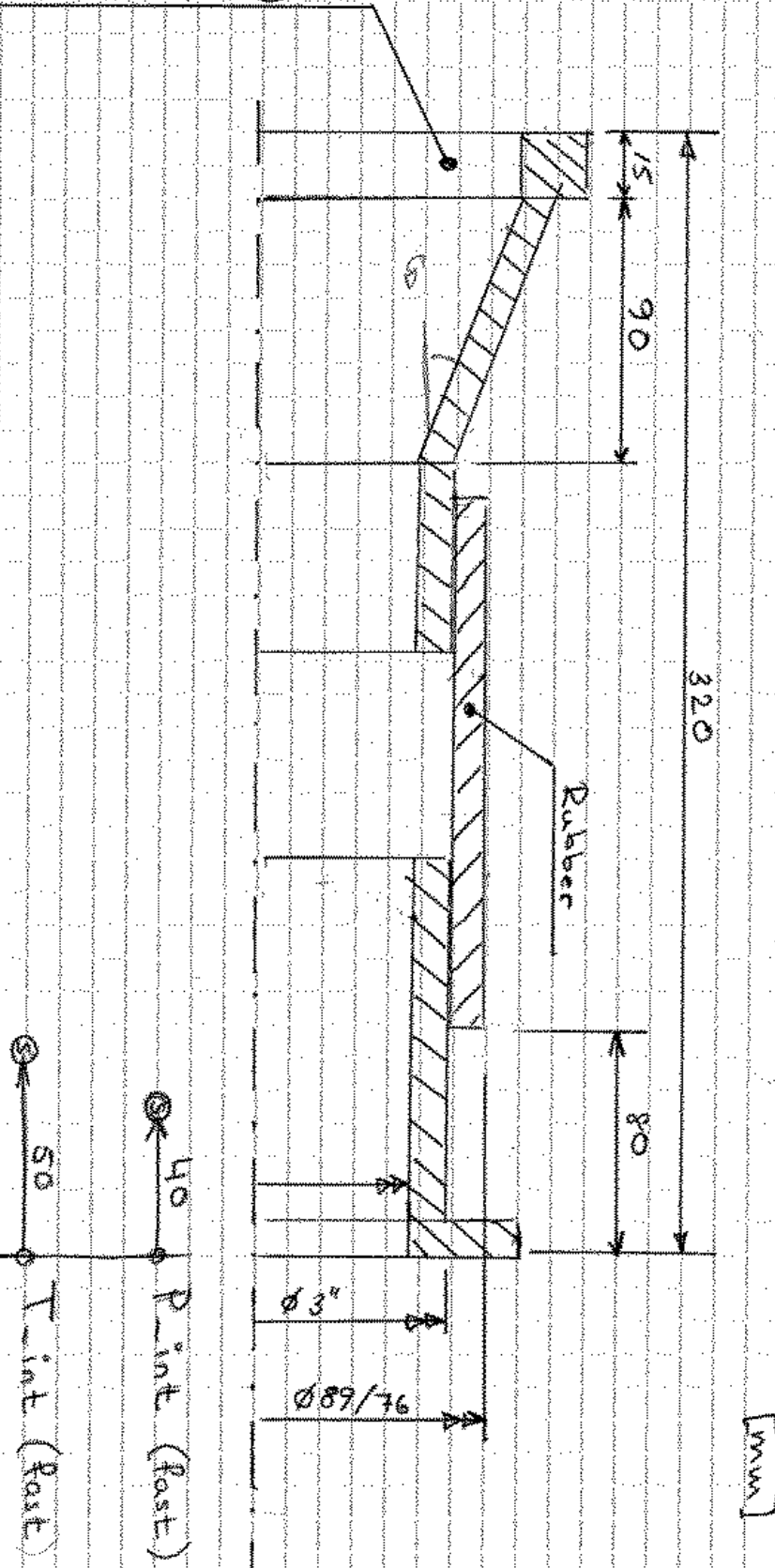


Figure 9.30 Drawing: inlet manifold

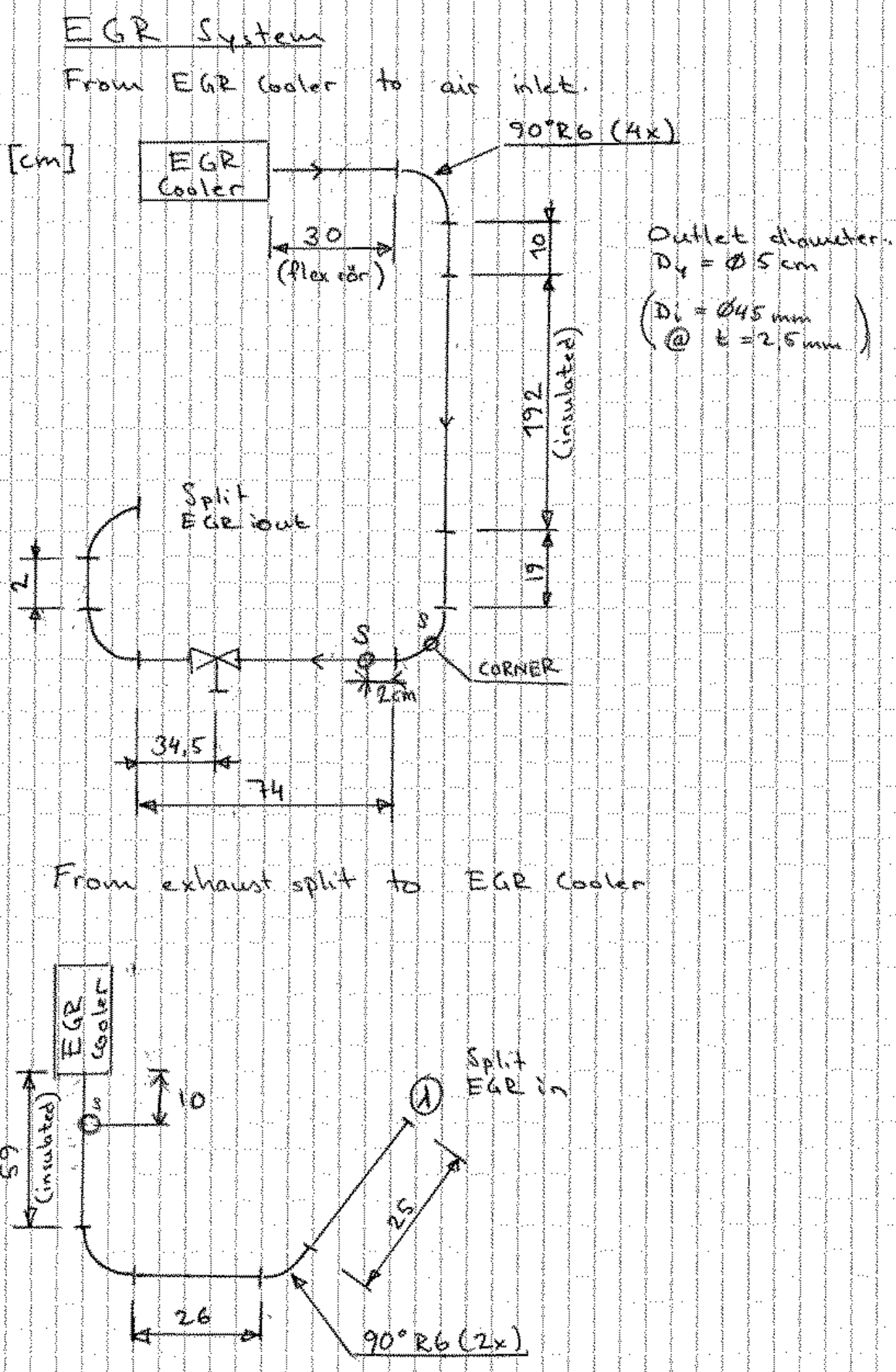


Figure 9.31 Drawing: EGR circuit

B - 2 Showing GT-Power case circuits

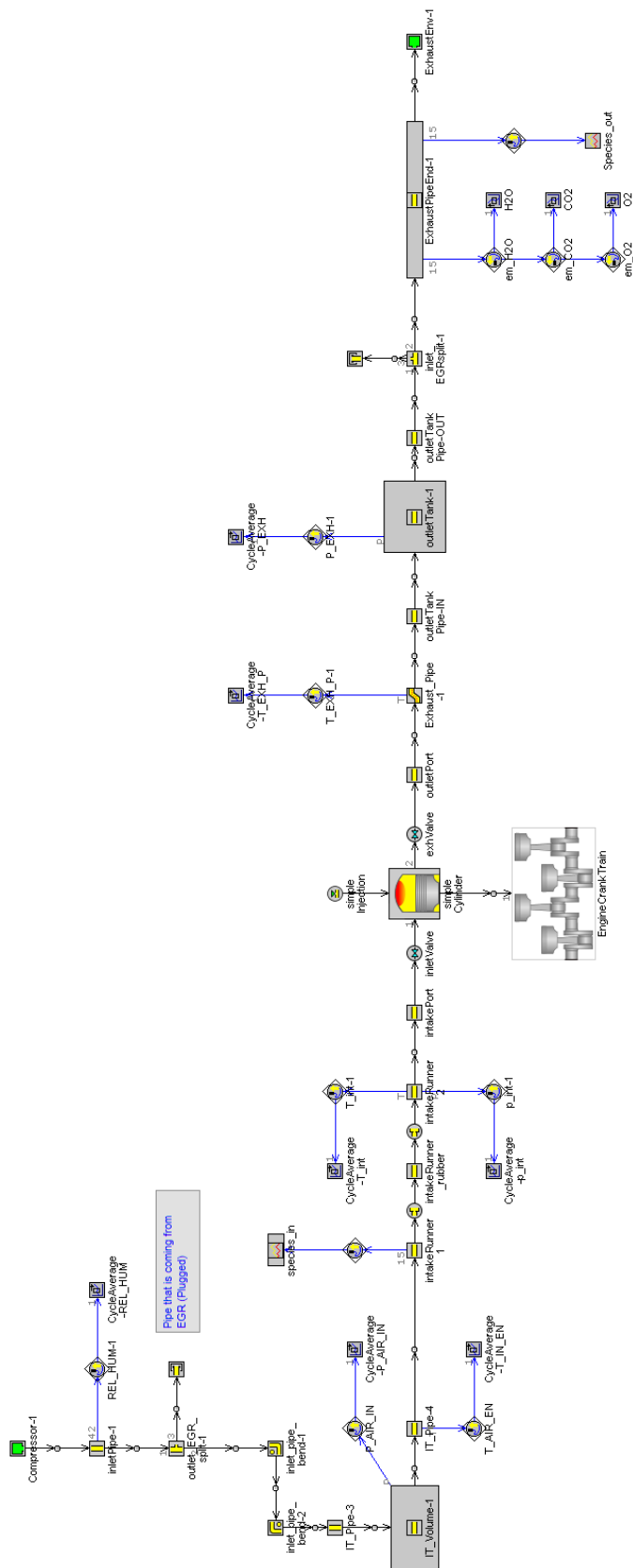


Figure 9.33 System circuit for case 1. No EGR circuit present.

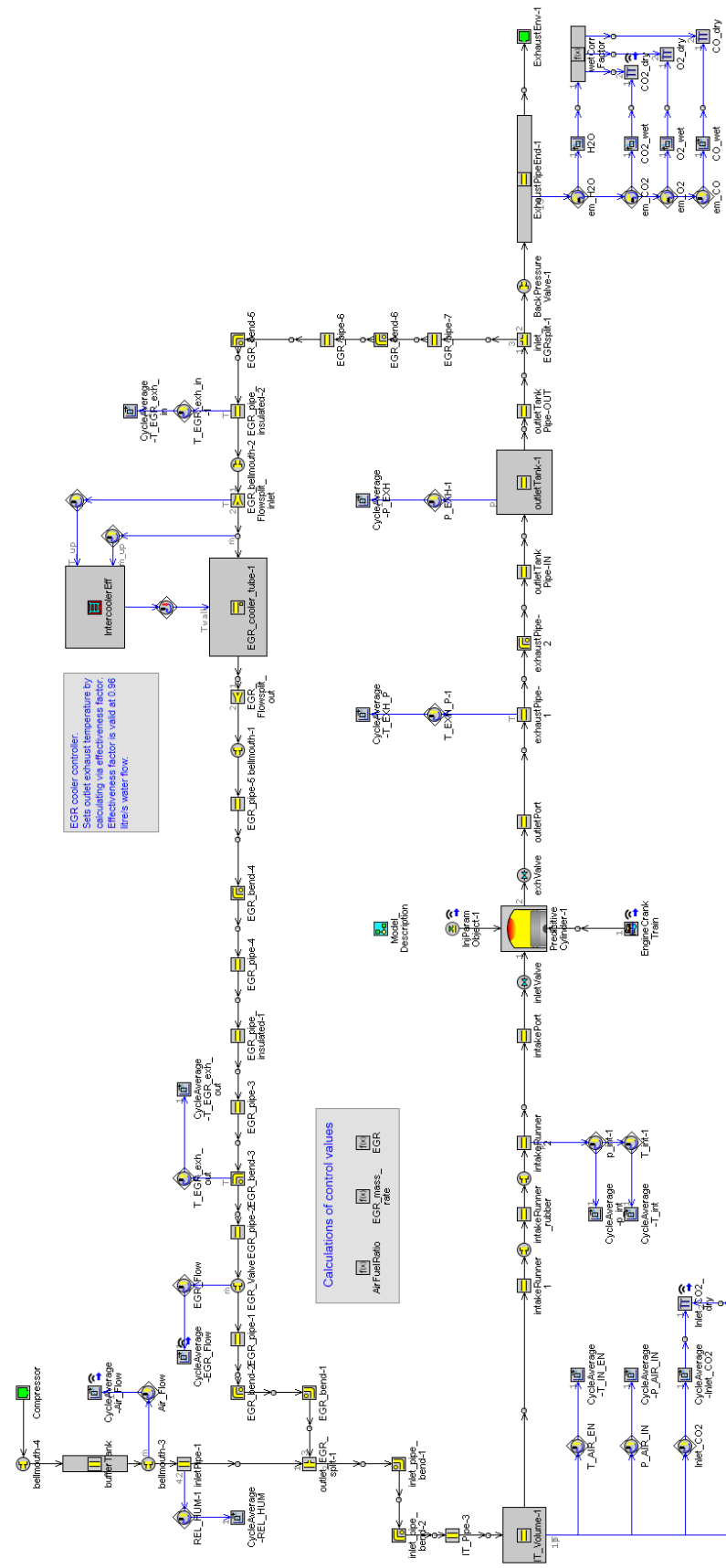


Figure 9.34 System circuit for case 4. Only difference between case 3 and 4 is the name of the cylinder part due to the predictive combustion model. Otherwise they are equal.

